Thesis On

INVESTIGATIONS ON IMPROVEMENT OF MATERIAL PROPERTIES AND PARAMETRIC OPTIMIZATION OF MRR, TWR AND ROUGHNESS USING POWDER MIXED DIELECTRIC IN EDM PROCESS

Submitted in partial fulfillment of the requirement for the award of the degree of

Master of Engineering

IN

PRODUCTION & INDUSTRIAL ENGINEERING

Submitted By

GURMAIL SINGH

Roll No. 800882002

Under the Guidance of

Dr. Ajay Batish
Associate Professor
Thapar University, Patiala

Anirban Bhattacharya
Assistant Professor
Thapar University, Patiala

Dr. Vinod Kumar Singla
Assistant Professor
Thapar University, Patiala

DEPARTMENT OF MECHANICAL ENGINEERING

THAPAR UNIVERSITY

PATIALA-147004, INDIA,

JULY-2010

DECLARATION

This is to certify that the thesis entitled **"INVESTIGATIONS ON IMPROVEMENT OF MATERIAL PROPERTIES AND PARAMETRIC OPTIMIZATION OF MRR, TWR AND ROUGHNESS USING POWDER MIXED DIELECTRIC IN EDM PROCESS "** is an authentic record of my study carried out as requirements for the award of the degree of **Master of Engineering in Mechanical (Production and Industrial) Engineering** to **Thapar University, Patiala,** under the guidance of **Dr. AJAY BATISH**, Associate Professor, **Mr. ANIRBAN BHATTACHARYA,** Assistant Professor and **Dr. VINOD KUMAR SINGLA,** Assistant Professor, Department of Mechanical Engineering, Thapar University, Patiala during **July 2009 to July 2010.** This matter embodied in this thesis has not been submitted in part or full to any other university or institute for the award of any degree.

Gurmail Singh

This is to certify that above declaration made by the student concerned is correct to the best of my knowledge & belief.

15/7/10

(Dr. AJAY BATISH)
Associate Professor,
Thapar University,
Patiala, 147004.

Anirban Bhattacharya

(ANIRBAN BHATTACHARYA)
Assistant Professor,
Thapar University,
Patiala, 147004.

(Dr. V.K. SINGLA)
Assistant Professor,
Thapar University,
Patiala, 147004.

Countersigned by:

(Dr. S.K. MOHAPATRA)
Professor & Head,
Department of Mechanical Engineering,
Thapar University, Patiala, 147004.

29.7.10

(Dr.R.K. SHARMA)
Dean of Academic Affairs,
Thapar University,
Patiala, 147004.

ACKNOWLEDGEMENTS

With deep sense of gratitude I express my sincere thanks to my guides, ***Dr. Ajay Batish*** , ***Mr. Anirban Bhattacharya*** and ***Dr. Vinod Kumar Singla*** for their valuable guidance, proper advice and constant encouragement during the my thesis work from the initial level to final level.I also feel very much obliged to ***Dr. S.K. Mohapatra***, Professor & Head, of Mechanical Engineering Department.

I would like also thanks to *Department of Science and Technology (DST)* for providing the equipment and other sources for my thesis work.

I would like to thanks all the members and employees of Mechanical Engineering Department, Thapar University, Patiala for their everlasting support.

I am also very thankful to my friends for their cooperation.

I offer my regards to all of those who supported me in any respect during the completion of the work.

Lastly, and most importantly, I wish to thank my parents. They supported me and loved me. To them I dedicate this thesis.

GURMAIL SINGH

Registration No. 800882002

ABSTRACT

Electric discharge machining (EDM) is one of the most popular machining methods to manufacture dies and press tools because of its capability to produce complicated shapes and machine very hard materials. The intent of the present study is to study the effect of different input parameters, namely, current, workpiece material, electrode material, dielectric medium, pulse on time, pulse off time and powder and some their interactions on the MRR, TWR, micro hardness and surface roughness. The effect of various input parameters on output responses have been analyzed using Analysis of Variance (ANOVA). Deposition of the powder material either in pure form or in compound form was also studied. XRD and microstructure analysis has been completed to understand the form and amount of deposition on the surface of the workpiece material. Main effect plot and interaction plot for significant factors and S/N ratio have been used to determine the optimal design for each output response.

ABBREVATIONS

ANOVA	Analysis of Variance
DC	Direct Current
Dof	Degree of Freedom
EDM	Electric Discharge Machining
HCHCr	High-Carbon High-Chromium
HDS	Hot Die Steel
RC	Relaxation Circuit
MRR	Material Removal Rate
TWR	Tool Wear Rate
SR	Surface Roughness
SEM	Scanning Electron Microscope
X-RD	X-Ray diffraction
S/N	Signal to Noise Ratio

OA	Orthogonal Array
A	Workpiece Material
B	Dielectric
C	Electrode Material
D	Pulse off Time
E	Pulse on Time
F	Current
G	Powder
Gr	Graphite Powder
W-Cu	Tungsten-Copper Electrode
Cu	Copper Electrode
CI	Confidence Interval
SS	Sum of Squares

CONTENTS

LIST OF FIGURES

LIST OF TABLES

CHAPTER 1

INTRODUCTION

1.1 INTRODUCTION TO NON-TRADITIONAL PROCESSES

Technologically advanced industries like aeronautics, automobiles, nuclear reactors, missiles, turbines etc. requires materials like high strength temperature resistant alloys which have higher strength, corrosion resistance, toughness, and other diverse properties. With rapid development in the field of materials it has become essential to develop cutting tool materials and processes which can safely and conveniently machine such new materials for sustained productivity, high accuracy and versatility at automation. Consequently, non-traditional techniques of machining are providing effective solutions to the problem imposed by the increasing demand for high strength temperature resistant alloys, the requirement of parts with intricate and compacted shapes and materials so hard as to defy machining by conventional methods. The processes are non-conventional in the sense that these don't employ a conventional tool for the material removal. Instead these utilize energy in direct form to remove the materials from workpiece. The range of applications of newly developed machining process is determined by workpiece properties like electrical and thermal conductivity, melting temperature, electrochemical equivalent etc. These techniques can be classified into three categories, i.e. mechanical, electro-thermal, and electrochemical machining processes. The mechanical non-conventional techniques (abrasive jet machining, ultrasonic machining, and water jet machining) utilizes kinetic energy of either abrasive particles or a water jet to remove the material. In electro-thermal method (plasma arc machining, laser beam machining, and electron beam machining) the energy is supplied in form of heat, light, and electron bombardment which results melting, or vaporization and melting both of work material. In the chemical machining, etching process is being done. On the other hand, in electrochemical machining an anodic dissolution process is going on in which high material removal rate can be achieved. The selection of a process is depend upon various factors like- process capabilities, physical parameters, shape to be machined, properties of workpiece material to be cut, and economics of process.

1.2 ELECTRIC DISCHARGE MACHINE

Electrical discharge machining (EDM) is one of the most extensively used non-conventional material removal processes. In this process the material is removed by a succession of electrical discharges, which occur between the electrode and the workpiece. There is no direct contact between the electrode tool and the workpiece. These are submersed in a dielectric liquid such as kerosene or deionised water. Its unique feature of using thermal energy to machine electrically conductive parts regardless of hardness has been its distinctive advantage. The electrical discharge machining process is widely used in the aerospace, automobile, die manufacturing and moulds industries to machine hard metals and its alloy [1, 2].

1.3 HISTORY OF ELECTRIC DISCHARGE MACHINING

In dates back to 1770, English chemist Joseph Priestly discovered the erosive effect of electrical discharges on metal. After a long time, in 1943 at the Moscow University where B.R. and N.I. Lazarenko decided to exploit the destructive effect of electrical discharges for constructive use. They developed a controlled process of machining to machine metals by vaporizing material from the surface of workpiece. Since then, EDM technology has developed rapidly and become indispensable in manufacturing applications such as die and mould making, micro-machining, prototyping, etc. In 1950s The RC (resistance–capacitance) relaxation circuit was introduced, in which provided the first consistent dependable control of pulse times and also a simple servo control circuit to automatically find and hold a given gap between the electrode (tool) and the workpiece. In the 1980s, CNC EDM was introduced which improved the efficiency of the machining operation.

1.4 WORKING PRINCIPLE OF EDM

The basic principle in EDM is the conversion of electrical energy into thermal energy through a series of discrete electrical discharges occurring between the electrode and work piece immersed in the dielectric fluid. The insulating effect of the dielectric is important in avoiding electrolysis of the electrodes during the EDM process. A spark is produced is at the point of smallest inter-electrode gap by a high voltage, overcoming the strength dielectric breakdown strength of the small gap between the cathode and anode at

a temperature in the range of 8000 to 12,000 °C. Erosion of metal from both electrodes takes place there. Duration of each spark is very short. The entire cycle time is usually few micro-seconds (μs).The frequency of pulsating direct current supply is about 20,000–30,000 Hz is turned off. There is a sudden reduction in the temperature which allows the circulating dielectric fluid to flush the molten material from the workpiece in the form of microscopic debris. After each discharge, the capacitor is recharged from DC source through a resistor, and the spark that follows is transferred to the next narrowest gap (Figure 1.1). The cumulative effect of a succession of sparks spread over the entire workpiece surface leads to erosion, or machining to a shape, which is approximately complementary to that of the tool [2].

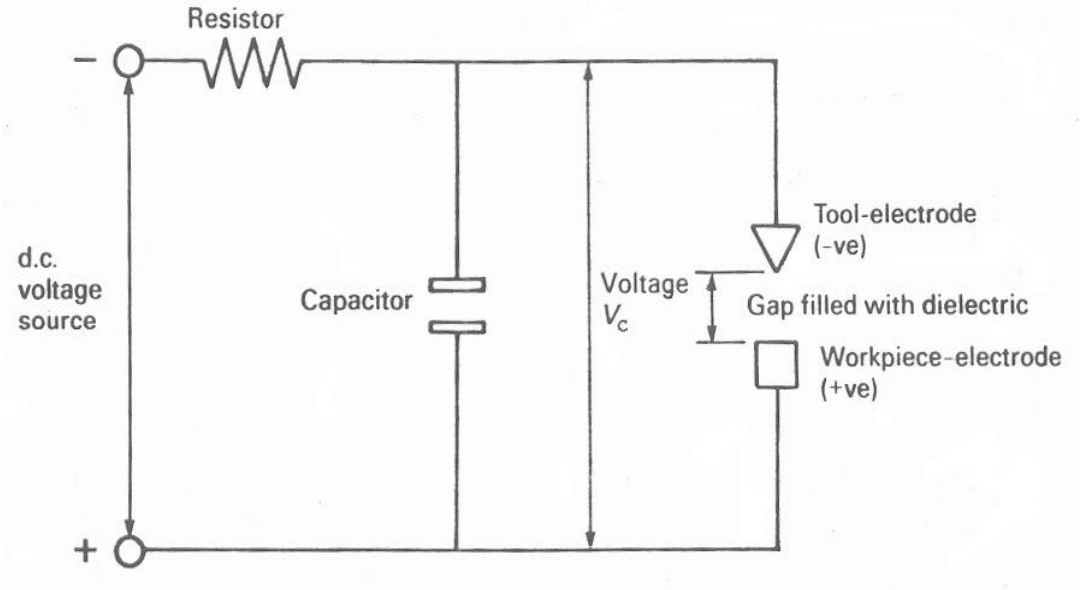

Figure 1.1 Relaxation circuit [3]

A servo system, which compares the gap voltage with a reference value, is employed to ensure that the electrode moves at a proper rate to maintain the right spark gap, and to retract the electrode if short-circuiting occurs. The Lazarenko RC circuit does not give good material removal rate (MRR), and higher MRR is possible only by sacrificing surface finish. As indicated in Figure 1.2, the increase in voltage of capacitor should be larger than the breakdown voltage and hence great enough to create a spark between electrode and workpiece, at region of least electrical resistance, which usually occurs at the smallest inter electrode gap [3].

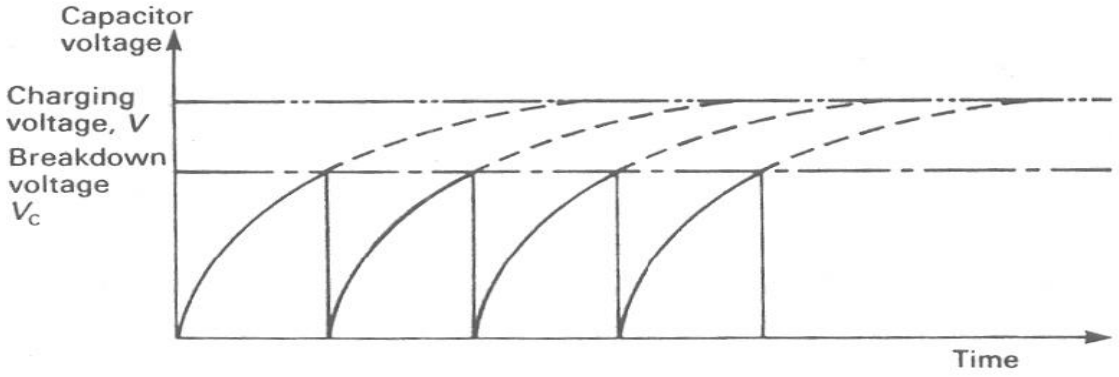

Figure 1.2 Variation of capacitor voltage with time [3]

This has been achieved with advent controlled pulse generator. It is typical wave forms are shown in Figure 1.3. In this, as comparison to RC circuit there is increase in pulse duration and less peak current value, shortened idle period.

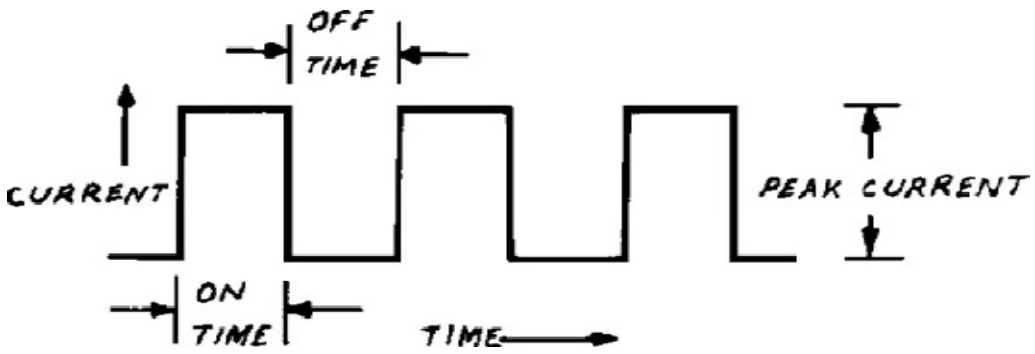

Figure 1.3 Pulse waveform of controlled pulse generator [3]

1.5 MECHANISM OF MATERIAL REMOVAL

The electro sparking method of metal working involves an electric erosion effect in which the breakdown of electrode material is done by electric discharge. The discharge is created by the ionization of dielectric which is spilled up of its molecules into ions and electrons. This discharge is created between two electrodes through a gaseous or liquid medium with the application of suitable voltage across the electrodes. The potential intensity of electric field between them is built up at some predetermined value; the

individual electrons will break loose from the surface of the anode under the influence of the field force. While moving in the inter-electrode space, the electrons collide with the neutral molecules of the dielectric, detaching electrons from them and causing ionization. At some time or other the ionization becomes such that a narrow channel of continuous conductivity is formed. When this happens there is a continuous flow of electrons along the channel to the electrode, resulting in the momentary current impulse or discharge. The

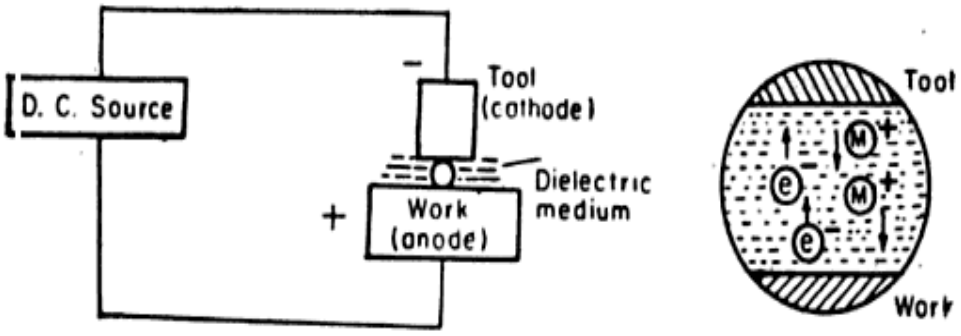

Figure 1.4 Mechanism of material removal [4]

liberation of energy accompanying the discharge leads to generation of high temperature. This high temperature plasma causes fusion or particle vaporization of metal and the dielectric fluid at the point of discharge. This leads to the formation of tiny crater at the point of discharge in the workpiece.

Comparatively less metal is eroded from the tool as compared to the workpiece due to following reasons:

a) The momentum with which positive ions strike the cathode surface is much less than the momentum with which the electron stream impinges on the anode surface.
b) A compressive force is generated on the cathode surface by spark which helps reduce tool wear.

The particles removed from the electrodes due to discharge fall in liquid, cool down and contaminate the area around the electrodes by forming colloidal suspension of metal. These suspensions, along with the products of decomposition of liquid dielectric are drawn into

the space between the electrodes during the initial part of discharge process and are distributed along the electric lines of force, thus forming current carrying ‘bridges’. The discharge then occurs along one of these brides as result of ionization [4].

1.6 SINKER EDM

Sinker EDM sometimes is also referred to as cavity type EDM or volume EDM. It consists of an electrode and workpiece that are submerged in an insulating liquid such as oil or dielectric fluid. In it, hydrocarbon dielectrics are normally used because surface roughness is better and tool electrode wear is lower compared to de-ionized water [5]. The electrode and workpiece are connected to a suitable power supply. The power supply generates an electrical potential between the two parts. As the electrode approaches the workpiece, dielectric breakdown occurs in the fluid forming an ionization channel, and a small spark is generated. The resulting heat and cavitation vaporize the work material, and to some extent, the electrode. These sparks strike one at a time in huge numbers at seemingly random locations between the electrode and the workpiece. As the base metal is eroded, the spark gap increases. Thus electrode is lowered automatically by the machine so that the process can continue uninterrupted. Several hundred thousand sparks occur per second in this process, with the actual duty cycle being carefully controlled by the setup parameters. These controlling cycles are sometimes known as "on time" and

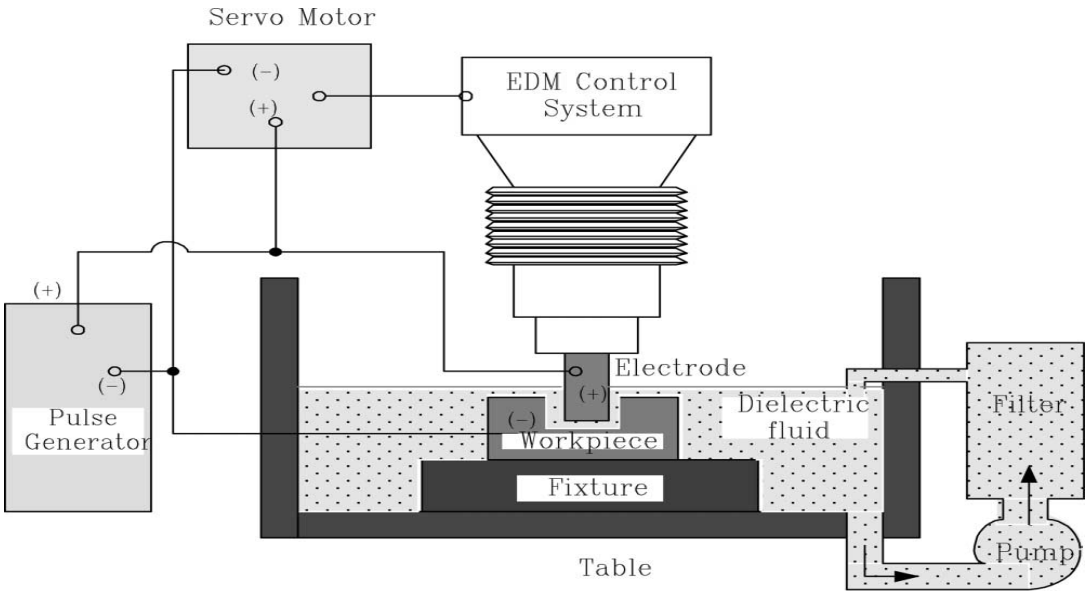

Figure 1.5 Schematic diagram of the Sinker EDM [6]

"off time". The on time setting determines the length or duration of the spark. Hence, a longer on time produces a deeper cavity for that spark and all subsequent sparks for that cycle creating a rougher finish on the workpiece. The reverse is true for a shorter on time. Off time is the period of time that one spark is replaced by another. A longer off time, allows the flushing of dielectric fluid through a nozzle to clean out the eroded debris, thereby avoiding a short circuit. These settings are maintained in micro seconds.

The workpiece can be formed, either by replication of a shaped tool electrode. The numerical control monitors the gap conditions (voltage and current) and synchronously controls the different axes and the pulse generator. The dielectric liquid is filtrated to remove debris particles and decomposition products [5].

1.7 EDM PROCESS PARAMETERS

1.7.1 Polarity

The Polarity normally used is normal polarity in which the tool is negative and workpiece is positive. Sometimes positive polarity can be used depending upon the requirement, where tool is positive and workpiece is negative. The negative polarity of the workpiece has an inferior surface roughness than that under positive polarity in EDM.

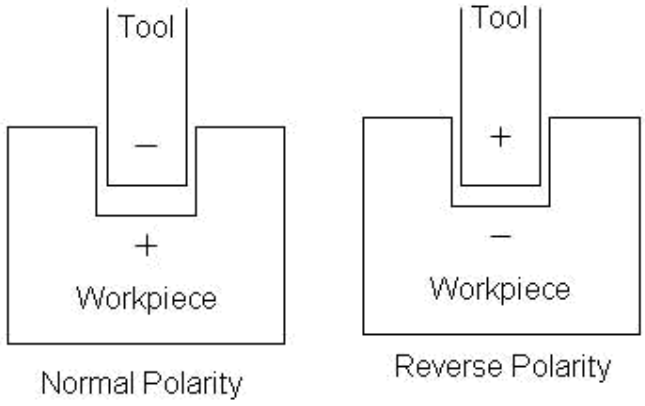

Figure 1.6 Normal Polarity and Reverse Polarity [7]

The current passing through the gap creates high temperatures causing material evaporation at both electrode spots. The plasma channel is composed of ion and electron flows. As the

electron processes has smaller mass than anions show quicker reaction, the anode material is worn out predominantly. This effect causes minimum wear to the tool electrodes and becomes of importance under finishing operations with shorter on-times. However, while running longer discharges, the early electron process predominance changes to positron process (proportion of ion flow increases with pulse duration), resulting in high tool wear. In general, polarity is determined by experiments and is a matter of tool material, work material, current density and pulse length combinations [7, 8].

1.7.2 Pulse on time

Pulse on-time is the time period during which machining takes place. MRR is directly proportional to amount of energy applied during pulse on-time. The energy of spark is controlled by the peak amperage and the length of the on-time. The longer the on-time pulse is sustained, the more workpiece material will be eroded. The resulting crater will be broader and deeper than a crater produced by a shorter on-time. These large craters will create a rougher surface finish. Extended on times gives more heat to workpiece, which means the recast layer will be larger and the heat affected zone will be deeper. Hence, excessive on-times can be counter-productive. When the optimum on-time for each electrode-work material combination is exceeded, material removal rate starts to decrease.

1.7.3 Pulse off time

Pulse off-time is the time during which re-ionization of dielectric takes place. The discharge between the electrodes leads to ionization of the spark gap. Before another spark can take place, the medium must de-ionize and regain its dielectric strength. This takes some finite time and power must be switched off during this time. Too low values of pulse off time may lead to short-circuits and arcing. A large value on other hand increases the overall machining time since no machining can take place during the off-time. Each cycle has an on-time and off-time that is expressed in units of microseconds.

1.7.4 Peak current

This is the amount of power used in discharge machining, measured in units of amperage, and is the most important machining parameter in EDM. In each on-time pulse, the current increases until it reaches a preset level, which is expressed as the peak current. Higher

value of peak current leads to rough surface finish operations and wider craters on work materials. Its higher value improves MRR, but at the cost of surface finish and tool wear. Hence it is more important in EDM because the machined cavity is a replica of tool electrode and excessive wear will hamper the accuracy of machining [8].

1.7.5 Discharge current

The discharge current (I_d) is a measure of the power supplied to the discharge gap. A higher current leads to a higher pulse energy and formation of deeper discharge craters. This increases the material removal rate (MRR) and the surface roughness (R_a) value. Similar effect on MRR and Ra is produced when the gap voltage (V_g) is increased. Once the current starts to flow, voltage drops and stabilizes at the working gap level. The preset voltage determines the width of the spark gap between the leading edge of the electrode and workpiece. Higher voltage settings increase the gap, which improves the flushing conditions and helps to stabilize the cut.

1.7.6 Pulse wave form

For higher surface finish, higher peak current values and short spark duration is required, a controlled pulse generator is used in EDM to generate proper pulse wave form. The pulses of high energy and low frequency are used in rough machining. The pulse shape is normally rectangular, but generators with other pulse shapes have also been developed. Using a generator which can produce trapezoidal pulses succeeded in reducing relative tool wear to very low values [8].

1.7 .7 Type of Dielectric medium

The fluids used as dielectric are generally hydrocarbon oils. The kerosene oil, paraffin oil, lubricating oil can be used. The deionised water gives high MRR and TWR [7]. However, the use of deionised water may result in higher levels of material removal rate in some special situations such as when a brass electrode at negative polarity is used ; pulse durations smaller than 500 µs are employed and machining of Ti–6A1–4V with a copper electrode . It has seen that machining a steel workpiece with a negative brass electrode in deionised water and with pulse time ranging from 400 to 1500 µs resulted in improved performance (higher material removal rate and lower electrode wear) when compared to

performing the same operation in a hydrocarbon oil. For a pulse time of 800 µs, material removal rate was approximately 60% higher and electrode wear 25% lower [9]. A good dielectric fluid should have following properties:

(a) It should have dielectric strength (i.e. behave as insulator until the required breakdown voltage between the electrodes is attained).
(b) It should take minimum possible time to breakdown, once the break down voltage is attained.
(c) It should able to deionise the gap immediately after the spark has occurred.
(d) It should serve as an effective cooling medium.
(e) It should have high degree of fluidity.

1.7.8 Type of flushing

It is basic requirement of dielectric that it should maintain its dielectric strength (insulating properties) during its whole operation. There is no problem at the start of EDM, but after discharge the debris are produced in the gap reduce the dielectric strength, which cause unwanted discharges which can damage to both tool and workpiece. Hence effective flushing is required to remove unwanted debris from the gap [3]. TWR and MRR are affected by the type of dielectric and the method of its flushing. In EDM, flushing can be achieved by following methods:

1.7.8.1 Suction flushing

In this, dielectric may be sucked through either the workpiece or the electrode. This technique is employed to avoid any tapering effect due to sparking between machining debris and the side walls of the electrodes. Suction flushing through the tool rather than through the workpiece is more effective.

1.7.8.2 Injection flushing

In this technique, dielectric is fed through either the workpiece or the tool which are pre-drilled to accommodate the flow. With the injection method, tapering of components arises due to the lateral discharge action occurring as a result of particles being flushed up the sides of electrodes [4].

1.7.8.3 Side flushing

When the flushing holes cannot be drilled either in the workpiece or the tool, side flushing is employed. If there is need of flushing of entire working area, special precautions have to taken for the pumping of dielectric.

1.7.8.4 Flushing by dielectric pumping

This method has been found particularly suitable in deep hole drilling. Flushing is obtained by using the electrode pulsation movement. When the electrode is raised, clean dielectric is sucked into mix with contaminated fluid, and as the electrode is lowered the particles are flushed out. [4].

1.7.9 Electrode gap

The servo feed system is used to control the working gap at a proper width. Mostly electro-mechanical (DC or stepper motors) and electro-hydraulic systems are used, and are normally designed to respond to average gap voltage [8]. Larger gap widths cause longer ignition delays, resulting in a higher average gap voltage. If the measured average gap voltage is higher than the servo reference voltage preset by the operator, the feed speed increases. On the contrary, the feed speed decreases or the electrode is retracted when the average gap voltage is lower than the servo reference voltage, which is the case for smaller gap widths resulting in a smaller ignition delay. Therefore short-circuits caused by debris particles and humps of discharge craters can be avoided. Also quick changes in the working surface area, when tool electrode shapes are complicated, does not result in hazardous machining. In some cases, the average ignition delay time is used in place of the average gap voltage to monitor the gap width [5].

1.7.10 Electrode material

The shape of electrode will be basically same as that of the product is desired. The electrode materials are classified as metallic material (copper, brass, tungsten, aluminium), non-metallic material (graphite), combined metallic and non-metallic (copper-graphite), and metallic coating as insulators (copper on moulded plastic, copper on ceramic) etc. Materials having high melting-point, good electrically conductivity, low wear rate and easily machinability are usually chosen as tool materials for EDM. They

should be cheap and readily shaped by conventional methods. High density graphite is used in pulsed EDM equipment, although the material does not perform satisfactorily in RC EDM work. It gives low wear due to its high melting temperature. Copper has the qualities for high stock metal removal. It is a stable material under sparking conditions. Brass as a tool material has high wear. Copper-boron and silver tungsten both exhibit extremely low wear. Sometimes copper tungsten is employed as the cathode metal. Its use yields high machining rates and very low wear. Due to its high cost and not so readily shaped, its applications are limited [7].

1.8 ORGANIZATION OF SEMINAR

Chapter 1 covers brief introduction to non-conventional machining, principle of electric discharge machining, mechanism of material removal and process parameters of EDM.

Chapter 2 presents an available literature of EDM process for surface modification. The available literature has been categorized in two broad classifications such as surface modification with powder mixing fluid and surface modification with electrode materials. Summary of the literature and gap in literature also discussed.

Chapter 3 presents the area of research work to be undertaken has been identified. Objective and work plan also discussed. Methodology to be adopted also described in brief.

Chapter 4 presents the analysis and results of the MRR. Results after the Analysis of Variance (ANOVA) and Taguchi Signal-to-Noise ratio are outlined in this chapter. Main effect plot and interaction plots for MRR are discussed in this chapter. Optimal design conditions have been discussed.

Chapter 5 presents the analysis and results of the TWR. Results after the Analysis of Variance (ANOVA) and Taguchi Signal-to-Noise ratio are outlined in this chapter. Main effect plot and interaction plots for TWR are discussed in this chapter. Optimal design conditions have been discussed.

Chapter 6 presents the analysis and results of the micro hardness at non-deposited and deposited region. Results after the Analysis of Variance (ANOVA) and Taguchi Signal-to-Noise ratio are outlined in this chapter. Main effect plot and interaction plots for non-

deposited and deposited region are discussed in this chapter. Optimal design conditions have been discussed.

Chapter 7 presents the analysis and results of the surface roughness (R_a). Results after the Analysis of Variance (ANOVA) and Taguchi Signal-to-Noise ratio are outlined in this chapter. Main effect plot and interaction plots for surface roughness (R_a) are discussed in this chapter. Optimal design conditions have been discussed.

Chapter 8 presents the analysis of surface properties. XRD and microstructure analysis has been completed to understand the form and amount of deposition on the surface of the workpiece material.

Chapter 9 presents the results, conclusions and recommendations from the experimental work.

CHAPTER 2
LITERATURE REVIEW

2.1 INTRODUCTION

A large work has been done on different aspects of EDM. This chapter covers the literature on EDM machine settings and other process parameters. Literature is divided into following three main categories**.**

1. According to powders used and their effect
2. According to electrode used and their effect
3. According to machine settings

2.1.1 According to Powders Used and Their Effect

Abbas et al. [10] reviews the research trends in EDM on ultrasonic vibration, dry EDM machining, EDM with powder additives, EDM in water and modelling technique in predicting EDM performances.

Wu et al. [11] has studied electrical discharge distribution effects can be achieved by the addition of aluminum (Al) powder in the dielectric. A fine surface roughness value of the workpiece is thus obtained. However, the electrostatic force among fine Al particles was found to agglomerate the Al powders in the dielectric. A surfactant can be adopted to separate the Al powder in the dielectric homogenously. Better surface even the mirror-like quality of the machined work piece is thus desired. In the study, the effect of surfactant and Al powders added in the dielectric on the surface status of the work piece after EDM is investigated. It was observed the best distribution effect is found when the concentrations of the Al powder and surfactant in the dielectric are 0.1 and 0.25 g/L, respectively. An optimal surface roughness (Ra) value of 0.172 mm is achieved by positive polarity, discharge current 0.3 A, pulse duration time 1.5 ms, open circuit potential 140 V, gap voltage 90 V, surfactant concentration 0.25 g/L. The surface roughness status of the work piece has been improved up to 60% as compared to that EDMed under pure dielectric with high surface roughness Ra of 0.434 mm.

Uno et al. [12] listed that the EDMed surface with metal powder mixed fluid has smaller surface roughness and higher resistance to corrosion because of the diffusion of electrode

and/or powder materials into the machined surface. They proposed a new surface modification technique to obtain high surface wear resistance using EDM with powder mixed fluid and also concluded that the EDMed surface with NPMF (Nickel powder mixed fluid) has a smaller surface roughness than that in EDM with kerosene type fluid. The resolidified layer containing nickel can be generated on EDMed surface and the thickness of the layer becomes larger and more uniform with the increase of nickel powder concentration in the machining fluid. The EDMed surface with NPMF becomes harder than that with pure kerosene type fluid and it also shows high resistance to sand abrasion. A hard layer containing TiC can be formed on the machined surface by EDM with CPMF (carbon powder mixed fluid) using titanium electrodes, which leads to higher surface wear resistance. By mixing carbon powder with the dielectric kerosene, thick hard layers with small surface roughness values can be obtained.

Peças and Henriques [13] has studied the addition of powder particles to the electrical discharge machining (EDM) dielectric fluid modifies some process variables and creates the conditions to achieve a higher surface quality in large machined areas. The analysis is carried out varying the silicon powder concentration and the flushing flow rate over a set of different processing areas. The evaluation of process is done by surface morphologic analysis. In experiment it has seen that with the addition of silicon powder in dielectric there is the reduction of crater dimensions (crater depth, crater diameter), white-layer thickness and surface roughness, but with increase the concentration of silicon powder the crater dimensions can be slightly reduced. An accurate control of the powder concentration and flushing flow is a requirement for achieving an improvement in the process polishing capability. It is observed that better surface morphology is by powder concentration in the range 2 to 3 g/l.

Kansal et al. [14] optimized the process parameters of powder mixed electrical discharge machining (PMEDM). The variables like Pulse on time, duty cycle, peak current and concentration of the silicon powder added into the dielectric fluid of EDM were selected to study the process performance in terms of material removal rate and surface roughness. Response surface methodology has been used to plan and analyze the experiments. They noted that by suspending silicon powder into the dielectric fluid of EDM and an enhanced rate of material removal and surface finish can be achieved. The material removal rate increases with the increase in the concentration of the silicon powder. The surface

roughness decreases with the increase in the concentration of the silicon powder. The combination of high peak current and high concentration yields more MRR and smaller SR.

Chiang [15] proposed mathematical models for the modeling and analysis of the effects of machining parameters on the performance characteristics in the EDM process of Al_2O_3+TiC mixed ceramic which are developed using the response surface methodology (RSM) to explain the influences of four machining parameters (the discharge current, pulse on time, duty factor and open discharge voltage) on the performance characteristics of the material removal rate (MRR), electrode wear ratio (EWR), and surface roughness (SR). He adopted the face-centered central composite design (CCD) to study the separable influence of individual machining parameters and the interaction between these parameters by using analysis of variance (ANOVA). The results show that the main two significant factors on the value of the material removal rate (MRR) are the discharge current and the duty factor. The discharge current and the pulse on time also have statistical significance on both the value of the electrode wear ratio (EWR) and the surface roughness (SR). The value of MRR first increases with an increase of pulse on time up to 200 μs, and then decreases with a further increase in the pulse on time. The value of MRR increases with an increase of discharge current, duty factor, and open discharge voltage. The value of EWR quickly decreases with an increase of pulse on time and then tends to stabilize. The value of EWR decreases with an increase of the discharge current, but it increases with an increase of duty factor and open discharge voltage. The value of SR first decreases with an increase of pulse on time before 150 μs and then increases further increase in the pulse on time. The value of SR increases with an increase of discharge current and open discharge voltage, but, decreases with an increase of duty factor.

Yan et al. [16] investigated the influence of the machining characteristics on pure titanium metals using an electrical discharge machining (EDM) with the addition of urea into distilled water. Machining parameters such as the dielectric type, peak current and pulse duration were changed to explore their effects on machining performance, including the material removal rate, electrode wear rate and surface roughness. The elemental distribution of nitrogen on the machined surface was qualitatively determined by Electronic Probe Micro-Analyzer (EPMA) to assess the effects on surface modification.

Micro hardness and wear resistance tests were performed to evaluate the effects of the reinforced surface. Experimental results indicate that the nitrogen element decomposed from the dielectric that contained urea, migrated to the work piece, forming a TiN hard layer, resulting in good wear resistance of the machined surface after EDM. It was concluded from experimental results that by adding urea into the dielectric, MRR and EWR increased with an increase in peak current. Moreover MRR and EWR declined as the pulse duration increased.

Prihandana et al. [17] observed that solutions are needed for increasing the material removal rate without degrading surface quality in micro-electrical discharge machining (m-EDM). They presented a new method that consists of suspending micro-MoS_2 powder in dielectric fluid and using ultrasonic vibration during m-EDM processes. The Taguchi method was adopted to optimize the process parameters to increase the material removal rate of dielectric fluid containing micro-powder in m-EDM using a L_{18} orthogonal array. Pareto analysis of variance was employed to analyze the four machining process parameters which were ultrasonic vibration of the dielectric fluid, concentration of micro-powder, tool electrode materials, and workpiece materials. The results showed that the introduction of MoS_2 micro-powder in dielectric fluid and using ultrasonic vibration significantly increase the material removal rate and improves surface quality by providing a flat surface free of black carbon spots.

Chowa et al. [18] investigated Micro-slit EDM process along with small discharge energy and SiC powder in pure water. SiC powder was added to pure water as a working fluid to verify the micro-slit EDM process performance. The result indicated that the addition of SiC powder would increase working fluid electrical conductivity, enlarge the electrode and workpiece gap, and also extrude debris easily, therefore increasing the material removal rate. Furthermore, the use of SiC powder helped bridge the electrode and workpiece gap and disperse discharge energy, thus creating two discrete discharging pulses from a single discharging period that could effectively disperse discharging energy into several increments. The discharging results could then generate a minor crater and debris since minor debris would ease gap exhaust and accelerate material removal rate. The minor crater could simultaneously refine the surface roughness.

Pecas and Henriques [19] compared the performance between EDM with powder mixed dielectric and conventional EDM when dealing with the generation of high-quality

surfaces. In particular the analysis of the effect of the electrode area in the surface quality measured by the surface roughness and craters morphology was carried out for both technologies. The results achieved evidenced a linear relationship between the electrode area and the surface quality measures as well as a significant performance improvement when the powder mixed dielectric is used.

Kung et al. [20] studied material removal rate (MRR) and electrode wear ratio (EWR) on the powder mixed electrical discharge machining (PMEDM) of cobalt-bonded tungsten carbide (WC-Co). In the PMEDM process, the aluminum powder particle suspended in the dielectric fluid disperses and makes the discharging energy dispersion uniform; it displays multiple discharging effects within a single input pulse. The study was made only for the finishing stages and has been carried out taking into account the four processing parameters: discharge current, pulse on time, grain size, and concentration of aluminium powder particle for the machinability evaluation of MRR and EWR. The response surface methodology (RSM) has been used to plan and analyze the experiments. The experimental plan adopts the face-centered central composite design (CCD). They highlighted the development of mathematical models for investigating the influence of processing parameters on performance characteristics.

Pecas and Henriques [21] studied that the addition of powder particles in suspension in the dielectric modifies some process variables and creates the conditions to achieve a high surface quality in large areas. They presented a new research work aiming to study the performance improvement of conventional EDM when used with a powder-mixed dielectric. A silicon powder was used and the improvement is assessed through quality surface indicators and process time measurements, over a set of different processing areas. The results showed the positive influence of the silicon powder in the reduction of the operating time, required to achieve a specific surface quality, and in the decrease of the surface roughness, allowing the generation of mirror-like surfaces.

Furutani et al. [22] described the influence of the discharge current and the pulse duration on the titanium carbide (TiC) deposition process by electrical discharge machining (EDM) with titanium (Ti) powder suspended in working oil. In the experiments, a 1-mm copper rod was used for an electrode to prevent the flushing of working oil from the gap between the electrode and a workpiece. Ti powder reacted with the cracked carbon from the working oil, then depositing a TiC layer on a workpiece

surface. A major criterion of the deposition or removal was the discharge energy over pulse duration of 10 μs. A thickness of the TiC layer became the maximum at a certain discharge current and pulse duration. Larger discharge energy and power promoted the removal by heat and pressure caused by the discharge. The removal was classified further into two patterns; cracks were observed on the Ti-rich surface in removal pattern 1 and a workpiece was simply removed in removal pattern 2. The maximum hardness of the deposition was 2000 Hv. The workpiece about 10 μm beneath its surface was also hardened because of the dispersion of TiC.

Wong et al. [23] proposed a near mirror finish phenomena in electrical discharge machining when powder is introduced into dielectric fluid as a suspension at the tool-workpiece or inter-electrode gap during machining. The dielectric flushing system of conventional die sinking EDM machine was specially modified to inject and distribute the powder into the dielectric fluid, especially at the gap between the tool and the workpiece. Machining was performed on various types of steel with different types of powder suspension at a peak current of around 1A. Particular combination of powder mixed dielectric and workpiece have been found to produce mirror surface or glossy machined surface. Close scrutiny of mirror finish surface reveals shallow overlapping resoldified discs with smooth rims, unlike typically EDMed surfaces, which are typically covered with deep craters, pock marks and globules. The various factors affecting the generation of mirror like surfaces were studied. The appropriate settings of electrode polarity and pulse parameters and correct combination of workpiece material and powder characteristics have a significant influence on the mirror finish condition. The use of negative electrode polarity (i.e. with tool as negative electrode, which condition is normally used for finishing EDM) is necessary to achieve the mirror finish condition. Other features of powder mixed dielectric EDM shorter machining time, more uniform dispersion of electrical discharge, and stable machining. Based on the results of the experimental investigation, types of material composition, powder properties and machine setting in bringing the near mirror condition were discussed.

2.1.2 According to Electrode Used and Their Effect

Che Haron et al. [24] investigated the machining characteristics when machining XW42 tool steel at two current settings (3A and 6 A), three diameter sizes (10, 15 and 20mm) and kerosene as the dielectric. The results showed that the material removal rate is higher

and the relative electrode wear ratio is lower with copper electrode than graphite electrode. The increase in the current and electrode diameter reduced tool wear rate as well as the material removal rate.

Tsai et al. [25] proposed a new method of blending the copper powders contained resin with chromium powders to form tool electrodes. Such electrodes are made at low pressure (20 MPa) and temperature (200°C) in a hot mounting machine. It was showed that using such electrodes facilitated the formation of a modified surface layer on the work piece after EDM, with remarkable corrosion resistant properties. The optimal mixing ratio, appropriate pressure, and proper machining parameters (such as polarity, peak current, and pulse duration) were used to investigate the effect of the material removal rate (MRR), electrode wear rate (EWR), surface roughness, and thickness of the recast layer on the usability of these electrodes. Their work also reveals that the composite electrodes obtained a higher MRR than Cu metal electrodes, the recast layer was thinner and fewer cracks were present on the machined surface.

A newly developed low-pressure and low-temperature technique was used to fabricate composite electrodes to conduct EDM on medium carbon steel. The conclusions based on the experimental results show that by using pure copper powders contained resin as electrodes, and adopting a positive polarity machining process can obtain a higher MRR than the Cu–Cr composite electrodes, but relatively the EWR is also higher. The MRR is higher when a sintering pressure of 20 or 30 MPa is used to fabricate composite electrodes than when a sintering pressure of 10 MPa is used. In the 10 MPa case, Cu and Cr particles easily drop out of the electrode due to their weak bonding, resulting in an unstable discharge state during the EDM process. The surface finish is poor when composite electrodes are used in negative polarity machining, because of very many Cu and Cr particles inside electrodes drop out accumulate or adhere to machined surfaces. With use the newly developed composite electrodes for EDM, causes both Cu and Cr particles to drop easily, such that the elements (Cu and Cr) in the electrode can also migrate to the machined surfaces during EDM, and the corrosion resistance increases with the percentage of added Cr particles. This result suggests that using such composite electrodes as tool electrode may improve the resistance of work piece surfaces to corrosion.

Simo et al. [26] studied surface alloying of various work piece materials using EDM. It can be achieved by using powder metallurgy (PM) tool electrodes and the use of powders

suspended in the dielectric fluid, typically aluminium, nickel, titanium, etc. They presented experimental results on the surface alloying of AISI H13 hot work tool steel during a die sink operation using partially sintered WC/Co electrodes operating in a hydrocarbon oil dielectric. An L_8 fractional factorial Taguchi experiment was used to identify the effect of key operating factors on output measures (electrode wear, work piece surface hardness, etc.). With respect to micro hardness, the percentage contribution ratios (PCR) for peak current, electrode polarity and pulse on time were ~24, 20 and 19%, respectively.

Mohri et al. [27] proposed a new method of surface modification by EDM using composite electrodes on workpieces of carbon steel or aluminum were carried out in hydrocarbon oil. Copper, aluminum, tungsten carbide and titanium were used for the materials of electrodes, it was revealed that there existed the electrode material in the work surface layer and the characteristics of the surface of material are changed. Surfaces have lesser cracks, high corrosion resistance and wear resistance.

Koshy et al. [28] used a rotating disk electrode which is more productive and accurate technique than use conventional electrode. Material removal rate, tool wear rate, relative electrode wear, corner reproduction accuracy and surface finish aspects of rotary electrode were compared with those of a stationary one. The effective flushing of the working gap improves material removal rate and machines surface with better finish. Despite the prevalent high tool wear rate, the reproduction accuracy is least affected as the wear gets uniformly distributed over the entire circumference of the disk. Machining of the sharp corner is possible even with aluminum electrode, whose relative electrode wear is greater than unity.

2.1.3 According to Machine Settings

Kanlayasiri and Boonmung [29] has investigated the effects of machining variables on the surface roughness of wire-EDMed DC53 die steel, which is an improvement over the familiar cold die steel SKD11. The machining variables investigated were pulse-peak current, pulse-on time, pulse-off time, and wire tension. Analysis of variance (ANOVA) technique was used to find out the variables affecting the surface roughness. The results from the analysis show that pulse-on time and pulse-peak current are significant variables to the surface roughness of wire-EDMed DC53 die steel. The surface roughness of the test specimen increases when these two parameters increase. A mathematical model was

developed using multiple regression method to formulate the pulse-on time and pulse-peak current to the surface roughness. The developed model was validated with a new set of experimental data, and the maximum prediction error of the model was less than 7%.

Wanga et al. [30] explores the feasibility of removing the recast layer (RCL) using etching and mechanical grinding for Ni-based super alloy materials by means of electrical discharge machining (EDM). Their experiment was divided into three stages. The first stage acquires a thick recast layer by using EDM with a larger discharging energy. The second stage optimizes the recast layer removal technique. This work determines the second stage setting using Taguchi's recommendation. Thus L_9 orthogonal array sets up the etching and mechanical grinding parameters and observes the recast layer removal quantity analysis. It was proved that the corrosive made up of phosphoric acid and hydrochloric acid under proper temperature could significantly enhance the recast layer removal rate for Inconel 718 alloy. The Electronic Probe Micro-Analyzer (EPMA) analysis of recast layer and base material before and after corrosion using phosphoric acid and hydrochloric acid proved that carbon decreases dramatically during the corrosion process. The micro-hardness test of recast layer and base material proved that corrosion using phosphoric acid and hydrochloric acid could only damage the structure of the recast layer and that base material hardness would not be damaged at all.

Keskin et al. [31] performed experiments to determine parameters effecting surface roughness. The data obtained for performance measures have been analyzed using the design of experiments methods. A considerably profound equation was obtained for the surface roughness using power, pulse time, and spark time parameters.

Singh et al. [32] carried out experimental investigation to study the effects of machining parameters such as pulsed current on material removal rate, diameteral overcut, electrode wear, and surface roughness in electric discharge machining of En-31 tool steel (IS designation: T105 Cr 1 Mn 60) hardened and tempered to 55 HRc. The work material was ED machined with copper, copper tungsten, brass and aluminium electrodes by varying the pulsed current at reverse polarity. The investigations indicate that the output parameters of EDM increase with the increase in pulsed current and the best machining rates are achieved with copper and aluminium electrodes.

2.2 SUMMARY OF LITERATURE REVIEW

A lot of work has been done in surface modification with electrical discharge machining. Surface modification has been done either with electrode material or with powder mixing in the dielectric medium. From the literature survey, it is observed that the field of surface modification using EDM process is still at the experimental stage. Many researchers [13], [14], [18], [21] used silicon metal powder in the kerosene dielectric fluid and investigated the various effects on the machining parameters such as surface roughness, tool wear rate, material removal rate. Some [11], [15], [20] studied effects on material removal rate and surface roughness value with adding aluminum powder in the kerosene dielectric fluid. Effects of MoS2 powders [17] also carried out. Effects of Ti powder [22] also carried out. The surface modification has shown by addition of urea into distilled water [16].

Surface modification by electrode materials also carried out. Many researchers [24], [25], [27], used copper electrode for machining of different materials and observed that a layer of electrode material has taken place on the surface of workpiece material which improve the surface properties. Some of researchers [27], [28] showed that aluminum electrode has positive effect on tool wear rate and surface finish. Tungsten copper electrode [26] improves the MRR without increase the TWR. The effect of machining variables [29], [31], [32] has been investigated on MRR, TWR and SR.

2.3 GAP IN LITERATURE

The field of surface modification using EDM process is still in at the experimental stage. A number of research studies have been carried out and feasibility of the process is well established. From the literature review, it is observed that no research work has been carried out on surface modification using graphite and aluminium powder in kerosene oil dielectric fluid along copper and tungsten- copper electrode. The surface modification in transformer oil as dielectric medium is missing. No work has been reported on H11 and HCHCr die steels with copper and tungsten-copper electrode in transformer oil. All these aspects will be addressed in research work.

3.1 PILOT EXPERIMENTATION

The effect of various input parameters i.e. pulse on, pulse off, current, electrode, workpiece and powder were investigated through the pilot experimentation. Two responses were selected for pilot experimentation namely material removal rate (MRR) and tool wear rate (TWR). The assignment of factors was carried out using statistical software MINITAB. All the factors were varied at three levels except workpiece material, which was varied at two levels. The degrees of freedom required for the experiment was calculated to be 11, thus the orthogonal array that can be used should have degrees of freedom (dof) greater than 11. L18 which can accommodate a combination of 2-level and 3-level factors was used for conduct of experiments to measures two response values namely, MRR and TWR. After the conduct of the 18 trials the mean values for MRR and TWR are tabulated in Table 3.1. For the analysis of the result, Analysis of Variance (ANOVA) was performed.

Table 3.1: L18 Orthogonal Array along with results for powder mixed EDM process during pilot experimentation

Trial No.	Work-piece	Pulse on (µs)	Current (Amp)	Pulse off (µs)	Electrode	Powder	MRR (mm^3/min)	TWR (mm^3/min)
1	HCHCr	10	2	38	Copper	Copper	2.98	0.011
2	HCHCr	10	5	57	Graphite	Graphite	11.92	5.024
3	HCHCr	10	8	85	W-Cu	Mix	37.26	0.616
4	HCHCr	50	2	38	Graphite	Graphite	0.99	1.256
5	HCHCr	50	5	57	W-Cu	Mix	14.03	0.136
6	HCHCr	50	8	85	Copper	Copper	14.03	0.449
7	HCHCr	100	2	57	Copper	Mix	1.36	0.112
8	HCHCr	100	5	85	Graphite	Copper	15.65	3.14
9	HCHCr	100	8	38	W-Cu	Graphite	1.61	1.57
10	H13	10	2	85	W-Cu	Graphite	4.91	0.205
11	H13	10	5	38	Copper	Mix	10.89	0.449
12	H13	10	8	57	Graphite	Copper	34.97	3.14
13	H13	50	2	57	W-Cu	Copper	3.89	0.068

14	H13	50	5	85	Copper	Graphite	9.87	0.112
15	H13	50	8	38	Graphite	Mix	1.43	4.71
16	H13	100	2	85	Graphite	Mix	3.35	0.628
17	H13	100	5	38	W-Cu	Copper	8.5	0.068
18	H13	100	8	57	Copper	Graphite	11.49	0.157

Table 3.2: ANOVA for MRR

Source	SS	v	V	F	F critical at 95% confidence level	P
Workpiece	6.16	1	6.160	0.10		0.766
Pulse off time	398.17	2	199.085	3.15		0.116
Current	593.65	2	296.827	5.22	5.14	0.049
Pulse on time	340.26	2	170.130	2.69		0.147
Electrode	38.88	2	19.441	0.31		0.746
Powder	135.21	2	67.605	1.07		0.401
Residual error	379.42	6	63.237			
Total	1891.76	17				

The relationship of MRR with current, pulse on time and pulse off time during the machining using copper, graphite and tungsten- copper electrode in powder mixed dielectric is shown in the Figure 3.1. It was observed that at low current, MRR is low but increases sharply with increased current. ANOVA for MRR is given in Table 3.2. The current was observed to be most significant factor affecting MRR. The MRR increased with increase in the pulse on time and decreased with increase in pulse off time. The workpiece material and the electrode material had insignificant effect on MRR. Further, the MRR was observed to increase when copper powder was suspended in dielectric and reduce with graphite powder.

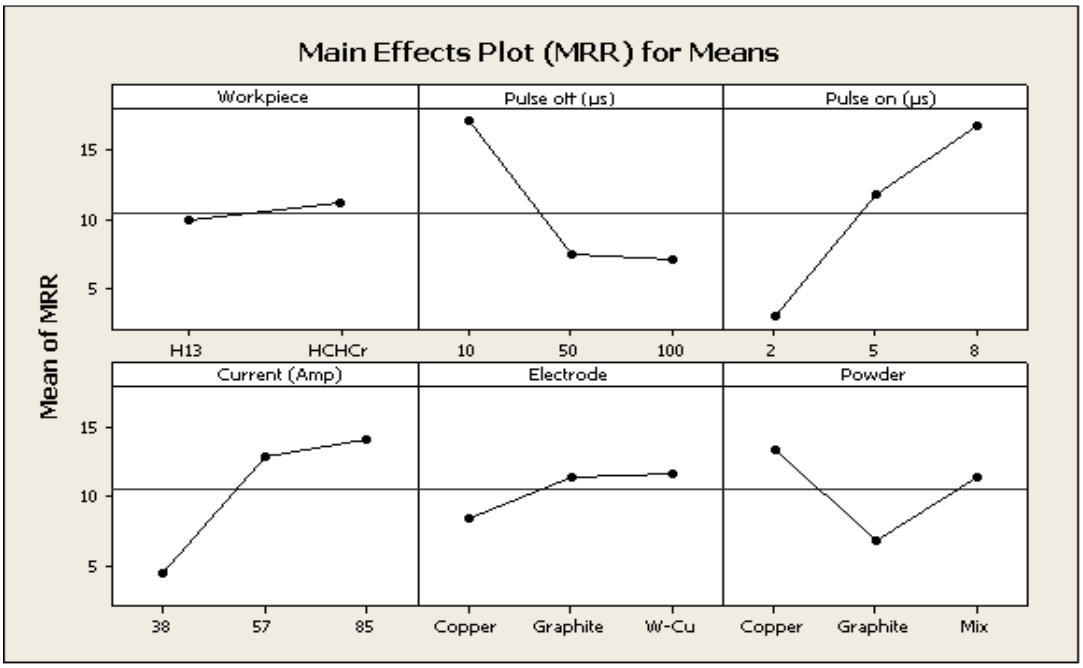

Figure 3.1: Main effect plot for MRR during pilot experimentation

Table 3.3: ANOVA for TWR

Source	SS	V	V	F	F critical at 95% confidence level	P
Workpiece	0.4284	1	0.4284	0.32		0.591
Pulse off	1.2608	2	0.6304	0.47		0.645
Current	6.5037	2	3.2519	2.44		0.168
Pulse on	1.1655	2	0.5827	0.44		0.665
Electrode	28.3231	2	14.1616	10.62	5.14	0.011
Powder	0.2748	2	0.1374	0.10		0.904
Residual error	8.0008	6	1.3335			
Total	45.9571	17				

The relationship of TWR with the current, pulse on and pulse off during the machining with copper, graphite and tungsten- copper electrode in powder mixed dielectric is shown in the Figure 3.2. The electrode material was found to be most significant factor effecting TWR. With copper electrode showing least TWR while graphite electrode has maximum TWR. Also, increase in current caused high tool wear, while all other factors had insignificant effect on TWR.

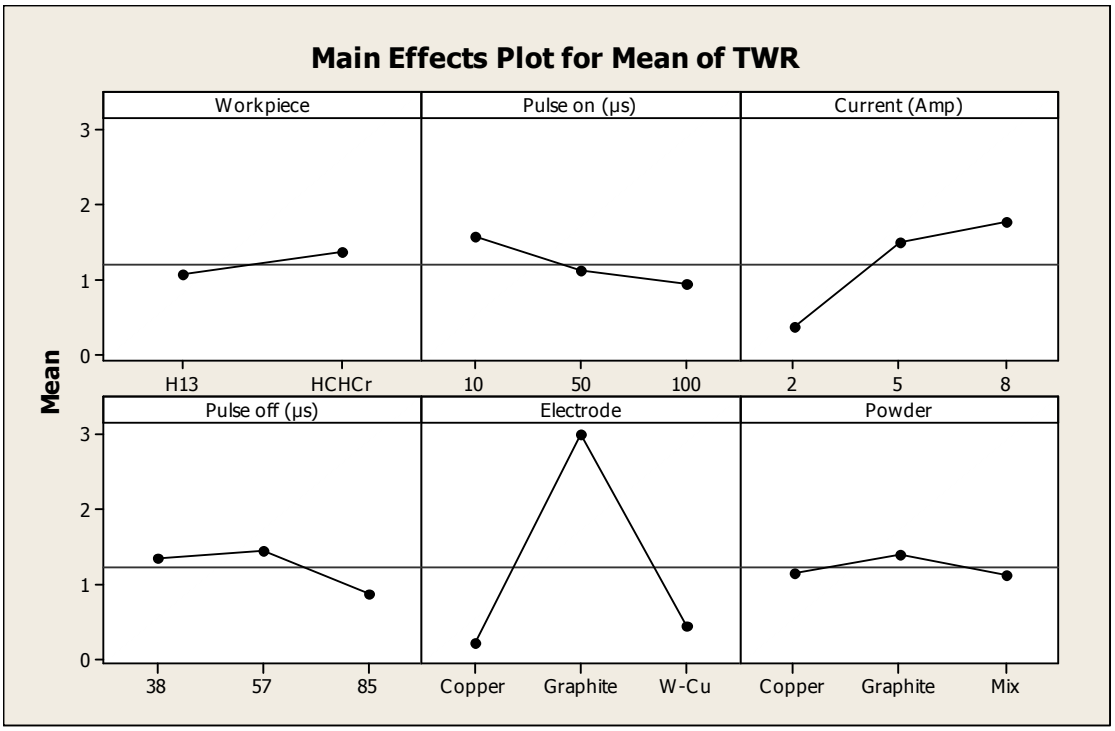

Figure 3.2: Main effect plot for TWR during pilot experimentation

3.2 METHODOLOGY

The full factorial design is referred as the technique of defining and investigating all possible conditions in an experiment involving multiple factors while the fractional factorial design investigates only a fraction of all the combinations. Although these approaches are widely used, they have certain limitations: they are inefficient in time and cost when the number of the variables is large; they require strict mathematical treatment in the design of the experiment and in the analysis of results; the same experiment may have different designs thus produce different results; further, determination of contribution of each factors is normally not permitted in this kind of design. The Taguchi method has been proposed to overcome these limitations by simplifying and standardizing the fractional factorial design. The methodology involves identification of controllable and uncontrollable parameters and the establishment of a series of experiments to find out the optimum combination of the parameters which has greatest influence on the performance and the least variation from the target of the design. The effect of various parameters (workpiece material, electrode, dielectric, pulse on time, pulse off time,

current and powder) and some of the effects of interactions between the main factors were also be studied using parameterization approach developed by Taguchi.

3.3 PROCEDURE OF EXPERIMENTAL DESIGN

The whole procedure of Taguchi method is as under.

1. Establishment of objective functions.
2. Selection of factors and/or interactions to be evaluated.
3. Identifications of uncontrollable factors and test conditions.
4. Selection of number of levels for the controllable and uncontrollable factors.
5. Calculation total degree of freedom needed
6. Select the appropriate Orthogonal Array (OA).
7. Assignment of factors and/or interactions to columns.
8. Execution of experiments according to trial conditions in the array.
9. Analyze results.
10. Confirmation experiments

3.4 ESTABLISHMENT OF OBJECTIVE FUNCTION

The objective of the study is to evaluate the main effects of workpiece material, dielectric, electrode, pulse off, pulse on time, current and powder on the MRR, TWR, surface roughness and micro hardness. Deposition of the powder material either in pure form or in compound form was also studied. XRD and microstructure analysis was completed to understand the form and amount of deposition on the surface of the workpiece material.

3.5 DEGREE OF FREEDOM (dof)

The number of factors and their interactions and level for factors determine the total degree of freedom required for the entire experiment. The degree of freedom for each factor is given by the number of levels minus one.

dof for each factor : k-1

where k is the number of level for each factor

dof for interactions between factors : $(k_A-1) \times (k_B-1)$

where k_A and k_B are number of level for factor A and B

3.6 DUMMY TREATMENT

The dummy treatment accommodates 2-level factor in a basic 3-level orthogonal array by using only two of possible levels for the factor and simply repeating one level from the previous of two levels for the indicated third level. Any one of the two levels for the factor can be repeated, so whichever is easiest, cheapest, or makes more sense should be repeated [33].

3.7 SELECTION OF FACTORS AND INTERACTION

The determination of which factors to investigate depends on the responses of interest. The factors affects the responses were identified using cause and effect analysis, brainstorming and pilot experimentation. The lists of factors studied with their levels are shown in the Table 3.4.

Table 3.4 Factors interested and their levels

FACTORS	LEVELS		
	Level-1	Level-2	Level-3
Worpiece material, *A*	EN 31	H11	HCHCr
Dielectric, *B*	Kerosene oil	Transformer oil	Kerosene oil**
Electrode, C	Copper	Tungsten-copper	Copper**
Pulse off (µs), *D*	38	57	85
Pulse on (µs), *E*	10	50	100
Current (Amp), *F*	2	5	8
Powder, G	No	Graphite	Aluminium

**= Dummy treated

Some of interactions between the main factors were believed to be of interest. The interaction identified for detailed statistical analysis is as under:

- Workpiece and Electrode, A × C
- Workpiece and Powder, A × G
- Electrode and Powder, C × G

The minimum dof required in the experiment are the sum of all the degrees of freedom of factors and interactions. In the present experiment setup, there are five 3-level factor and two, electrode and dielectric are 2-level factor. The number of dof for factors A, D, E, F and G are two and for factor B and C is one. The total dof for the experiment including the interaction is given in Table 3.5. As the dof required for the experiment is 20, the orthogonal array (OA) to be used should have more than 20 dof. The most suitable orthogonal array that can be used for this experiment is L27, which has 26 dof assigned to its various columns. The additional six dof were used to measure the random error.

Table 3.5 Degree of freedom

Factor	A	B	C	D	E	F	G	Ax C	A x G	C x G	Total
Degree of Freedom	2	1	1	2	2	2	2	2×1 = 2	2×2 = 4	1×2 = 2	20

3.8 ORTHOGONAL ARRAY

OA plays a critical part in achieving the high efficiency of the Taguchi method. OA is derived from factorial design of experiment by a series of very sophisticated mathematical algorithms including combinatorics, finite fields, geometry and error-correcting codes. The algorithms ensure that the OA to be constructed in a statistically independent manner that each level has an equal number of occurrences within each column; and for each level within one column, each level within any other column will occur an equal number of times as well. Then, the columns are called orthogonal to each other. OA's are available with a variety of factors and levels in the Taguchi method. Since each column is orthogonal to the others, if the results associated with one level of a specific factor are much different at another level, it is because changing that factor from one level to the next has strong impact on the quality characteristic being measured. Since the levels of the other factors are occurring an equal number of times for each level of the strong factor, any effect by these other factors will be ruled out. The Taguchi method apparently has the following strengths:

1. Consistency in experimental design and analysis.
2. Reduction of time and cost of experiments.
3. Robustness of performance without removing the noise factors.

The selection of orthogonal array depends on:

- The number of factors and interactions of interest
- The number of levels for the factors of interest

Taguchi's orthogonal arrays are experimental designs that usually require only a fraction of the full factorial combinations. The arrays are designed to handle as many factors as possible in a certain number of runs compared to those dictated by full factorial design. The columns of the arrays are balanced and orthogonal. This means that in each pair of columns, all factor combinations occur same number of times. Orthogonal designs allow estimating the effect of each factor on the response independently of all other factors. Once the degrees of freedom are known, the next step, selecting the orthogonal array (OA) is easy. The number of treatment conditions is equal to the number of rows in the orthogonal array and it must be equal to or greater than the degrees of freedom. The interactions to be evaluated will require an even larger orthogonal array. Once the appropriate orthogonal array has been selected, the factors and interactions can be assigned to the various columns.

The linear graph used for assignment of factors in L27 array is shown in Figure 3.3. The L27 array has 13 columns and each column has two dof associated with it. In the linear graph, each vertex of the triangle represents a column in L27 array [33].

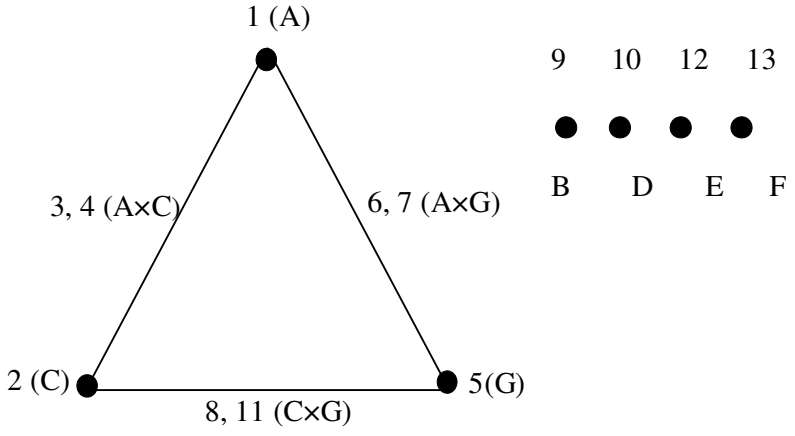

Figure 3.3: L27 Linear Graph [33]

Factor A has been assigned to column 1, factor B to column 2 and factor G to column 5. Each connecting line of the triangle represents interaction and also the column merged for the purpose. Column 3 and 4 were merged to measure the interaction of factor A×*C,* column 6 and 7 and column 8 and 11 were merged to measure the interaction of factor A×G and C×G respectively. The remaining factors B, D, E and F were assigned to columns 9, 10, 12 and 13 respectively. Two factors, dielectric fluid and electrode material, were varied at two levels each and the third level was dummy treated. To calculate the variation due to error a comparison of average response value of level 1 and 1** (repeated dummy treatment experiment) was calculated [33].

The 27 trial conditions represented by Taguchi's L27 are given in Table 3.6. The dummy treated levels are marked by using ** against the repeated level.

Table 3.6: L27 Experimental design

Trial no.	Workpiece	Dielectric	Electrode	Pulse off	Pulse on	Current	Powder
1	EN31	Kerosene	Cu	38	10	2	No
2	EN31	Transformer oil	Cu	57	50	5	Gr
3	EN31	Kerosene**	Cu	85	100	8	Al
4	EN31	Transformer oil	W	57	100	8	No
5	EN31	Kerosene**	W	85	10	2	Gr
6	EN31	Kerosene	W	38	50	5	Al
7	EN31	Kerosene**	Cu**	85	50	5	No
8	EN31	Kerosene	Cu**	38	100	8	Gr
9	EN31	Transformer oil	Cu**	57	10	2	Al
10	H11	Transformer oil	Cu	85	50	8	No
11	H11	Kerosene**	Cu	38	100	2	Gr
12	H11	Kerosene	Cu	57	10	5	Al
13	H11	Kerosene**	W	38	10	5	No
14	H11	Kerosene	W	57	50	8	Gr
15	H11	Transformer oil	W	85	100	2	Al
16	H11	Kerosene	Cu**	57	100	2	No

17	H11	Transformer oil	Cu**	85	10	5	Gr
18	H11	Kerosene**	Cu**	38	50	8	Al
19	HCHCr	Kerosene**	Cu	57	100	5	No
20	HCHCr	Kerosene	Cu	85	10	8	Gr
21	HCHCr	Transformer oil	Cu	38	50	2	Al
22	HCHCr	Kerosene	W	85	50	2	No
23	HCHCr	Transformer oil	W	38	100	5	Gr
24	HCHCr	Kerosene**	W	57	10	8	Al
25	HCHCr	Transformer oil	Cu**	38	10	8	No
26	HCHCr	Kerosene**	Cu**	57	50	2	Gr
27	HCHCr	Kerosene	Cu**	85	100	5	Al

** = Dummy Treated

To ensure that the suspended powder particles do not clog the filtering system special mild steel tank was designed for the conducting experiments. This tank of size 330 × 180 × 187 mm was made of 3mm thick mild steel and had capacity of 9 litre. The tank was installed in EDM machine as shown in Figure 3.6. A stirrer rotating at 1400 rpm was used in the tank for proper mixing of the powder in the dielectric.

3.9 EXPERIMENTAL SET UP

The experiments have been conducted on the Electrical Discharge Machine model T-3822 of Victory Electromech available at Thapar University, Patiala in Machine Tool lab. A large number of input parameters which can be varied in the EDM process, i.e. discharge voltage, pulse on, pulse off, polarity, peak current, electrode gap and type of flushing, each having its own effect on the output parameters such as tool wear rate, material removal rate, surface finish and hardness of machined surface. Current, pulse on and pulse off are the parameters which were varied on the machine for experimentation. The ranges of these parameters for the experimental work have been selected on the basis of results of pilot experiments. The input parameters have been fixed for during the whole experimentation, as given in the Table 3.7.

Table 3.7: Constant input parameter

S.No	Parameter	Value
1	Open circuit voltage	135+/-5%
2	Polarity	Positive
3	Machining time	10 mintues
4	Spark energy	Low
5	Powder concentration	10 gm/l

To avoid the entrance of suspended powder in filtering system especially tank is designed of mild steel. The inside dimensions of tank are length 330 mm, breadth 180mm, height 187mm and plate thickness 3mm. Capacity of the tank is 9 liters. A stirrer of 1400 rpm was used in the tank for the properly mix of the powder in dielectric.

Figure 3.4 Electrical Discharge Machine

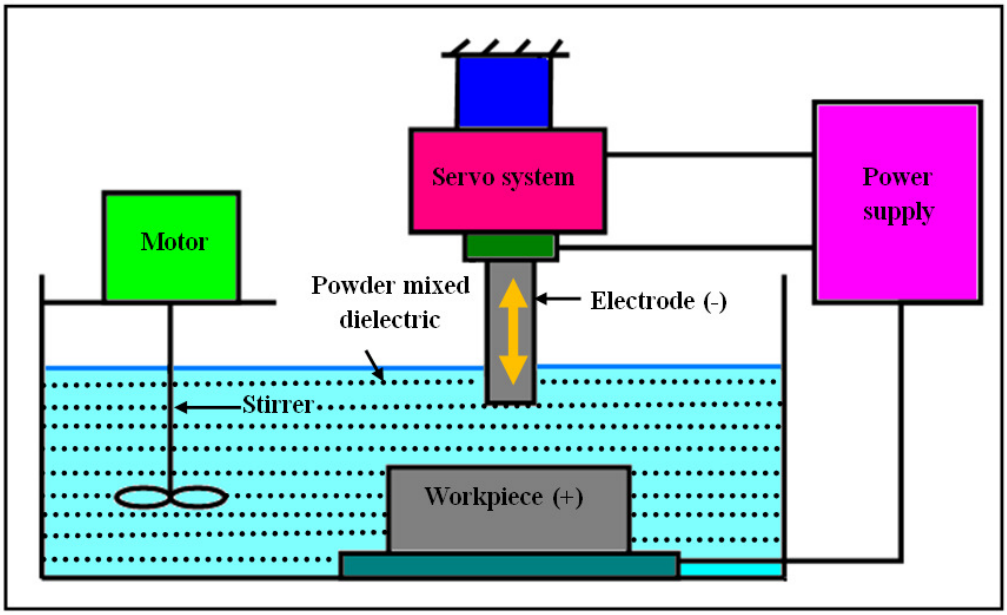

Figure 3.5: Schematic Diagram of Experimental Setup

Figure 3.6: Dielectric Tank with Stirrer Attachment

3.10 MEASURING AND TEST EQUIPMENT USED

Micro hardness and surface roughness tests were conducted on all the samples, produced after each of the 27 trials. Also, MRR was measured using a weighing machine, while TWR was measured using a Vernier Calliper. The details of important test equipment used in experimental study are given below:

3.10.1Surface Roughness Tester

Surface roughness was measured using the Perthometer, model M4Pi of Mahr, Germany available in the Metrology lab of Thapar University, Patiala. The equipment uses the stylus method of measurement, has profile resolution of 12 nm and measure roughness up to 100µm. A tracing length of 4.8 mm was used for analysis. Surface roughness of each sample was measured at three different positions namely, centre, left and right of each machined sample. The left and right positions were taken at 7mm form center on each side.

3.10.2 Micro Hardness Tester

Micro hardness was measured on a computer interfaced Micro Hardness Tester, (model MVH-2) Metatech industries, Pune, India, available at Thapar University, Patiala. The micro hardness measurement is dependent on the diameter of indentation on the samples. The indents formed in the pyramid shaped indenter were measured with Quantimet software using a load of 1 kg for 20 seconds. The micro hardness was measured at deposition as well as non deposition region

3.10.3 X-Ray Diffraction Machine

XRD analysis was carried out on X-Ray Diffraction machine, (model ME 210 LA 2) of Rigaku corporation, Japan, available in Material Testing lab of Thapar University, Patiala. The range of 2θ from the 5^0 to 100^0 was used at a scan speed of 5^0/minute for each test.

3.10.4 Scanning Electron Microscope (SEM) Machine

Microstructure was carried out of some selected samples on Scanning Electron Microscope, (model JSM-840A) of Joel, Japan, available in Material Testing lab of Thapar University, Patiala. The range of magnification from 10× to 3,00,000×. SEM of samples was carried out on three ranges, namely, 200×, 500× and 1000×.

3.11 ANALYSIS OF RESULTS

Signal-to-noise ratio

The parameters that influence the output can be categorized into two classes, namely controllable (or design) factors and uncontrollable (or noise) factors. Controllable factors are those factors whose values can be set and easily adjusted by the designer. Uncontrollable factors are the sources of variation often associated with operational environment. The best settings of control factors as they influence the output parameters are determined through experiments. From the analysis point of view, there are three possible categories of the response characteristics explained below.

r is the number of tests in a trial (noise of repetitions regardless of noise levels)

$\sum_{i=1}^{r} y^2{}_i$ = summation of all response values under each trial

MSD = Mean square deviation

y_j = Observed value of the response characteristic

y_0 = nominal or target value of the results

The three different response characteristics are given by the following.

1) Higher is Better. The S/N for higher the better is given by:

$(S/N)_{HB} = -10 \log (MSD_{HB})$ (Equation....3.1)

Where $MSD_{HB} = \frac{1}{r}\sum_{j=1}^{r}\left(\frac{1}{y_j^{\,2}}\right)$ (Equation....3.2)

MSD_{HB} = Mean Square Deviation for higher-the-better response.

2) Nominal is Better. The S/N for nominal is better is:

$(S/N)_{NB} = -10 \log (MSD_{NB})$ (Equation....3.3)

Where $MSD_{NB} = \frac{1}{r}\sum_{j=1}^{r}(y_j - y_0)^2$ (Equation....3.4)

3) Lower is Better. In this design situation, response is the type of ‘‘lower is better’’, which is a logarithmic function based on the mean square deviation (MSD), given by

$$S/N_{LB} = -10\log(MSD) = -10\log[(\frac{1}{r}\sum_{i=1}^{r} y^2{}_i) \quad \text{(Equation....3.5)}$$

Where $MSD_{LB} = \frac{1}{r}\sum_{j=1}^{r}\left(y_j{}^2\right)$ (Equation....3.6)

Signal to noise ratio for response characteristics

The parameters that influence the output can be categorized in two categories, controllable factors and uncontrollable factors. The control factors that may contribute to reduced variation can be quickly identified by looking at the amount of variation present in response. The uncontrollable factors are the sources of variation often associated with operational environment. For this experimental work, response characteristics have given in the Table 3.8.

Table 3.8: Response Characteristics

Response name	Response type	Units
Material Removal Rate (MRR)	Higher the better	mm^3/min
Tool Wear Rate (TWR)	Lower the better	mm^3/min
Micro Hardness	Higher the better	HVN
Surface Roughness	Lower the better	Microns

Measurement of F-value of Fisher's F ratio

The principle of the *F* test is that the larger the *F* value for a particular parameter, the greater the effect on the performance characteristic due to the change in that process parameter. *F* value is defined as:

$$F = \frac{MS\ for\ a\ term}{MS\ for\ the\ error\ term} \quad \text{(Equation....3.7)}$$

Computation of average performance:

Average performance of a factor at certain level is the influence of the factor at this level on the mean response of the experiments.

Analysis of variance

The knowledge of the contribution of individual factors is critically important for the control of the final response. The analysis of variance (ANOVA) is a common statistical technique to determine the percent contribution of each factor for results of the experiment. It calculates parameters known as sum of squares (*SS*), pure *SS*, degree of freedom (DOF), variance, F-ratio and percentage of each factor. Since the procedure of ANOVA is a very complicated and employs a considerable of statistical formulae, only a brief description of is given as following.

The Sum of Squares (SS) is a measure of the deviation of the experimental data from the mean value of the data.

Let '*A*' be a factor under investigation

$$SS_T = \sum_{i=1}^{N} (y_i - \overline{T})^2 \qquad \text{(Equation....3.8)}$$

Where N = Number of response observations, $\overline{T}$ is the mean of all observations y_i is the i th response

Factor Sum of Squares (SS_A) - Squared deviations of factor (*A*) averages from overall average

$$SS_A = \left[\sum_{i=1}^{k_A} \left(\frac{A_i^2}{n_{Ai}} \right) \right] - \frac{T^2}{N} \qquad \text{(Equation....3.9)}$$

Where

A_i =Average of all obseravtions under A_i level = A_i / n_{Ai}

T = sum of all observations

$\overline{T}$ = Average of all observations = T / N

n_{Ai} = Number of obsernations under A_i level

Error Sum of Squares (SS_e) - Squared deviations of observations from factor (A) averages

$$SS_e = \sum_{j=1}^{k_A} \sum_{i=1}^{n_{Ai}} \left(y_i - \overline{A}_j \right)^2 \qquad \text{(Equation....3.10)}$$

Sum of Squares ($SS_{A\times B}$) for interactions

$$SS_{A\times B} = \left[\sum_{i=1}^{c} \left(\frac{(A\times B)_i^2}{n_{(A\times B)i}} \right) \right] - \frac{T^2}{N} - SS_A - SS_B \qquad \text{(Equation....3.11)}$$

Sum of Squares of factors for dummy treatment level

The level symbols for A_1 & $A_{1^{**}}$, both indicate the same test condition w.r.t. factor A. Therefore

$$SS_A = \frac{(A_1 + A^{**}_1)^2}{n_{A1} + n_{A1^{**}}} + \frac{A_2^2}{n_{A2}} - \frac{T^2}{N} \qquad \text{(Eequation....3.12)}$$

$$SS_e = \frac{(A_1 - A_1^{**})^2}{n_{A1} + n_{A1^{**}}} \qquad \text{(Equation....3.13)}$$

$$SS_{A\times B} = \left[\sum_{i=1}^{c} \left(\frac{(A\times B)_i^2}{n_{(A\times B)i}} \right) \right] - \frac{T^2}{N} - SS_A - SS_B - SS_e \qquad \text{(Equation....3.14)}$$

3.12 TEST RESULTS FOR WORKPIECE & ELECTRODE MATERIAL

Three workpiece materials High-Carbon High-Chromium (HCHCr), Hot Die Steel (H11) and EN31 and two electrode materials Graphite and Tungsten-Copper were used. Before the start of experimentation, the chemical composition of workpiece and electrode material was measured on an Optical Emission Spectrometer DV-6. The percentage composition of the workpiece and electrode material is provided in Table 3.9 and 3.10 respectively.

Table 3.9 Chemical composition of workpiece materials

Work-piece	% composition													
	Fe	C	Si	Mn	P	S	Cr	Mo	Ni	Co	Cu	Ti	V	W
H11	91.7	0.39	1.0	0.5	0.03	0.02	4.75	1.1		.01	0.01		0.5	
HCHCr	83.5	1.6	0.5	0.55	0.03	0.03	13.3	0.05	0.07	0.01	0.05	0.02	-	0.02
EN31	92.3	0.3	1.0	0.4	0.04		5.0						1.0	

Table 3.10 Chemical composition of electrode materials

Electrode	% Composition					
	W	Cu	Ni	Z	Ti	Lead
Tungsten-copper	79.36	19.46	0.121	0.047	0.014	0.026
Copper	-	99.78	.045	0.09	0.029	0.044

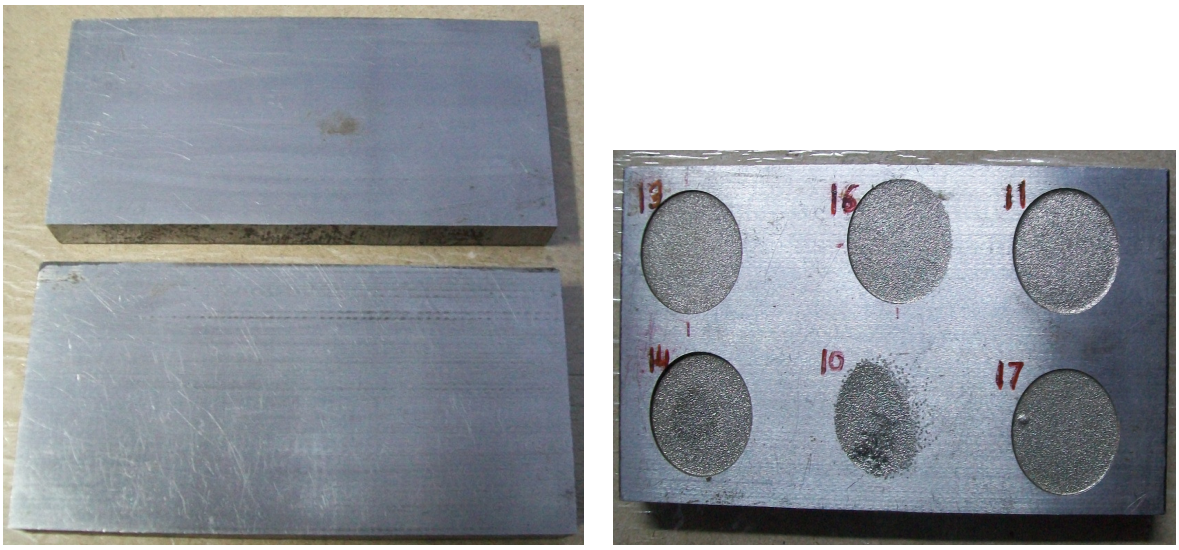

(a) **(b)**

Figure 3.7 Workpiece materials a) Before Machining b) After Machining

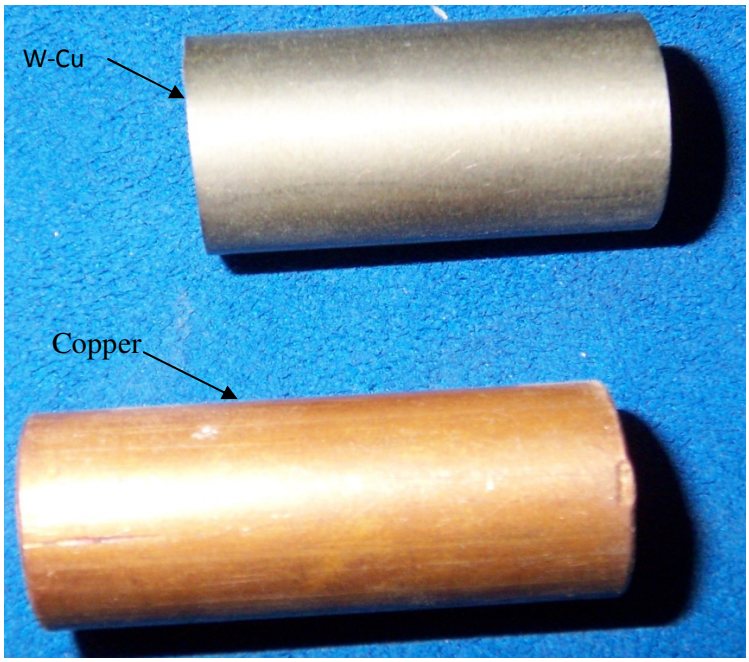

Figure 3.8 Electrodes used

The surface of workpiece has ground on the surface grinder to remove the scaling. Micro hardness of workpiece measured at three different positions before machining which are given in the Table 3.11.

Table 3.11 Micro hardness of workpiece materials before machining

Workpiece material	HCHCr	H11	EN31
Micro hardness (HVN)	576	538	552

CHAPTER 4

RESULTS AND ANALYSIS OF MRR

4.1 INTRODUCTION

The effects of parameters i.e. workpiece, dielectric, electrode, pulse on time, pulse off time, current, powder and some of their interactions were evaluated using ANOVA and factorial design analysis. A confidence interval of 99% has been used for the analysis. One repetition for each of 27 trails was completed to measure the Signal to Noise ratio(S/N Ratio).

4.2 RESULTS FOR MRR

The results for MRR for each of the 27 treatment conditions with repetition are given in Table 4.1. MRR of each sample is calculated from weight difference of workpiece before and after the performance trial, which is given by:

$$\text{MRR} = \frac{(\text{Wi}-\text{Wf})}{\rho \times t} \times 1000 \text{ mm}^3/\text{min} \qquad \text{(Equation ....4.1)}$$

Where Wi ,= Initial weight of workpiece material (gms)
Wf = Final weight of workpiece material (gms)
t = Time period of trails in minutes
ρ = Density of workpiece in gms/cc

Table 4.1: Results for MRR

Trial no.	Work-piece	Dielectric	Elec-trode	Pulse off	Pulse on	Current	Pow-der	MRR mm^3/min		Mean MRR mm^3/min	S/N Ratio
								I	II		
1	EN31	Kerosene	Cu	38	10	2	No	5.16	6.23	5.69	15.0
2	EN31	Transformer oil	Cu	57	50	5	Gr	13.11	13.38	13.24	22.43
3	EN31	Kerosene**	Cu	85	100	8	Al	27.29	26.09	26.69	28.52
4	EN31	Transformer oil	W	57	100	8	No	28.31	27.68	27.99	28.94
5	EN31	Kerosene**	W	85	10	2	Gr	0.264	1.32	0.794	-8.72
6	EN31	Kerosene	W	38	50	5	Al	12.85	14.83	13.84	22.75
7	EN31	Kerosene**	Cu**	85	50	5	No	13.25	13.38	13.31	22.48
8	EN31	Kerosene	Cu**	38	100	8	Gr	27.55	27.42	27.48	28.78
9	EN31	Transformer oil	Cu**	57	10	2	Al	3.88	2.79	3.335	10.11

10	H11	Transformer oil	Cu	85	50	8	No	17.09	18.42	17.75	24.96
11	H11	Kerosene**	Cu	38	100	2	Gr	1.939	1.69	1.82	5.13
12	H11	Kerosene	Cu	57	10	5	Al	9.69	8.42	9.05	19.07
13	H11	Kerosene**	W	38	10	5	No	14.18	13.45	13.81	22.79
14	H11	Kerosene	W	57	50	8	Gr	12.25	14.61	13.42	22.45
15	H11	Transformer oil	W	85	100	2	Al	3.77	4.00	3.88	11.77
16	H11	Kerosene	Cu**	57	100	2	No	4.73	4.61	4.67	13.38
17	H11	Transformer oil	Cu**	85	10	5	Gr	8.36	6.06	7.21	16.82
18	H11	Kerosene**	Cu**	38	50	8	Al	28.73	28.97	28.85	29.20
19	HCHCr	Kerosene**	Cu	57	100	5	No	18.19	19.6	18.89	25.50
20	HCHCr	Kerosene	Cu	85	10	8	Gr	2.51	1.08	1.79	2.927
21	HCHCr	Transformer oil	Cu	38	50	2	Al	3.77	3.95	3.85	11.72
22	HCHCr	Kerosene	W	85	50	2	No	5.39	4.00	4.51	13.15
23	HCHCr	Transformer oil	W	38	100	5	Gr	19.57	18.89	19.23	25.67
24	HCHCr	Kerosene**	W	57	10	8	Al	1.75	1.88	1.81	5.16
25	HCHCr	Transformer oil	Cu**	38	10	8	No	11.49	10.65	11.07	20.86
26	HCHCr	Kerosene**	Cu**	57	50	2	Gr	0.549	0.53	0.54	-5.29
27	HCHCr	Kerosene	Cu**	85	100	5	Al	15.09	14.42	14.75	23.37

** Dummy treated factor

4.3 ANALYSIS OF VARIANCE - MRR

The results for MRR were analyzed using ANOVA for identifying the significant factors affecting the performance measures. The Analysis of Variance (ANOVA) for the mean MRR at 99% confidence interval is given in Table 4.2. The variance data for each factor and their interactions were F-tested to find significance of each. The principle of the *F* test is that the larger the *F* value for a particular parameter, the greater the effect on the performance characteristic due to the change in that process parameter. ANOVA table shows that current (F value 186.82), pulse on time (F value 89.05), workpiece (F value 33.5), pulse off time (F value 16.28), powder (F value 11.30) factors that significantly affect the MRR. The interaction of electrode × powder (F value 47.16) is significant. All other factors namely, electrode and dielectric are insignificant to affect the MRR. Table 4.3 shows the ranks of various factors in terms their relative significance. Current has the highest rank signifying highest contribution to MRR and electrode has the lowest and was observed to be insignificant in affecting MRR. Main effects plot for the MRR are shown in Figure 4.1 which shows the variation of MRR with the input parameters. As can be seen MRR increases with increase in current from 2 Amp to 8 Amp. MRR is decreased with addition of powder in dielectric as compared to without powder mixed dielectric.

The interaction plots are shown in the Figure 4.2 which shows interaction of electrode × powder is significant for the MRR.

Table 4.2: ANOVA for MRR

Sources	SS	v	V	F	F (Critical)	SS'	% contri-bution
Workpiece, A	174.89	2	87.45	33.50	10.9	161.69	7.71
Dielectric, B	3.32	1	3.32	1.27			
Electrode, C	2.41	1	2.41	0.92			
Pulse off, D	84.98	2	42.49	16.28		71.78	3.42
Pulse on, E	464.85	2	232.43	89.05	10.9	451.65	21.53
Current, F	975.19	2	487.60	186.82	10.9	961.99	45.86
Powder, G	59.00	2	29.50	11.30	10.9	45.80	2.18
A×C	18.27	2	9.14	3.50			
A×G	52.74	4	13.18	5.05			
C×G	246.18	2	123.09	47.16	10.9	232.98	11.11
Error	15.66	6	2.61				
TOTAL	2097.50	26	80.67				
e-pooled	92.41	14	6.60			171.61	8.18

Table 4.3: Response table for means of MRR

Level	Workpiece	Dielectric	Electrode	Pulse off	Pulse on	Current	Powder
1	14.711	22.220	11.669	13.963	6.065	3.255	11.787
2	11.711	11.954	11.055	10.332	12.170	13.707	9.505
3	8.517			10.100	16.158	17.432	13.101
Delta	6.194	0.734	0.614	3.863	10.093	14.176	3.596
Rank	3	6	7	4	2	1	5

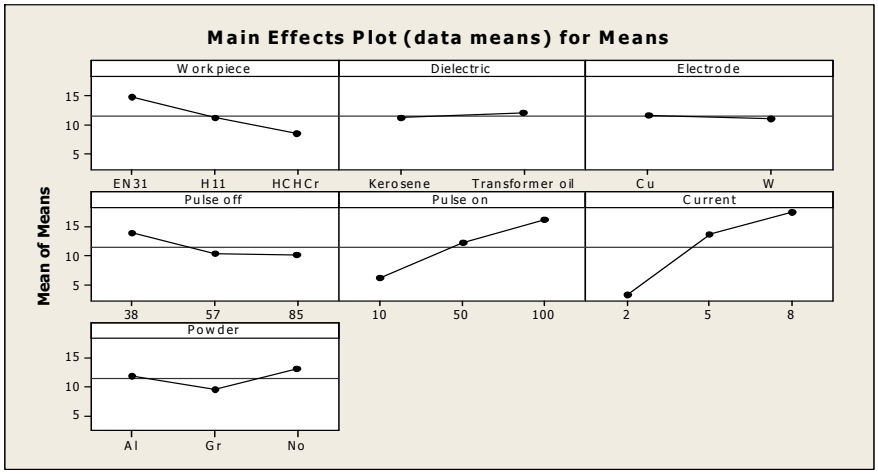

Figure 4.1: Main effects plot of MRR for Means

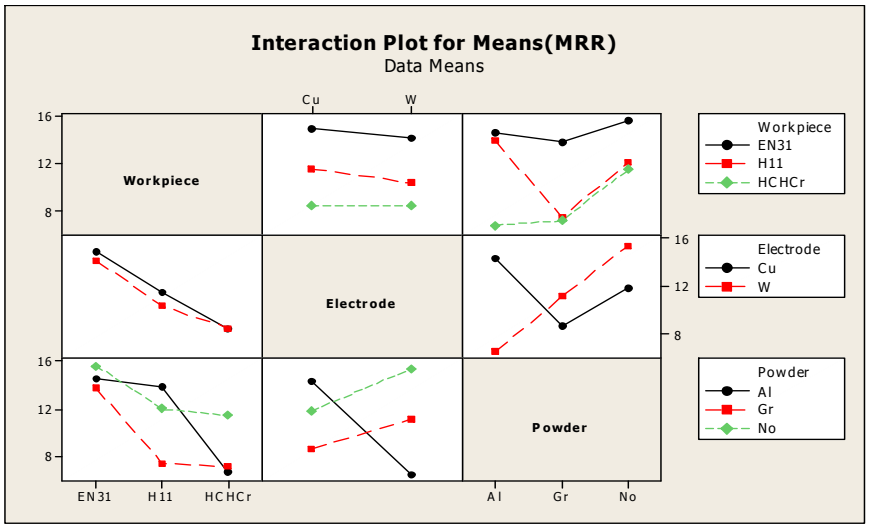

Figure 4.2: Interaction plot for MRR

4.4 RESULTS FOR S/N RATIO OF MRR

The S/N ratio consolidates several repetitions into one value and is an indication of the amount of variation present. The S/N ratios have been calculated to identify the major contributing factors and interactions that cause variation in the MRR. MRR is "Higher is better" type response which is given by:

$$(S/N)_{HB} = -10 \log (MSD_{HB}) \qquad \text{(Equation ....4.2)}$$

$$\text{Where } MSD_{HB} = \frac{1}{r}\sum_{j=1}^{r}\left(\frac{1}{y_j^{\,2}}\right) \qquad \text{(Equation ....4.3)}$$

MSD_{HB} = Mean Square Deviation for higher-the-better response.

Table 4.4 shows the ANOVA results for S/N ratio of MRR at 99% confidence interval. Current was observed to be the most significant factor affecting the MRR, followed by pulse on time, powder according to F test. All the interactions are insignificant. Main effects plot and interaction plot of S/N ratio for MRR are shown in the figure 4.3 and 4.4 respectively.

Table 4.4: ANOVA for S/N ratio of MRR

Sources	SS	v	V	F	F (Critical)	SS'	% contribution
Workpiece, A	150.44	2	75.22	6.14			
Dielectric, B	68.78	1	68.78	5.61			
Electrode, C	13.56	1	13.56	1.11			
Pulse off, D	141.79	2	70.89	5.78			
Pulse on, E	440.77	2	220.38	17.98	10.9	368.57	13.34
Current, F	1258.87	2	629.44	51.36	10.9	1186.67	42.96
Powder, G	340.85	2	170.43	13.91	10.9	268.65	9.72
A×C	107.79	2	53.90	4.40			
A×G	42.44	4	10.61	0.87			
C×G	123.66	2	61.83	5.04			
Error	73.53	6	12.26				
TOTAL	2762.50	26	106.25				
e-pooled	722.01	20	36.10			938.61	33.98

Table 4.5: Response table for S/N ratio of MRR

Level	Workpiece	Dielectric	Electrode	Pulse off	Pulse on	Current	Powder
1	18.923	15.872	17.502	20.215	11.560	7.362	17.966
2	18.403	19.258	15.998	15.755	18.210	22.326	12.248
3	13.676			15.033	21.233	21.314	20.789
Delta	5.247	3.386	1.504	5.182	9.673	14.965	8.541
Rank	4	6	7	5	2	1	3

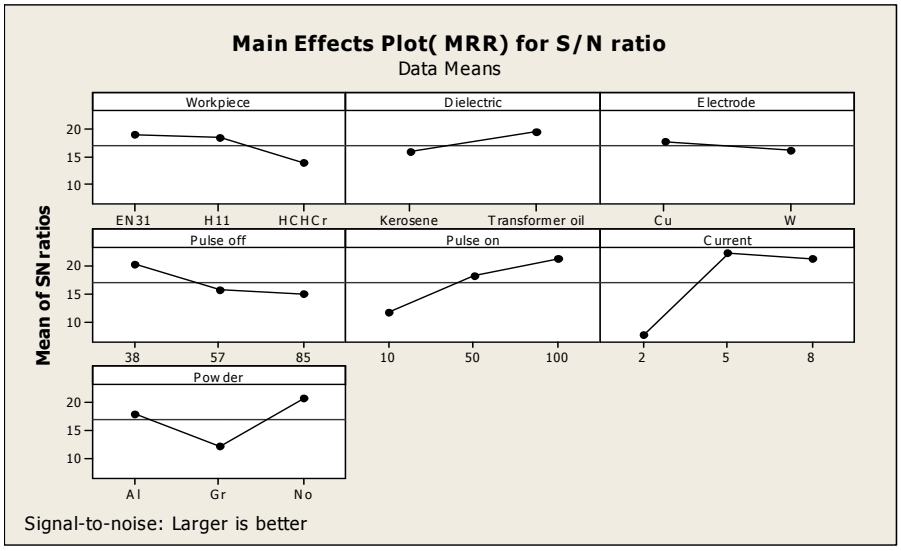

Figure 4.3: Main effects plot for MRR of S/N ratio

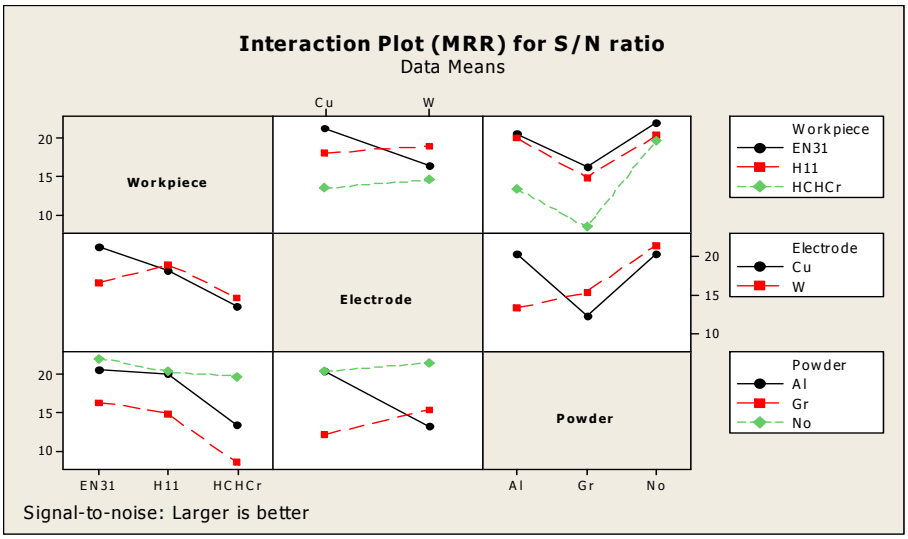

Figure 4.4: Interaction plot for MRR of S/N ratio

4.5 OPTIMAL DESIGN FOR MRR

The same level of all the significant factors provide a higher mean value and reduced variability so nothing has to be compromised. The level of factors which improves average and uniformity may conflict, so a compromise may have to be reached. Also a compromise has to occur when multiple responses are considered and the same factor level may cause one response to improve and other to deteriorate [33].

In this experimental analysis, the main effect plot and interaction plot in Figure 4.1 and Figure 4.2 used to estimate the mean MRR. From the, Table 4.6 it is concluded that highest MRR was observed when EN-31 was machined at pulse off time 38µs, current 5Amp pulse on time 100 µs, current 8Amp. In S/N ratio highest MRR was observed when workpiece material was machined at pulse on time 100 µs, current 5Amp without powder mixing. It is observed that current at 5Amp has optimal value for higher MRR because it decreases variation. Also, it was observed that there was interaction between electrode and powder affects MRR .The results were conflicting according to their relative significance .The best MRR value was compromised to get best result. MRR assumed to be achieved best result if EN-31workpicee is machined at pulse on time100 µs, pulse off time 38µs, current 5Amp with copper-tungsten electrode and aluminium powder mixing in dielectric.

Table 4.6: Significant factors and interactions

Factor	Affecting mean		Affecting variation	
	Contribution	Best level	Contribution	Best level
Workpiece, *A*	significant	Level-1(EN-31)	insignificant	-
Dielectric, *B*	insignificant	-	insignificant	-
Electrode, C	insignificant	-	insignificant	-
Pulse off, *D*	significant	Level-1(38 µs)	insignificant	-
Pulse on, *E*	significant	Level-3(100 µs)	significant	Level-3(100 µs)
Current, *F*	significant	Level-3 (8Amp)	significant	Level-2 (5Amp)
Powder, G	significant	Level-1(no powder)	significant	Level-1(no powder)
A×C	insignificant	-	insignificant	-
A×G	insignificant	-	insignificant	-
C×G	significant	C_3G_3	insignificant	-

Estimating the mean

In experimental analysis, the MRR is a higher average response is better (HB) characteristic. Depending on the characteristic, different treatment combinations has chosen to obtain satisfactory results. After conducting the experiments the optimum treatment condition within the experiments determined on the basis of prescribed combination of factor levels is determined to one of those in the experiment [33].

Mean value for MRR

$$\mu_{A_1 D_1 E_3 F_2 G_3} = \overline{C_3 G_3} + \overline{A_1} + \overline{D_1} + \overline{E_3} + \overline{F_2} - 4\overline{T}$$

$$= 15.65 + 14.709 + 13.96 + 16.15 + 13.70 - 4 * 11.46 = 28.32 \text{ mm}^3/\text{min}$$

Confidence Interval around the Estimated Mean

The confidence interval is a maximum and minimum value between which the true average should fall at some stated percentage of confidence. The estimate of the mean µ is only a point estimate based on the averages of results obtained from the experiment. Statistically this provides a 50% chance of the true averages being greater than µ and a 50% chance of the true average being less than µ [33].

Confidence Interval around the estimated MRR mean

$$CI_1 = \sqrt{\frac{F_{\alpha,v_1,v_2} V_e}{n_{eff}}}$$

Where $F_{\alpha v_1 v_2} = F\ ratio$

$\alpha = risk\ (0.01)$ $\quad confidence = 1 - \alpha$

$v_1 = dof\ for\ mean\ which\ is\ always = 1$

$v_2 = dof\ for\ error = v_e$

n_{eff} = Number of tests under that condition using the participating factors

$$n_{eff} = \frac{N}{1 + dof_{A,D,E,F,CG}} = \frac{27}{1+2+2+2+2+2} = 2.45$$

$$CI_1 = \sqrt{\frac{F_{\alpha,v_1,v_2} V_e}{n_{eff}}} = \sqrt{\frac{0.14 \times 6.60}{2.45}} = 0.37$$

So the confidence interval around the MRR is given by 28.32±0.37mm^3/min.

CHAPTER 5

RESULTS AND ANALYSIS OF TWR

5.1 INTRODUCTION

The effects of parameters i.e. workpiece, dielectric, electrode, pulse on time, pulse off time, current, powder and some of their interactions were evaluated using ANOVA and factorial design analysis. A confidence interval of 99% has been used for the analysis. One repetition for each of 27 trails was completed to measure the Signal to Noise ratio(S/N Ratio).

5.2 RESULTS FOR TWR

The results for TWR for each of the 27 treatment conditions with repetition are given in Table 5.1. The TWR is calculated from the loss in length in electrode during performance trial:

$$\text{TWR} = \frac{A \times L}{\text{t}} \ \text{mm}^3/\text{min} \qquad \text{(Equation 5.1)}$$

Where A = front area of electrode (mm^2)

L = Loss in length of electrode (mm)

t = time period of trial (minutes)

Table 5.1: Results for TWR

Trial no.	Work-piece	Dielectric	Electrode	Pulse off	Pulse on	Current	Powder	TWR mm^3/min		Mean TWR mm^3/min	S/N ratio
								I	II		
1	EN31	Kerosene	Cu	38	10	2	No	0.22	0.21	0.21	13.39
2	EN31	Transformer oil	Cu	57	50	5	Gr	1.12	1.13	1.13	-1.05
3	EN31	Kerosene**	Cu	85	100	8	Al	1.95	1.72	1.83	-5.28
4	EN31	Transformer oil	W	57	100	8	No	2.19	2.10	2.15	-6.63
5	EN31	Kerosene**	W	85	10	2	Gr	0.30	0.32	0.31	10.05
6	EN31	Kerosene	W	38	50	5	Al	0.72	0.74	0.74	2.66
7	EN31	Kerosene**	Cu**	85	50	5	No	1.29	1.33	1.31	-2.35

8	EN31	Kerosene	Cu**	38	100	8	Gr	1.50	1.61	1.55	-3.84
9	EN31	Transformer oil	Cu**	57	10	2	Al	0.20	0.21	0.21	13.64
10	H11	Transformer oil	Cu	85	50	8	No	1.74	1.82	1.78	-5.01
11	H11	Kerosene**	Cu	38	100	2	Gr	0.33	0.34	0.34	9.42
12	H11	Kerosene	Cu	57	10	5	Al	0.77	0.79	0.78	2.18
13	H11	Kerosene**	W	38	10	5	No	1.05	1.06	1.06	-0.48
14	H11	Kerosene	W	57	50	8	Gr	1.43	1.48	1.46	-3.27
15	H11	Transformer oil	W	85	100	2	Al	0.52	0.53	0.52	5.63
16	H11	Kerosene	Cu**	57	100	2	No	1.12	1.13	1.12	-1.02
17	H11	Transformer oil	Cu**	85	10	5	Gr	1.21	1.23	1.22	-1.75
18	H11	Kerosene**	Cu**	38	50	8	Al	1.91	1.91	1.91	-5.63
19	HCHCr	Kerosene**	Cu	57	100	5	No	1.73	1.74	1.73	-4.79
20	HCHCr	Kerosene	Cu	85	10	8	Gr	1.45	1.46	1.46	-3.26
21	HCHCr	Transforme	Cu	38	50	2	Al	0.38	0.39	0.39	8.22
22	HCHCr	Kerosene	W	85	50	2	No	0.20	0.22	0.21	13.46
23	HCHCr	Transformer oil	W	38	100	5	Gr	0.80	0.77	0.78	2.06
24	HCHCr	Kerosene**	W	57	10	8	Al	1.03	1.04	1.03	-0.31
25	HCHCr	Transformer oil	Cu**	38	10	8	No	2.09	2.09	2.10	-6.44
26	HCHCr	Kerosene**	Cu**	57	50	2	Gr	0.26	0.25	0.26	11.83
27	HCHCr	Kerosene	Cu**	85	100	5	Al	1.35	1.36	1.35	-2.65

** Dummy treated factor

5.3 ANALYSIS OF VARIANCE - TWR

The results for TWR were analyzed using ANOVA for identifying the significant factors affecting the performance measures. The Analysis of Variance (ANOVA) for the mean TWR at 99% confidence interval is given in Table 5.2. The variance data for each factor and their interactions were F-tested to find significance of each. ANOVA table shows that current (F value 149.06), powder (F value 13.39), electrode (F value 12.54) factors that affects the TWR. All remaining factors and the interactions are insignificant to affect TWR. It is observed that the current is the most significant factor which contributes TWR followed by powder and electrode. Main effects plot for TWR are shown in the Figure 5.1 that shows TWR increases with increase in current from 2 Amp to 8 Amp and also

increases with increase in pulse on time from 50µs to 100µs. Electrode wear in tungsten-copper electrode as comparison to copper electrode is much less. TWR decreases with powder mixing in dielectric. The interaction plots have shown in the Figure 5.2 shows that none of interaction is significant for the TWR. Table 5.3 shows ranks to various factors; current has highest rank, most significant that affecting TWR. The workpiece material, pulse off time and dielectric are least significant in TWR.

Table 5.2: ANOVA for TWR

Sources	SS	v	V	F	F (Critical)	SS'	% contribution
Workpiece, A	0.05	2	0.02	0.95			
Dielectric, B	0.07	1	0.07	2.56			
Electrode, C	0.32	1	0.32	12.54	13.7	0.25	2.43
Pulse off, D	0.05	2	0.03	1.07			
Pulse on, E	0.54	2	0.27	10.59			
Current, F	7.64	2	3.82	149.06	10.9	7.49	73.55
Powder, G	0.69	2	0.34	13.39	10.9	0.54	5.30
A×C	0.53	2	0.26	10.29			
A×G	0.08	4	0.02	0.74			
C×G	0.07	2	0.04	1.37			
Error	0.15	6	0.03				
TOTAL	10.18	26	0.39				
e-pooled	1.54	21	0.07			1.91	18.72

Table 5.3: Response table for means of TWR

Level	Workpiece	Dielectric	Electrode	Pulse off	Pulse on	Current	Powder
1	1.0497	1.0380	1.1499	1.0097	0.9317	0.3974	0.9746
2	1.1326	1.1424	0.9187	1.0964	1.0201	1.1239	0.9463
3	1.0362			1.1123	1.2667	1.6971	1.2976
Delta	0.0963	0.1044	0.2312	0.1027	0.3350	1.2997	0.3512
Rank	7	5	4	6	3	1	2

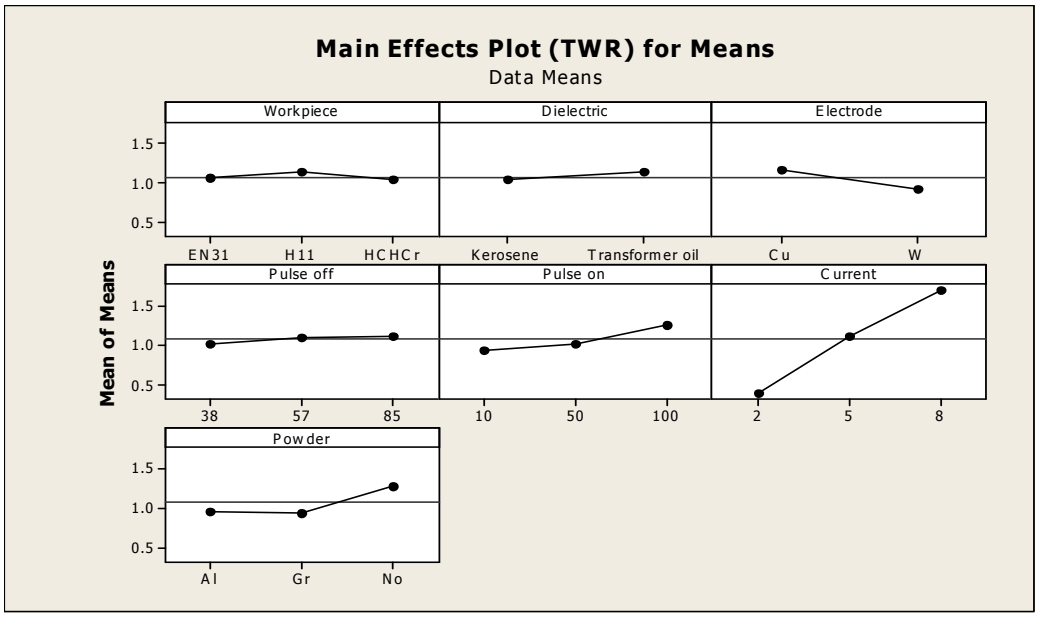

Figure 5.1: Main effects plot for TWR

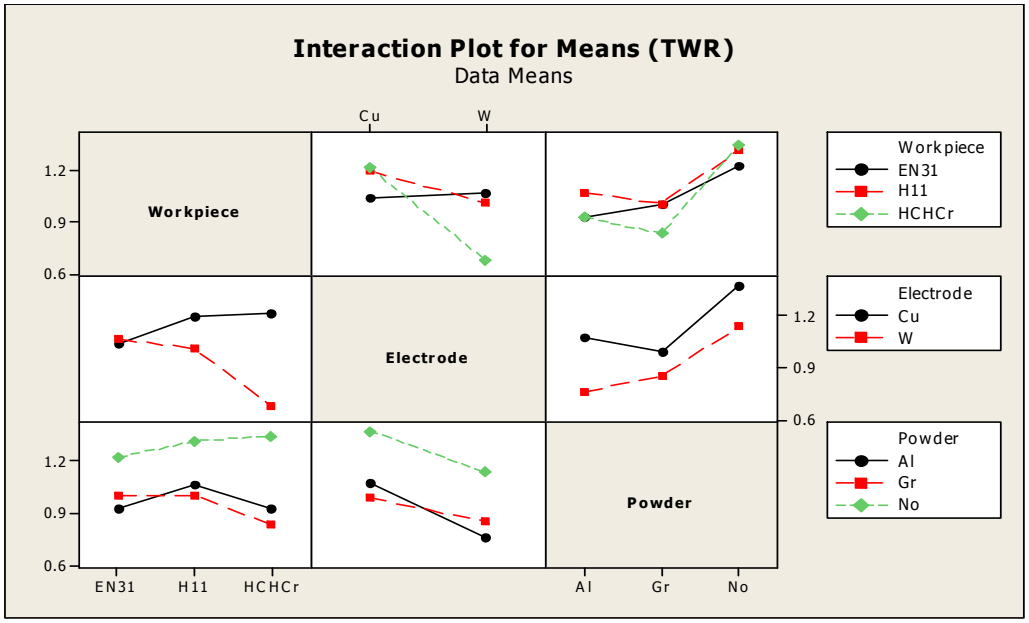

Figure 5.2: Interaction plot for TWR

5.4 ANOVA FOR S/N RATIO FOR TWR

The S/N ratio consolidates several repetitions into one value and is an indication of the amount of variation present. The S/N ratios have been calculated to identify the major contributing factors and interactions that cause variation in the TWR. TWR is 'Lower is better' type response which is given by:

$$S/N_{LB} = -10\log(MSD) = -10\log[(\frac{1}{r}\sum_{i=1}^{r} y^2{}_i) \quad \text{(Equation ....5.2)}$$

$$\text{Where } MSD_{LB} = \frac{1}{r}\sum_{j=1}^{r}\left(y_j{}^2\right) \quad \text{(Equation ....5.3)}$$

Table 5.4 shows the ANOVA for S/N ratio for TWR at 99% confidence interval. The current is the most significant in affecting TWR followed by pulse on time, electrode according to F test. The interaction between workpiece and electrode also affects TWR. Main effect plot and interaction plot of S/N ratios for TWR are shown in the Figure 5.3 and figure 5.4 respectively.

Table 5.4: ANOVA for S/N of TWR

Sources	SS	v	V	F	F (Critical)	SS'	% contribution
Workpiece, A	27.91	2	13.96	8.77			
Dielectric, B	3.02	1	3.02	1.89			
Electrode, C	17.56	1	17.56	11.03	13.7	11.30	0.95
Pulse off, D	7.08	2	3.54	2.22			
Pulse on, E	70.53	2	35.27	22.15	10.9	58.02	4.90
Current, F	919.52	2	459.76	288.77	10.9	907.00	76.63
Powder, G	27.46	2	13.73	8.62			
A×C	57.15	2	28.57	17.95	10.9	44.64	3.77
A×G	15.46	4	3.86	2.43			
C×G	28.39	2	14.19	8.91			
Error	9.55	6	1.59				
TOTAL	1183.61	26	45.52				
e-pooled	118.86	19	6.26			162.65	13.74

Table 5.5 Response table for S/N ratio of TWR

Level	Workpiece	Dielectric	Electrode	Pulse off	Pulse on	Current	Powder
1	2.28664	1.67326	0.86671	2.15221	3.00229	9.40506	2.05149
2	0.00744	0.96416	2.57726	1.17651	2.09663	-0.68561	2.24405
3	2.01660			0.98197	-0.78824	-4.40877	0.01515
Delta	2.27920	0.70909	1.71055	1.17024	3.79052	13.81382	2.22890
Rank	3	7	5	6	2	1	4

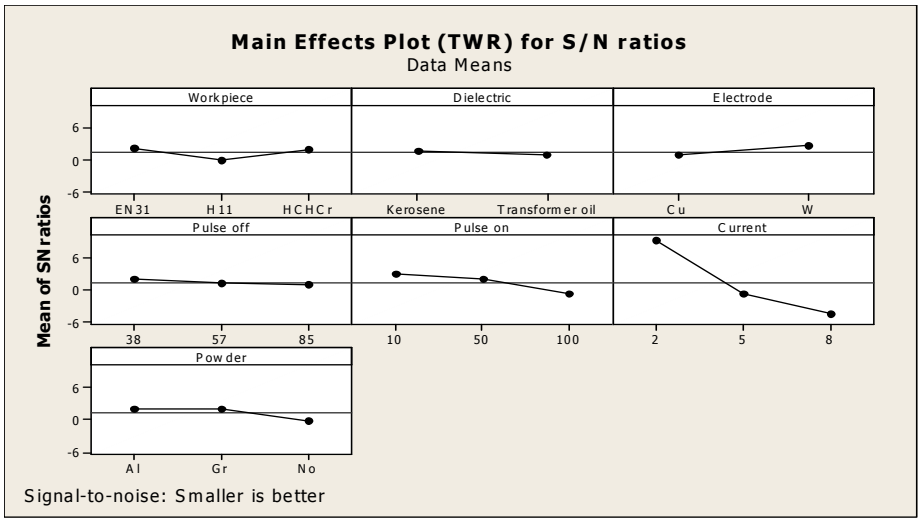

Figure 5.3 Main effects plot of TWR for S/N ratio

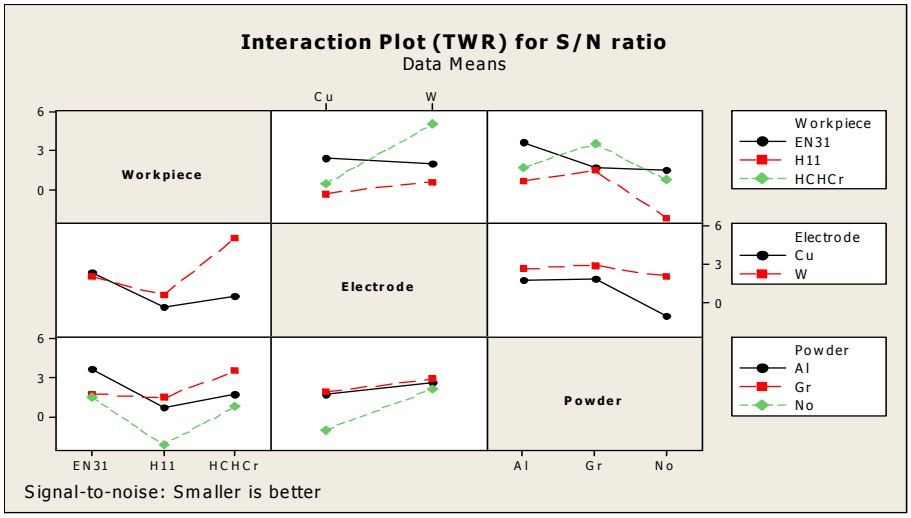

Figure 5.4 Interaction plot of TWR for S/N ratio

5.5 OPTIMAL DESIGN FOR TWR

In this experimental analysis, the main effect plot and interaction plot in Figure 5.1 and Figure 5.2 used to estimate the mean TWR. From the, Table 5.6 it is concluded that the lowest TWR was to be observed when workpiece was machined with tungsten-copper at current 8Amp without powder mixing. In S/N ratio highest TWR was to be observed when workpiece material was machined with tungsten-copper electrode at pulse on time 10 µs and current 2Amp. The level of factors which improves average and uniformity were conflicting, so a compromise may have to be reached. So, best value of TWR was suggested if EN31 workpiece machined at current 2 Amp and pulse on time10 µsec with tungsten-copper electrode without powder mixing in dielectric.

Table 5.6 Significant factors and interactions

Factors	Affecting mean		Affecting variation (S/N ratio)	
	Contribution	Best level	Contribution	Best level
Workpiece (A)	insignificant	-	insignificant	-
Dielectric (B)	insignificant	-	insignificant	-
Electrode (C)	significant	Level-2(W-Cu)	significant	Level-2 (W-Cu)
Pulse off (D)	insignificant	-	insignificant	-
Pulse on (E)	insignificant	-	significant	Level-1(10µs)
Current (F)	significant	Level-3 (8Amp)	significant	Level-1(2Amp)
Powder (G)	significant	Level-1(no powder)	insignificant	-
(A × C)	insignificant	-	significant	A_1C_2
(A × G)	insignificant	-	insignificant	-
(C × G)	insignificant	-	insignificant	-

Estimating the mean foe TWR

In experimental analysis, the TWR is a lower average response is better (LB) characteristic. Depending on the characteristic, different treatment combinations has chosen to obtain satisfactory results. After conducting the experiments the optimum treatment condition within the experiments determined on the basis of prescribed combination of factor levels was determined to one of those in the experiment [33].

Mean value for TWR

$\mu_{A_1E_1F_1C_2G_1} = \overline{A_1C_2} + \overline{E_1} + \overline{F_1} + \overline{G_1} - 3\overline{T} = 1.065+0.397+1.697+1.297-3*1.073=1.237$ mm^3/min

Confidence Interval around the Estimated Mean

The confidence interval is a maximum and minimum value between which the true average should fall at some stated percentage of confidence.

Confidence Interval around the estimated TWR mean

$$CI_1 = \sqrt{\frac{F_{\alpha,v_1,v_2} V_e}{n_{eff}}}$$

Where $F_{\alpha v_1 v_2} = F\ ratio$

$\alpha = risk\ (0.01)$ $\quad confidence = 1-\alpha$

$v_1 = dof\ for\ mean\ which\ is\ always = 1$

$v_2 = dof\ for\ error = v_e$

$n_{eff} =$ Number of tests under that condition using the participating factors

$$n_{eff} = \frac{N}{1 + dof_{AC,E,F,G}} = \frac{27}{1+2+2+2+2} = 3$$

$$CI_1 = \sqrt{\frac{F_{\alpha,v_1,v_2} V_e}{n_{eff}}} = \sqrt{\frac{0.21 \times 0.07}{3}} = 0.07$$

So the confidence interval around the TWR is given by 1.237 ± 0.07mm^3/min.

CHAPTER 6

RESULTS AND ANALYSIS OF MICRO HARDNESS

6.1 INTRODUCTION

The effects of parameters i.e. workpiece, dielectric, electrode, pulse on time, pulse off time, current, powder and some of their interactions were evaluated using ANOVA and factorial design analysis. A confidence interval of 99% has been used for the analysis. One repetition for each of 27 trails was completed to measure the Signal to Noise ratio(S/N Ratio).

6.2 RESULTS FOR MICRO HARDNESS OF NON-DEPOSITED REGION

The micro hardness measurement is dependent on the diameter of indentation on the samples. The indents formed in the pyramid shaped indenter were measured with Quantimet software using a load of 1 kg for 20 seconds. The micro hardness was measured at deposition as well as non deposition region. The results for micro hardness at non deposited region for each of the 27 treatment conditions with repetition are shown in Table 6.1.

Table 6.1: Results for micro hardness at non-deposited yellow region

Trial no.	Worpiece	Dielectric	Electrode	Pulse off	Pulse on	Current	Powder	Micro hardness		Mean Micro hardness	SN ratio Micro hardness
								I	II		
1	EN31	Kerosene	Cu	38	10	2	No	826	868	847	58.54
2	EN31	Transformer oil	Cu	57	50	5	Gr	876	942	909	59.15
3	EN31	Kerosene**	Cu	85	100	8	Al	956	924	940	59.45
4	EN31	Transformer oil	W	57	100	8	No	938	886	912	59.18
5	EN31	Kerosene**	W	85	10	2	Gr	798	816	807	58.13
6	EN31	Kerosene	W	38	50	5	Al	926	898	912	59.19
7	EN31	Kerosene**	Cu**	85	50	5	No	873	861	867	58.75
8	EN31	Kerosene	Cu**	38	100	8	Gr	883	914	898	59.06
9	EN31	Transformer oil	Cu**	57	10	2	Al	775	816	796	58.00
10	H11	Transformer oil	Cu	85	50	8	No	756	797	777	57.79
11	H11	Kerosene**	Cu	38	100	2	Gr	894	931	912	59.19
12	H11	Kerosene	Cu	57	10	5	Al	818	810	814	58.21

13	H11	Kerosene**	W	38	10	5	No	758	728	743	57.41
14	H11	Kerosene	W	57	50	8	Gr	877	916	896	59.04
15	H11	Transformer oil	W	85	100	2	Al	814	757	786	57.88
16	H11	Kerosene	Cu**	57	100	2	No	787	722	754	57.5
17	H11	Transformer oil	Cu**	85	10	5	Gr	821	889	855	58.61
18	H11	Kerosene**	Cu**	38	50	8	Al	935	920	928	59.34
19	HCHCr	Kerosene**	Cu	57	100	5	No	770	741	755	57.55
20	HCHCr	Kerosene	Cu	85	10	8	Gr	799	813	806	58.12
21	HCHCr	Transformer oil	Cu	38	50	2	Al	913	879	896	59.04
22	HCHCr	Kerosene	W	85	50	2	No	746	772	759	57.60
23	HCHCr	Transformer oil	W	38	100	5	Gr	836	835	836	58.43
24	HCHCr	Kerosene**	W	57	10	8	Al	847	855	851	58.59
25	HCHCr	Transformer oil	Cu**	38	10	8	No	771	790	781	57.84
26	HCHCr	Kerosene**	Cu**	57	50	2	Gr	822	806	814	58.21
27	HCHCr	Kerosene	Cu**	85	100	5	Al	829	791	810	58.16

** dummy treated factor

6.3 ANALYSIS OF VARIANCE - MICRO HARDNESS AT NON-DEPOSITED REGION

ANOVA Table 6.2 shows that powder is the most significant factor which is affecting the micro hardness. Table 6.3 shows relative ranks of various input parameters according to significance. The workpiece and powder are most significant according to their ranks. The interaction between workpiece and powder is significant for the micro hardness at non deposited region. Main effect plots had shown in the Figure 6.1 shows that micro hardness has increased with addition of powder in dielectric medium. The micro hardness increased with increase in current. The interaction plot for micro hardness is shown in Figure 6.2.

Table 6.2: ANOVA for micro hardness at non-deposited yellow region

Sources	SS	v	V	F	F (Critical)	SS'	% contribution
Workpiece, A	3969.21	2	1984.60	5.65			
Dielectric, B	8.53	1	8.53	0.02			
Electrode, C	453.97	1	453.97	1.29			
Pulse off, D	7155.70	2	3577.85	10.19			
Pulse on, E	12135.79	2	6067.90	17.27	10.9	9618.08	11.99
Current, F	10164.84	2	5082.42	14.47	10.9	7647.12	9.54

Powder, G	21314.18	2	10657.09	30.34	10.9	18796.47	23.44
A×C	3969.21	2	1984.60	5.65			
A×G	16432.58	4	4108.15	11.69	9.15	11397.16	14.21
C×G	2477.38	2	1238.69	3.53			
Error	2107.71	6	351.29				
TOTAL	80189.09	26	3084.20				
e-pooled	20141.70	16	1258.86			32730.26	40.82

Table 6.3: Response table for means of micro hardness at non-deposited yellow region

Level	Workpiece	Dielectric	Electrode	Pulse off	Pulse on	Current	Powder
1	876.4	839.7	842.2	861.4	811.0	819.0	859.1
2	829.4	838.4	833.5	833.6	861.9	833.4	859.3
3	811.9			822.9	844.9	865.4	799.4
Delta	64.5	1.3	8.7	38.5	50.9	46.4	59.9
Rank	1	7	6	5	3	4	2

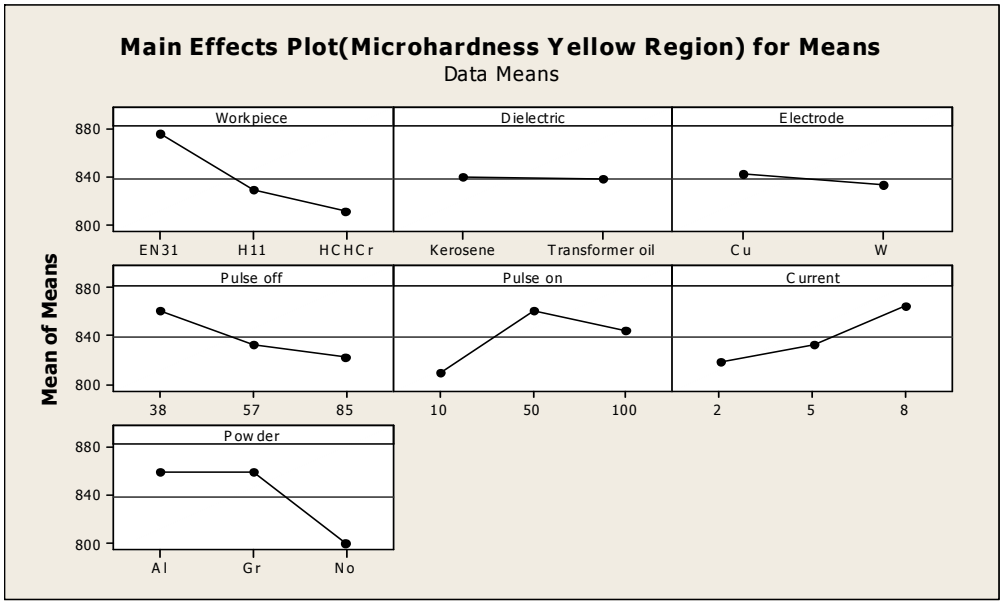

Figure 6.1: Main effect plot for micro hardness at non-deposited yellow region

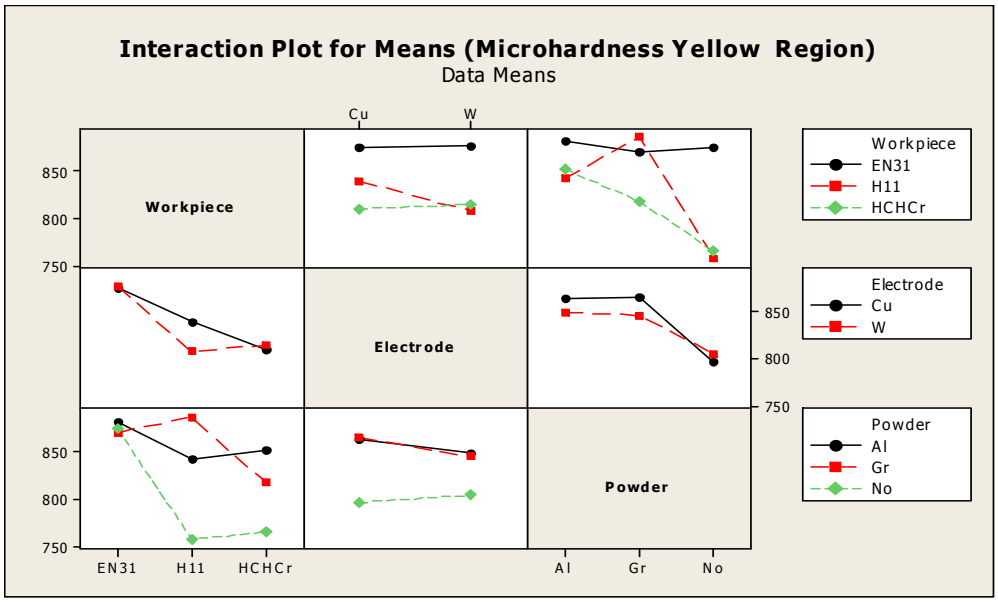

Figure 6.2: Interaction plot of means micro hardness at non- deposited yellow region

6.4 ANOVA FOR S/N RATIO OF MICROHARDNESS AT NON-DEPOSITED YELLOW REGION

Micro hardness is "Higher is better" type response, for which S/N ratio was calculated by using equation 4.2. Table 6.4 shows the ANOVA for S/N ratio for micro hardness at 99% confidence interval. Among all the factors current and powder have factors which are significant. Current has most significant which has highest contribution in micro hardness according to F value and percentage contribution. Among the interactions interaction between workpiece and powder is significant for micro hardness. Main effect plot and interaction plot of S/N ratio for micro hardness shown in the Figure 6.3 and Figure 6.4

Table 6.4: ANOVA of S/N ratio for micro hardness at non-deposited yellow region

Sources	SS	v	V	F	F (Critical)	SS'	% contribution
Workpiece, A	0.40	2	0.20	5.63			
Dielectric, B	0.00	1	0.00	0.03			
Electrode, C	0.05	1	0.05	1.38			
Pulse off, D	0.75	2	0.38	10.58			
Pulse on, E	1.23	2	0.62	17.32	10.9	1.02	
Current, F	1.08	2	0.54	15.19	10.9	0.87	10.10
Powder, G	2.41	2	1.21	33.97	10.9	2.21	25.54
A×C	0.40	2	0.20	5.63			

A×G	1.86	4	0.47	13.12	9.15	1.45	16.80
C×G	0.24	2	0.12	3.43			
Error	0.21	6	0.04				
TOTAL	8.65	26	0.33				
e-pooled	2.06	20	0.10			3.09	35.72

Table 6.5: Response table for S/N ratios of micro hardness at non-deposited yellow region

Level	Workpiece	Dielectric	Electrode	Pulse off	Pulse on	Current	Powder
1	58.83	58.45	58.48	58.68	58.17	58.24	58.66
2	58.34	58.44	58.39	58.39	58.68	58.39	58.67
3	58.18			58.28	58.50	58.72	58.03
Delta	0.66	0.01	0.09	0.40	0.52	0.48	0.64
Rank	1	7	6	5	3	4	2

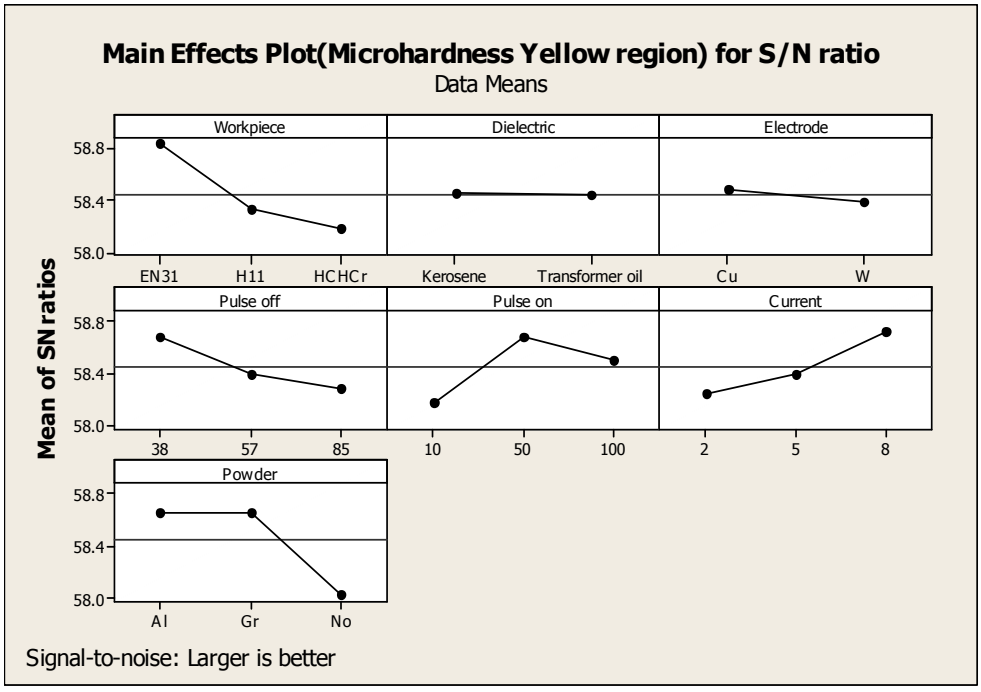

Figure 6.3: Main effects plot for S/N ratio of micro hardness at non-deposited yellow region

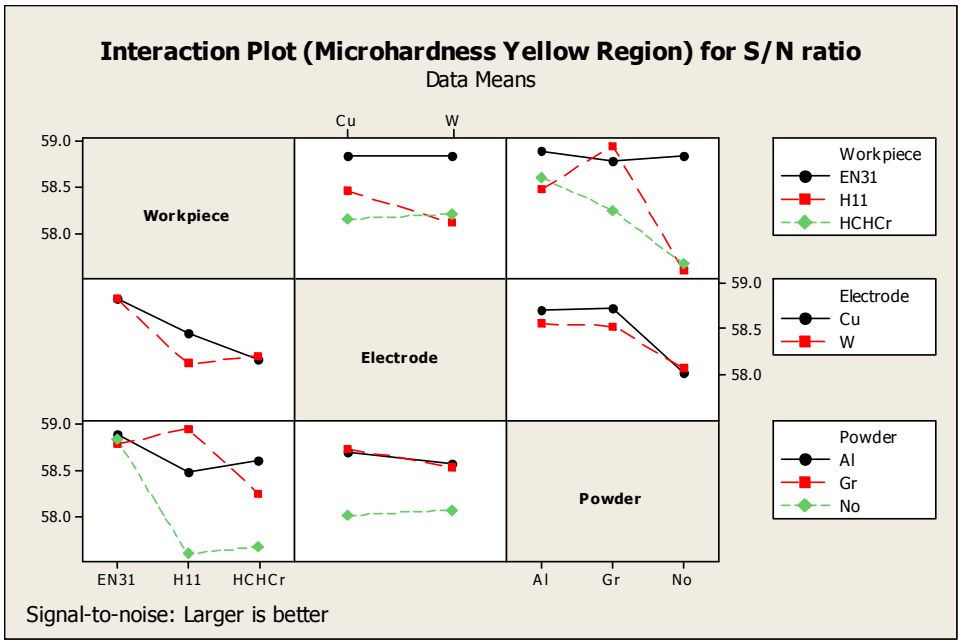

Figure 6.4: Interaction plot of S/N ratio for micro hardness at non- deposited yellow region

6.5 OPTIMAL DESIGN FOR MICRO HARDNESS OF NON-DEPOSITED REGION

In this experimental analysis, the main effect plot and interaction plot in Figure 6.1 and Figure 6.2 used to estimate the mean micro hardness. From Table 6.6 it is concluded that highest micro hardness was observed that when workpiece was machined at current 8Amp with pulse on time of 50 µs with graphite powder mixing. In S/N ratio highest micro harness was to be observed when workpiece material was machined with tungsten-copper electrode at current 8Amp with graphite powder mixing. So, to achieve higher micro hardness the best design was suggested that workpiece of H11 machined at pulse on time of 50 µsec and current at 8Amp in graphite mixed dielectric.

Table 6.6: significant factors and their interactions

Factor	Affecting mean		Affecting variation	
	Contribution	Best level	Contribution	Best level
Workpiece , *A*	insignificant	-	insignificant	-
Dielectric, *B*	insignificant	-	insignificant	-
Electrode, C	insignificant	-	insignificant	-
Pulse off , *D*	insignificant	-	insignificant	-
Pulse on, *E*	significant	Level-2(50µs)	insignificant	-

Current , *F*	significant	Level-3 (8Amp)	significant	Level-3(8Amp)
Powder, G	significant	Level-2(Gr powder)	significant	Level-2(Gr powder)
A×C	insignificant	-	insignificant	-
A×G	significant	A_2G_2	significant	A_2G_2
C×G	insignificant	-	insignificant	-

Estimating the mean for Micro Hardness

In experimental analysis, the micro hardness is a higher average response is better (HB) characteristic. Different treatment combinations have been chosen to get satisfactory results. After conducting the experiments the optimum treatment condition within the experiments determined on the basis of prescribed combination of factor levels is determined to one of those in the experiment.

Mean value for micro hardness (Yellow region)

$\mu_{E_2F_3A_2G_2} = \overline{E_2} + \overline{F_3} + \overline{A_2G_2} - 2\overline{T} = 862+865+887-2*921=772$ hvn .

Confidence Interval around the Estimated Mean Micro Hardness

Statistically confidence interval provides a 50% chance of the true averages being greater than μ and a 50% chance of the true average being less than μ.

$$CI_1 = \sqrt{\frac{F_{\alpha,v_1,v_2}V_e}{n_{eff}}} \quad \text{Where} \quad F_{\alpha v_1 v_2} = F\ ratio$$

$\alpha = risk$ (0.01) $\qquad confidence = 1-\alpha$

$v_1 = dof\ for mean which is always = 1$

$v_2 = dof\ for error = v_e$

n_{eff} = Number of tests under that condition using the participating factors

$$n_{eff} = \frac{N}{1+dof_{E,F,AG}} = \frac{27}{1+2+2+4} = 3$$

$$CI_1 = \sqrt{\frac{F_{\alpha,v_1,v_2}V_e}{n_{eff}}} = \sqrt{\frac{0.16\times1256.86}{3}} = 8.18$$

So the confidence interval around the micro hardness of non-deposited region is given by 772 ± 8.18 hvn.

6.6 RESULTS FOR MICRO HARDNESS OF DEPOSITED BLACK REGION

There was two deposited different region (black and red) has been seen during micro hardness experimentation. The results for micro hardness at deposited black region for each of the 27 treatment conditions with repetition are given in Table 6.7

Table 6.7: Results for Micro hardness at deposited black region

Trial no.	Work-piece	Dielectric	Elec-trode	Pul-se off	Puls e on	Cur-rent	Powder	Micro hardness		Mean Micro hardn ess	S/N Ratio
								I	II		
1	EN31	Kerosene	Cu	38	10	2	No	895	865	880	58.88
2	EN31	Transformer oil	Cu	57	50	5	Gr	1109	1071	1090	60.74
3	EN31	Kerosene**	Cu	85	100	8	Al	1026	1031	1028	60.24
4	EN31	Transformer oil	W	57	100	8	No	1033	1046	1033	60.34
5	EN31	Kerosene**	W	85	10	2	Gr	912	934	923	59.30
6	EN31	Kerosene	W	38	50	5	Al	997	950	973	59.76
7	EN31	Kerosene**	Cu**	85	50	5	No	973	921	947	59.52
8	EN31	Kerosene	Cu**	38	100	8	Gr	1014	1048	1134	63.37
9	EN31	Transformer oil	Cu**	57	10	2	Al	926	900	913	59.21
10	H11	Transformer oil	Cu	85	50	8	No	1079	1052	1065	60.55
11	H11	Kerosene**	Cu	38	100	2	Gr	981	939	960	59.64
12	H11	Kerosene	Cu	57	10	5	Al	1084	1065	1074	60.62
13	H11	Kerosene**	W	38	10	5	No	938	946	942	59.48
14	H11	Kerosene	W	57	50	8	Gr	1144	1056	1100	60.81
15	H11	Transformer oil	W	85	100	2	Al	947	917	932	59.38
16	H11	Kerosene	Cu**	57	100	2	No	906	862	884	58.92
17	H11	Transformer oil	Cu**	85	10	5	Gr	1036	1004	1020	60.17
18	H11	Kerosene**	Cu**	38	50	8	Al	1043	1063	1053	60.45
19	HCHCr	Kerosene**	Cu	57	100	5	No	945	938	941	59.48
20	HCHCr	Kerosene	Cu	85	10	8	Gr	1060	1046	1053	60.45
21	HCHCr	Transformer oil	Cu	38	50	2	Al	949	919	934	59.40
22	HCHCr	Kerosene	W	85	50	2	No	897	882	889	58.98
23	HCHCr	Transformer oil	W	38	100	5	Gr	1111	1101	1106	60.87
24	HCHCr	Kerosene**	W	57	10	8	Al	1061	1129	1090	60.77
25	HCHCr	Transformer oil	Cu**	38	10	8	No	1005	983	994	59.95
26	HCHCr	Kerosene**	Cu**	57	50	2	Gr	985	905	945	59.48
27	HCHCr	Kerosene	Cu**	85	100	5	Al	992	986	989	59.90

** dummy treated factor

6.7 ANALYSIS OF VARIANCE - MICRO HARDNESS AT DEPOSITED BLACK REGION

The results for micro hardness were analyzed using ANOVA for identifying the significant factors affecting the performance measures. The ANOVA for the mean micro hardness at 99% confidence interval is shown in Table 6.8. The variance data for each factor and their interactions were F-tested to find significance of each. ANOVA table shows that current (F value 117.13), powder (F value 39.25) are significant factors. The current (F value 117.13) has the highest F value is most significant factor. Table 6.9 shows ranks to various input parameters in terms their relative significance. The current is the most significant factor that affects micro hardness and dielectric has the least significant factor in micro hardness according to their rank. The interaction between workpiece × electrode is significant for the micro hardness at deposited region. Main effect plots had shown in the Figure 6.5 shows that micro hardness has increased with addition of graphite powder in dielectric medium. It is observed that micro hardness increases when current increases from 5Amp to 8 Amp. The micro hardness is more when machined with copper electrode than tungsten-copper electrode. The interaction plot for micro hardness is shown in Figure 6.6.

Table 6.8: ANOVA for micro hardness at deposited black region

Sources	SS	v	V	F	F (Critical)	SS'	% contribution
Workpiece, *A*	765.58	2	382.79	0.94			
Dielectric, *B*	2474.57	1	2474.57	6.10			
Electrode, C	97.72	1	97.72	0.24			
Pulse off, *D*	2833.59	2	1416.79	3.49			
Pulse on, *E*	936.84	2	468.42	1.15			
Current, *F*	94977.91	2	47488.95	117.13	10.9	93518.93	62.11
Powder, G	31833.69	2	15916.84	39.25	10.9	30374.71	20.17
A×C	9150.59	2	4575.29	11.28	10.9	7691.61	5.1
A×G	4407.68	4	1101.92	2.717			
C×G	641.23	2	320.61	0.79			
Error	2432.56	6	405.42				
TOTAL	150552.01	26	5790.46				
e-pooled	14589.81	20	729.49			18966.75	12.59

Table 6.9: Response table for mean of micro hardness of deposited black region

Level	Workpiece	Dielectric	Electrode	Pulse off	Pulse on	Current	Powder
1	1487.8	1237.4	1242.6	1493.1	988.3	917.8	999.2
2	1003.4	1010.4	1000.1	1009.2	999.7	1009.3	1532.5
3	994.1			983.1	1497.3	1558.2	953.7
Delta	493.7	227.0	242.6	510.1	509.1	640.4	578.8
Rank	5	7	6	3	4	1	2

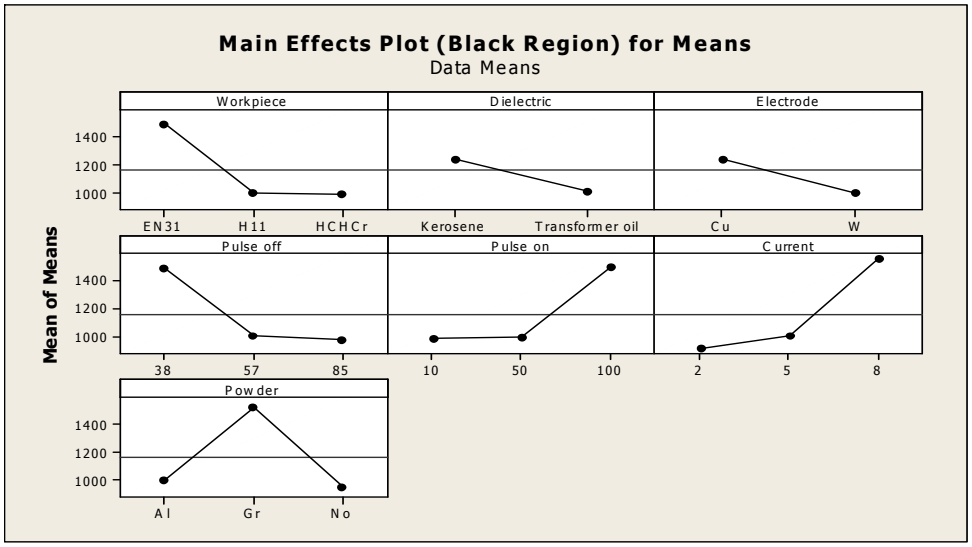

Figure 6.5: Main effect plot for micro hardness at deposited black region

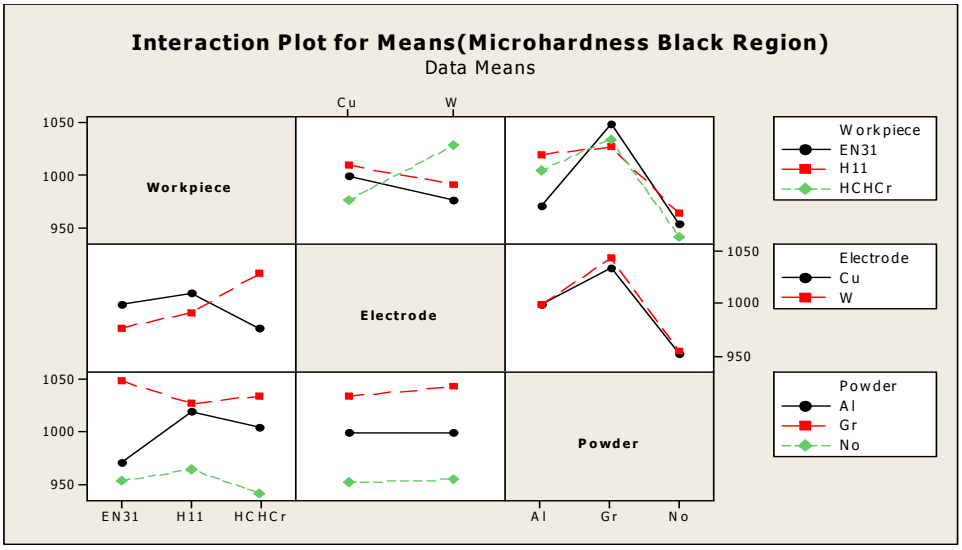

Figure 6.6: Interaction plot of micro hardness at deposited black region

6.8 ANOVA FOR S/N RATIO OF MICROHARDNESS AT DEPOSITED BLACK REGION

Table 6.10 shows the ANOVA for S/N ratio of micro hardness at 99% confidence interval. The current and powder are significant factors. Current has most significant which has highest contribution in micro hardness according to F test. All interactions are insignificant interactions for micro hardness. Main effect plot and interaction plot of S/N ratio for micro hardness shown in the Figure 6.7 and Figure 6.8.

Table 6.10: ANOVA for S/N ratio of micro hardness at deposited black region

Sources	SS	v	V	F	F (critical)	SS'	% contribution
Workpiece, *A*	0.25	2	0.12	1.10			
Dielectric, *B*	0.02	1	0.02	0.22			
Electrode, C	0.05	1	0.05	0.41			
Pulse off, *D*	0.61	2	0.31	2.75			
Pulse on, *E*	0.66	2	0.33	2.95			
Current, *F*	10.47	2	5.23	47.01	10.9	9.83	45.20
Powder, G	4.29	2	2.14	19.27	10.9	3.65	16.80
A×C	1.99	2	0.99	8.93			
A×G	1.71	4	0.43	3.84			
C×G	1.04	2	0.52	4.67			
Error	0.67	6	0.11				
TOTAL	21.75	26	0.84				
e-pooled	6.99	22	0.32			8.26	38.00

Table 6.11: Response table for S/N ratio of micro hardness at black region

Level	Workpiece	Dielectric	Electrode	Pulse off	Pulse on	Current	Powder
1	35.58	35.56	35.57	35.59	35.54	35.45	35.56
2	35.56	35.57	35.56	35.57	35.56	35.57	35.64
3	35.55			35.54	35.60	35.67	35.50
Delta	0.03	0.01	0.01	0.05	0.05	0.22	0.14
Rank	5	7	6	4	3	1	2

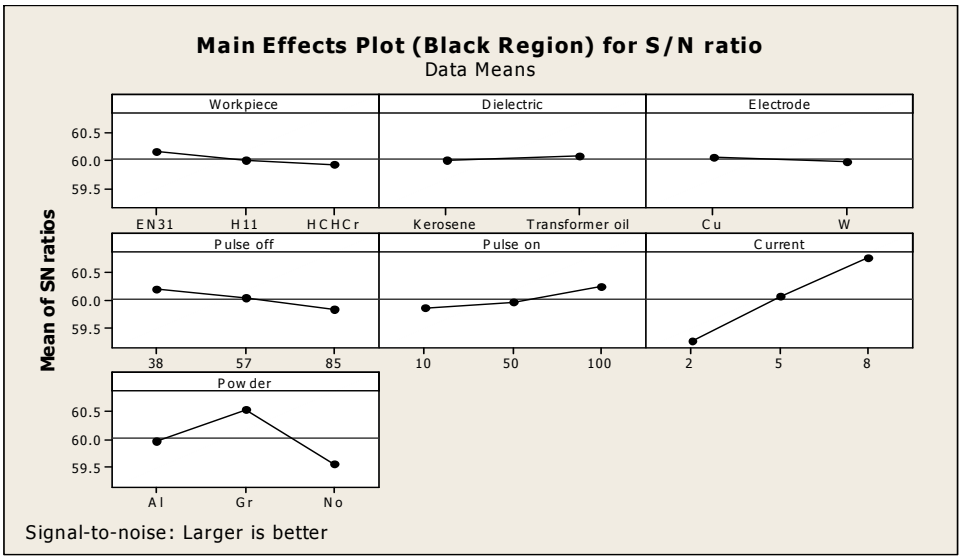

Figure 6.7: Main effects plot for S/N ratio of micro hardness at deposited black region

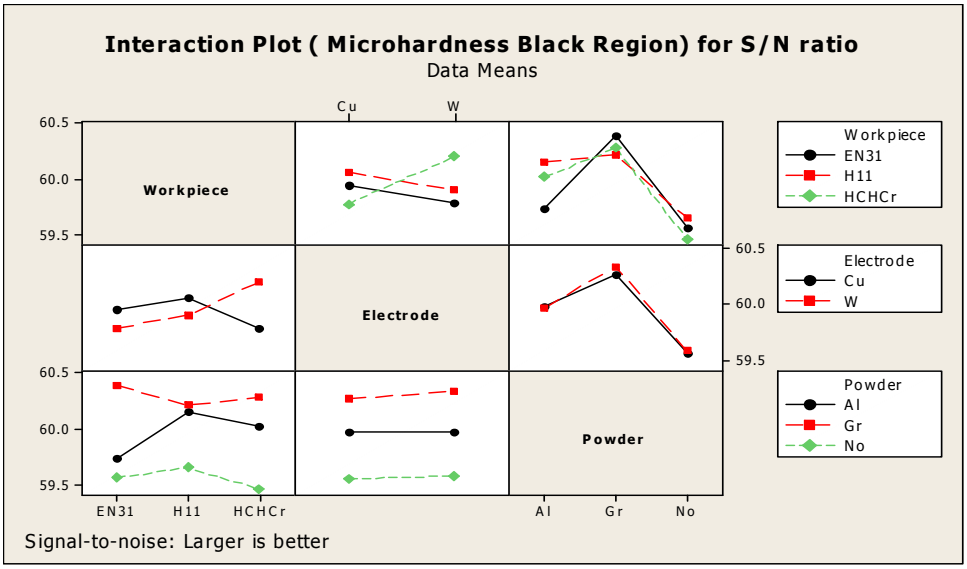

Figure 6.8: Interaction plot of S/N ratio for micro hardness at deposited black region

6.9 OPTIMAL DESIGN FOR MICRO HARDNESS FOR DEPOSITED REGION (BLACK REGION)

In this experimental analysis, the main effect plot and interaction plot in Figure 6.5 and Figure 6.6 used to estimate the mean micro hardness. From the, Table 6.12 it is concluded that highest micro hardness was to be observed when workpiece was machined at current 8Amp with graphite powder mixing. In S/N ratio highest micro hardness was to be

observed when workpiece material was machined with tungsten-copper electrode at current 2Amp with graphite. The interaction between workpiece has shown significant, so best micro hardness value was to be suggested if HCHCr workpiece should be machined with tungsten-copper electrode at current of 8Amp in graphite powder mixed dielectric.

Table 6.12: Significant factors and interactions

Factor	Affecting mean		Affecting variation	
	Contribution	Best level	Contribution	Best level
Workpiece , *A*	insignificant	-	insignificant	-
Dielectric, *B*	insignificant	-	insignificant	-
Electrode, C	insignificant	-	insignificant	-
Pulse off , *D*	insignificant	-	insignificant	-
Pulse on, *E*	insignificant	-	insignificant	-
Current , *F*	significant	Level-3 (8 Amp)	significant	Level-3(8Amp)
Powder, G	significant	Level-2(Gr powder)	significant	Level-2(Gr powder)
A×C	significant	A_3C_2	insignificant	-
A×G	insignificant	-	insignificant	-
C×G	insignificant	-	insignificant	-

Mean value for micro hardness (Black region)

$$\mu_{A_3C_2F_3G_2} = \overline{F_3} + \overline{G_2} + \overline{A_3C_2} - 2\overline{T} = 061+1036+1028-2*996=1133 \text{ hvn.}$$

Confidence Interval around the Estimated Mean

$$n_{eff} = \frac{N}{1 + dof_{F,G,AC}} = \frac{27}{1+2+2+2} = 3.857$$

$$CI_1 = \sqrt{\frac{F_{\alpha,v_1,v_2} V_e}{n_{eff}}} = \sqrt{\frac{0.2 \times 729.49}{3.857}} = 6.15$$

So the confidence interval around the micro hardness of non-deposited region is given by 1133 ± 6.15 hvn.

6.10 RESULTS FOR MICRO HARDNESS OF DEPOSITED RED REGION

The results for micro hardness at deposited red region for each of the 27 treatment conditions with repetition are shown in Table 6.13.

Table 6.13: Results for Micro hardness at deposited red region

Trial no.	Work-piece	Dielectric	Electrode	Pulse off	Pulse on	Cur-rent	Powder	Micro hardness		Mean Micro-hard-ness	SN ratio Micro-hardness
								I	II		
1	EN31	Kerosene	Cu	38	10	2	No	878	814	846	58.53
2	EN31	Transformer oil	Cu	57	50	5	Gr	1010	942	976	59.77
3	EN31	Kerosene**	Cu	85	100	8	Al	1005	963	984	59.85
4	EN31	Transformer oil	W	57	100	8	No	1042	1024	1033	60.28
5	EN31	Kerosene**	W	85	10	2	Gr	904	918	911	59.19
6	EN31	Kerosene	W	38	50	5	Al	904	943	923	59.30
7	EN31	Kerosene**	Cu**	85	50	5	No	877	857	867	58.76
8	EN31	Kerosene	Cu**	38	100	8	Gr	1055	1007	1031	60.26
9	EN31	Transformer oil	Cu**	57	10	2	Al	859	901	880	58.88
10	H11	Transformer oil	Cu	85	50	8	No	835	844	839	58.48
11	H11	Kerosene**	Cu	38	100	2	Gr	954	874	914	59.19
12	H11	Kerosene	Cu	57	10	5	Al	972	992	982	59.84
13	H11	Kerosene**	W	38	10	5	No	885	881	883	58.92
14	H11	Kerosene	W	57	50	8	Gr	966	1006	986	59.87
15	H11	Transformer oil	W	85	100	2	Al	884	893	888	58.97
16	H11	Kerosene	Cu**	57	100	2	No	845	849	847	58.56
17	H11	Transformer oil	Cu**	85	10	5	Gr	925	967	946	59.51
18	H11	Kerosene**	Cu**	38	50	8	Al	947	997	972	59.74
19	HCHCr	Kerosene**	Cu	57	100	5	No	884	858	871	58.79
20	HCHCr	Kerosene	Cu	85	10	8	Gr	878	836	857	58.65
21	HCHCr	Transformer oil	Cu	38	50	2	Al	845	827	836	58.44
22	HCHCr	Kerosene	W	85	50	2	No	833	887	860	58.68
23	HCHCr	Transformer oil	W	38	100	5	Gr	966	974	970	59.74

24	HCHCr	Kerosene**	W	57	10	8	Al	930	944	937	59.44
25	HCHCr	Transformer oil	Cu**	38	10	8	No	921	906	913	59.21
26	HCHCr	Kerosene**	Cu**	57	50	2	Gr	906	910	908	59.16
27	HCHCr	Kerosene	Cu**	85	100	5	Al	949	963	956	59.60

** dummy treated factor

6.11 ANALYSIS OF VARIANCE - MICRO HARDNESS AT DEPOSITED REGION (RED REGION)

The results for micro hardness were analyzed using ANOVA for identifying the significant factors affecting the performance measures. The Analysis of Variance (ANOVA) for the mean micro hardness at 99% confidence interval is shown in Table 6.14. ANOVA table shows that current (F value 108.8), powder (F value 54.9), workpiece (F value 38.6) and pulse on time (F value 16.6) are significant factors. It is observed current is the most significant factor. Table 6.15 shows ranks to various input parameters in terms their relative significance. The current is the most significant in micro hardness and dielectric is the least significant in micro hardness according to their relative ranks. The interaction between electrode and powder is significant for the micro hardness at deposited red region. Main effect plots had shown in the Figure 6.9 shows that micro hardness has increased with addition of graphite powder in dielectric medium. The micro hardness increased with increase in current and pulse on time. The micro hardness value is more with tungsten-copper electrode than copper electrode. The interaction plot for micro hardness had shown in Figure 6.10.

Table 6.14: ANOVA for micro hardness at deposited red region

Sources	SS	v	V	F	F (Critical)	SS'	% contribution
Workpiece, *A*	10166.9	2	5083.5	38.6	10.9	9372.5	12.0
Dielectric, *B*	179.8	1	179.8	1.4			
Electrode, C	329.8	1	329.8	2.5			
Pulse off, *D*	1378.4	2	689.2	5.2			
Pulse on, *E*	4379.7	2	2189.9	16.6	10.9	3585.3	4.6
Current, *F*	28639.5	2	14319.8	108.8	10.9	27845.0	35.8
Powder, G	14461.6	2	7230.8	54.9	10.9	13667.1	17.6

A×C	10166.9	2	5083.5	38.6	10.9	9372.5	12.0
A×G	2883.4	4	720.9	5.5			
C×G	4465.5	2	2232.7	17.0	10.9	3671.0	4.7
Error	789.8	6	131.6				
e-pooled	5561.2	14	397.2			10327.9	13.3
TOTAL	77841.4	26	2993.9				

Table 6.15: Response table for mean of micro hardness of deposited red region

Level	Workpiece	Dielectric	Electrode	Pulse off	Pulse on	Current	Powder
1	939.1	918.6	912.0	921.0	906.2	876.7	928.8
2	917.6	920.3	932.4	935.6	907.6	930.5	944.3
3	900.9			901.0	943.8	950.3	884.4
Delta	38.1	1.6	19.9	34.6	37.7	73.6	59.9
Rank	3	7	6	5	4	1	2

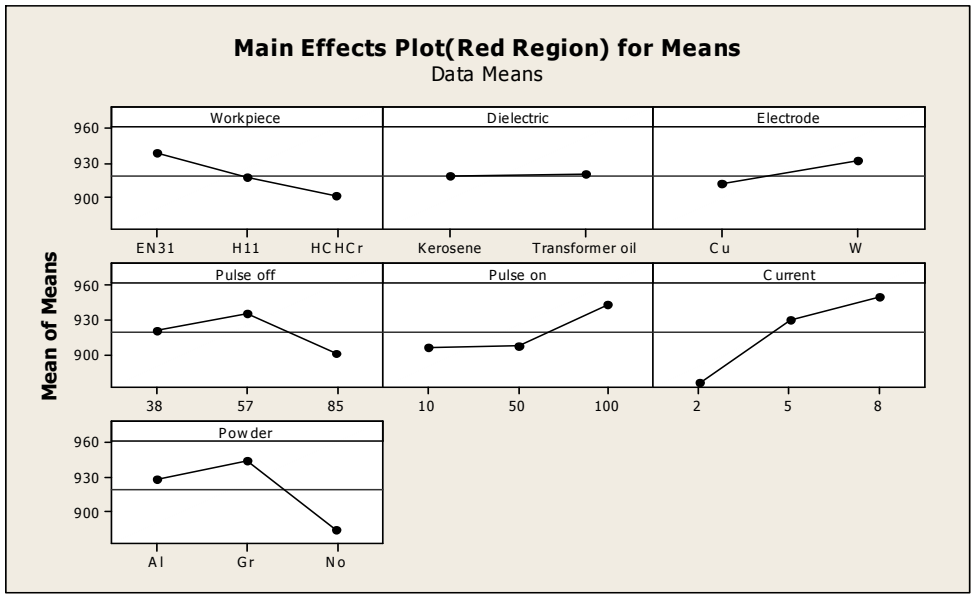

Figure 4.9: Main effect plot for micro hardness at deposited red region

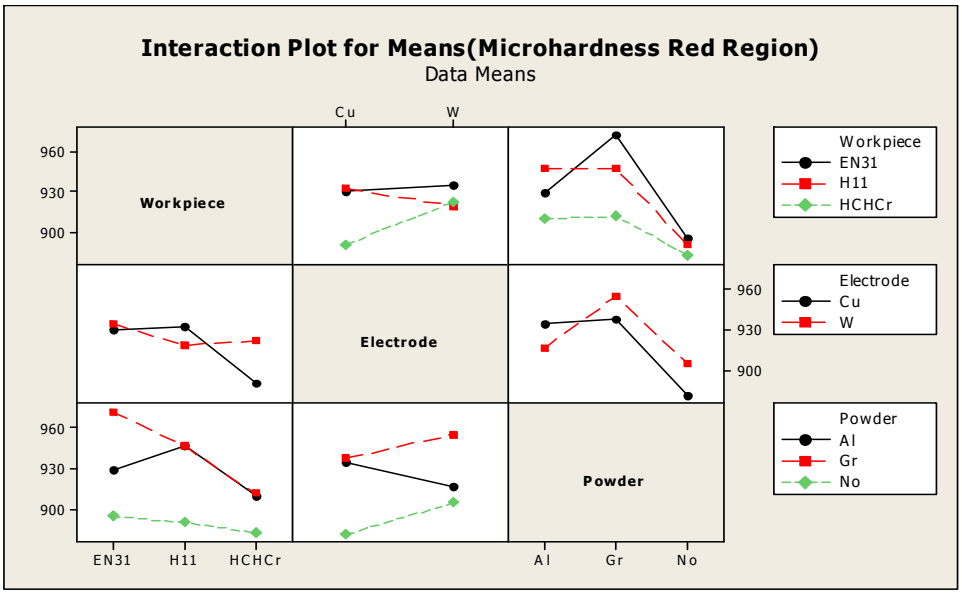

Figure 4.10: Interaction plot of means for micro hardness at deposited red region

6.12 ANOVA FOR S/N RATIO OF MICROHARDNESS AT DEPOSITED RED REGION

Table 6.16 shows the ANOVA for S/N ratio for micro hardness at 99% confidence interval. Among all the factors current and powder have factors which are significant. Current has most significant which has highest contribution in micro hardness according to F value and percentage contribution. All interactions are insignificant interactions for micro hardness. Main effect plot and interaction plot of S/N ratio for micro hardness shown in the Figure 6.11 and Figure 6.12.

Table 6.16 ANOVA for S/N ratio of micro hardness at deposited red region

Sources	SS	v	V	F	F (Critical)	SS'	% contribution
Workpiece, *A*	0.58	2	0.29	6.83			
Dielectric, *B*	0.00	1	0.00	0.02			
Electrode, C	0.23	1	0.23	5.34			
Pulse off, *D*	0.47	2	0.23	5.49			
Pulse on, *E*	0.70	2	0.35	8.16			
Current, *F*	2.30	2	1.15	26.96	10.9	1.90	23.95
Powder, G	1.59	2	0.80	18.62	10.9	1.19	14.97
A×C	0.58	2	0.29	6.83			
A×G	0.56	4	0.14	3.29			

C×G	0.66	2	0.33	7.67			
Error	0.26	6	0.04				
TOTAL	7.93	26	0.30				
e-pooled	4.03	20	0.20			4.84	61.08

Table 6.17 Response table for S/N ratio of micro hardness at deposited red region

Level	Workpiece	Dielectric	Electrode	Pulse off	Pulse on	Current	Powder
1	35.48	35.48	35.44	35.45	35.44	35.39	35.47
2	35.45	35.45	35.47	35.48	35.44	35.47	35.49
3	35.43			35.43	35.49	35.49	35.40
Delta	0.05	0.00	0.03	0.05	0.05	0.10	0.08
Rank	3	7	6	5	4	1	2

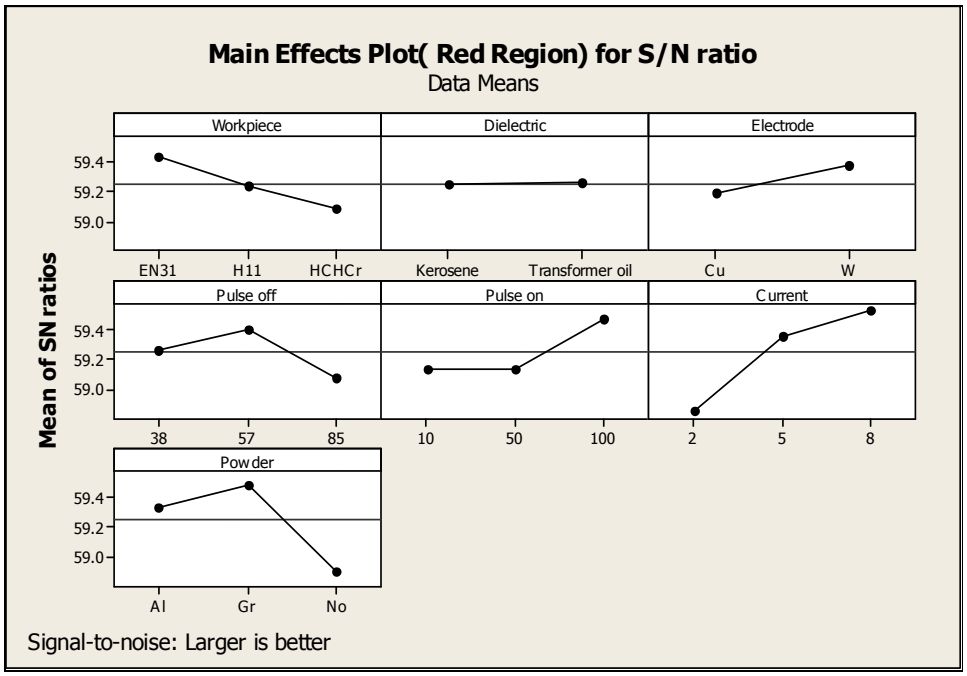

Figure 6.11 Main effects plot for S/N ratio of micro hardness at deposited red region

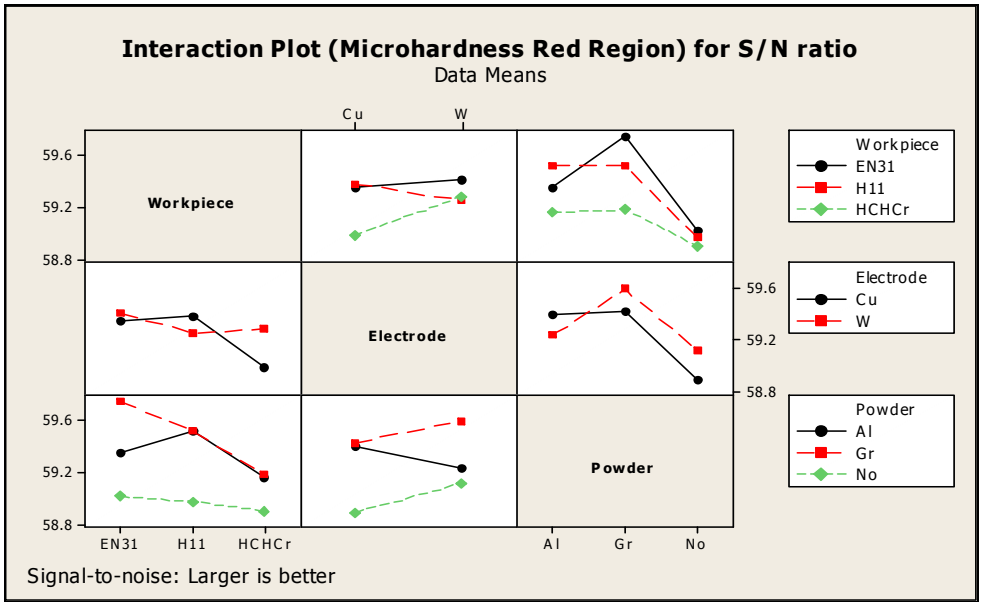

Figure 4.12 Interaction plot of S/N ratio for micro hardness at deposited red region

6.13 OPTIMAL DESIGN FOR DEPOSITED REGION (RED REGION)

In this experimental analysis, the main effect plot and interaction plot in Figure 6.9 and Figure 6.10 were used to be estimate the mean micro hardness. From the, Table 6.18 it was concluded that highest micro hardness was to be observed when EN-31 workpiece was machined at current 8Amp on 100µs pulse on time with graphite powder mixing. The interactions workpiece v/s electrode and electrode v/s powder were found to be significant. In S/N ratio highest micro hardness was to be observed when workpiece material was machined with tungsten-copper electrode at current 2 Amp with graphite. The best value of micro hardness was obtained when H11 workpiece machined at pulse off 100 µs and current at 8Amp with tungsten-copper electrode in graphite mixed dielectric.

Table 6.18: Significant factors and interactions

Factor	Affecting mean		Affecting variation	
	Contribution	Best level	Contribution	Best level
Workpiece , *A*	significant	(EN-31)	insignificant	-
Dielectric, *B*	insignificant	-	Insignificant	-
Electrode, C	insignificant	-	Insignificant	-
Pulse off , *D*	insignificant	-	Insignificant	-
Pulse on, *E*	significant	Level-3(100µs)	insignificant	-

Current , *F*	significant	Level-3 (8Amp)	significant	Level-3(8Amp)
Powder, G	significant	Level-2(Gr	significant	Level-2(Gr powder)
A×C	significant	A_2C_1	insignificant	-
A×G	insignificant	-	insignificant	-
C×G	significant	C_2G_2	insignificant	-

Mean value for Micro hardness(Red Region)

$$\mu_{A_2E_3F_2G_1} = \overline{E_3} + \overline{F_3} + \overline{A_2C_1} + \overline{C_2G_2} - 3\overline{T}$$

=944+951+923+960-3*921=1015 hvn

Confidence Interval around the estimated mean micro hardness

$$n_{eff} = \frac{N}{1 + dof_{E,F,AC,CG}} = \frac{27}{1+2+2+2+2} = 3$$

$$CI_1 = \sqrt{\frac{F_{\alpha,v_1,v_2} V_e}{n_{eff}}} = \sqrt{\frac{0.14 \times 397.2}{3}} = 4.31$$

So the confidence interval around the micro hardness of non-deposited region is given by 1015 ± 4.31hvn.

CHAPTER 7

RESULTS AND ANALYSIS OF SURFACE ROUGHNESS

7.1 INTRODUCTION

In this experiment work surface roughness (R_a) has measured at three positions i.e. position 1 (center), position 2 (left) and position 3 (right) at each samples. The center position is at center of machined area and left position at 7 mm left from the center and right position at 7 mm right from the center. The results for surface roughness at position 1 (center) for each of the 27 treatment conditions with repetition are shown in Table 7.1.

Table 7.1: Results for Surface Roughness (R_a) at position 1, 2, 3

Trial no.	Roughness Position 1		Mean	S/N ratio position 1	Roughness Position 2		Mean	S/N ratio position 2	Roughness Position 3		Mean	SN ratio position 3
	I	II			I	II			I	II		
1	5.26	4.88	5.06	-14.09	3.28	4.60	3.94	-12.03	4.26	5.0	4.65	-13.37
2	7.27	7.24	7.25	-17.20	7.18	7.18	7.18	-17.12	7.87	7.87	7.87	-17.92
3	10.3	10.2	10.3	-20.23	10.4	10.1	10.2	-20.22	10.4	10.3	10.38	-20.33
4	8.12	7.90	8.01	-18.07	7.89	7.93	7.91	-17.96	7.94	8.31	8.13	-18.20
5	1.86	1.87	1.87	-5.41	2.19	2.43	2.31	-7.27	1.29	0.75	1.04	-0.62
6	6.85	6.12	6.49	-16.25	6.58	6.99	6.78	-16.63	6.85	7.48	7.16	-17.10
7	8.82	7.25	8.03	-18.14	6.48	7.52	7.00	-16.93	7.10	7.16	7.13	-17.06
8	9.54	9.49	9.52	-19.57	9.77	9.29	9.53	-19.58	9.31	9.18	9.25	-19.32
9	4.59	4.31	4.45	-12.97	4.72	4.57	4.64	-13.34	4.37	4.34	4.36	-12.78
10	7.90	7.83	7.87	-17.91	9.29	9.09	9.19	-19.27	8.34	8.36	8.36	-18.44
11	4.92	5.11	5.02	-14.01	5.18	4.96	5.06	-14.06	5.10	5.17	5.14	-14.22
12	5.32	6.59	5.96	-15.55	6.18	7.04	6.60	-16.48	5.98	7.84	6.91	-16.87
13	5.23	4.48	4.85	-13.75	5.38	4.69	5.03	-14.06	5.37	5.58	5.47	-14.77
14	6.86	6.42	6.64	-16.44	8.36	8.43	8.39	-18.47	8.06	8.49	8.27	-18.36
15	6.39	6.17	6.28	-15.96	5.88	6.43	6.15	-15.79	6.78	6.72	6.75	-16.58
16	5.70	5.25	5.48	-14.78	4.96	5.54	5.25	-14.42	4.76	5.66	5.21	-14.36
17	6.09	6.11	6.09	-15.70	6.46	6.42	6.43	-16.17	5.94	5.95	5.95	-15.48
18	7.96	8.04	8.00	-18.06	7.57	8.56	8.06	-18.14	6.86	8.36	7.61	-17.67
19	7.58	8.58	8.08	-18.17	8.39	6.89	7.64	-17.70	6.93	7.11	7.01	-16.92
20	3.31	4.61	3.96	-12.07	6.65	6.38	6.52	-16.28	4.38	4.62	4.49	-13.06
21	4.78	4.47	4.63	-13.31	4.23	4.05	4.14	-12.35	4.31	4.30	4.31	-12.69
22	5.52	4.72	5.12	-14.21	5.21	4.04	4.62	-13.36	5.00	3.96	4.48	-13.09
23	6.70	6.52	6.61	-16.40	7.18	6.38	6.78	-16.64	5.99	6.09	6.04	-15.62
24	7.76	7.91	7.84	-17.88	7.36	7.19	7.27	-17.23	7.72	7.74	7.73	-17.76
25	5.35	5.54	5.44	-14.71	6.13	5.98	6.05	-15.64	6.49	6.43	6.46	-16.20
26	1.82	2.05	1.93	-5.74	2.50	1.86	2.18	-6.86	3.12	2.93	3.02	-9.61
27	7.57	7.19	7.38	-17.36	6.65	7.11	6.88	-16.76	6.38	6.71	6.54	-16.32

7.2 ANALYSIS OF VARIANCE - SURFACE ROUGHNESS (R_a) AT POSITION 1

The results for surface roughness were analyzed using ANOVA for identifying the significant factors affecting the performance measures. ANOVA for the mean surface roughness at 99% confidence interval is given in Table 7.2. The current, pulse on time, powder, workpiece and electrode are input parameters which effects the surface roughness. Main effect plots had shown in the Figure 7.1 shows that the surface roughness increases with increase in the current and pulse on time. The surface roughness decreases with graphite powder mixing in the dielectric. The workpiece material also affects the surface roughness. Table 7.3 shows ranks to various input parameters in terms their relative significance. The all of interactions are significant in surface roughness.

Table 7.2 ANOVA for Roughness at position 1 (center)

Sources	SS	v	V	F	F (Criti-cal)	SS'	% contribution
Workpiece, A	5.52	2	2.76	91.02	10.9	5.44	5.24
Dielectric, B	0.06	1	0.06	1.92			
Electrode, C	0.92	1	0.92	30.26	13.7	0.88	0.85
Pulse off, D	0.12	2	0.06	1.92			
Pulse on, E	24.78	2	12.39	408.82	10.9	24.70	23.80
Current, F	46.36	2	23.18	764.81	10.9	46.28	44.59
Powder, G	9.15	2	4.58	150.97	10.9	9.07	8.74
A×C	11.26	2	5.63	185.74	10.9	11.18	10.77
A×G	3.77	4	0.94	31.11	9.15	3.61	3.48
C×G	1.69	2	0.84	27.83	10.9	1.61	1.55
Error	0.18	6	0.03				
TOTAL	103.80	26	3.99				
e-pooled	0.36	9	0.04			1.03	0.99

Table 7.3 Response table for means of Roughness at position 1 (center)

Level	Workpiece	Dielectric	Electrode	Pulse off	Pulse on	Current	Powder
1	6.772	6.193	6.359	6.179	5.058	4.425	6.810
2	6.242	6.292	5.966	6.181	6.217	6.749	5.431
3	5.665			6.319	7.404	7.504	6.438
Delta	1.107	0.099	0.391	0.140	2.347	3.079	1.378
Rank	4	7	5	6	2	1	3

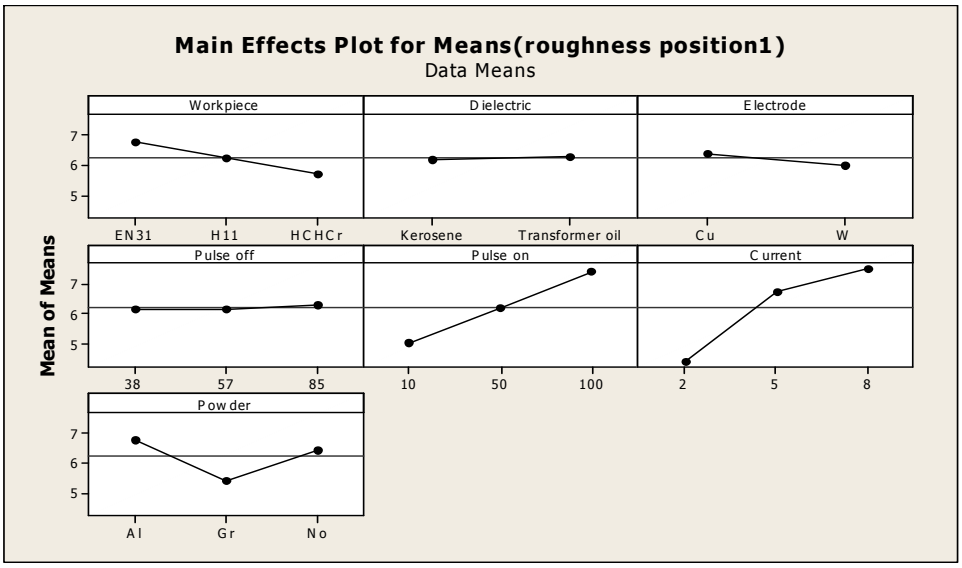

Figure 7.1: Main effects plot for surface roughness at position 1

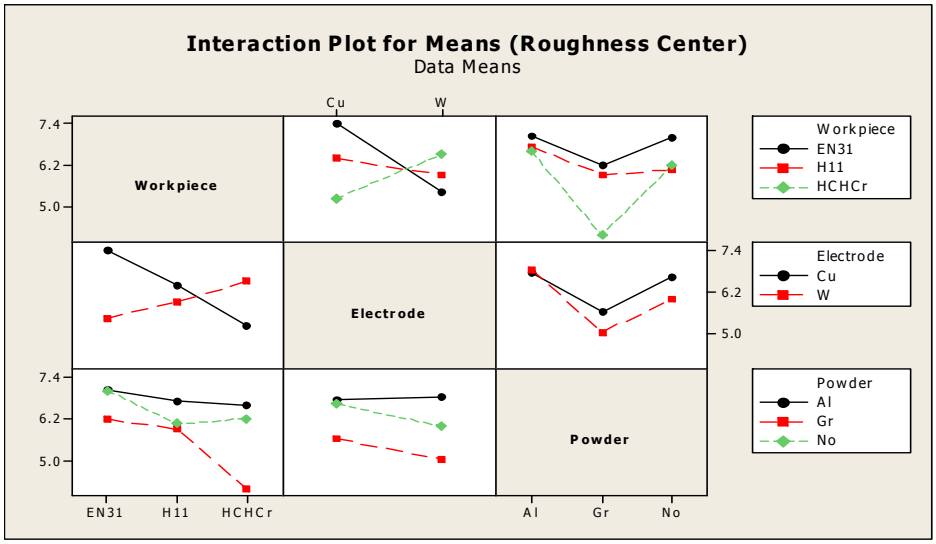

Figure 7.2: Interaction plot surface roughness at position 1

7.3 ANOVA FOR S/N RATIO FOR ROUGHNESS (R_a)

The S/N ratio several repetitions into one value which reflects the amount of variation present. The values of all the results according to Taguchi array parameter design layout are presented in this section. The S/N ratios have been calculated to identify the major contributing factors and interactions for variation in the roughness values at position1 (Center), position 2(Left) and position 3(Right). In this design situation,

roughness is the type of 'lower is better', which is a logarithmic function based on the mean square deviation (MSD), given by

$$S/N_{LB} = -10\log(MSD) = -10\log[(\frac{1}{r}\sum_{i=1}^{r} y^2{}_i)$$

Where $MSD_{LB} = \frac{1}{r}\sum_{j=1}^{r}\left(y_j{}^2\right)$

Table 7.4 shows the ANOVA for S/N ratio for roughness at 99% confidence interval. Among all the factors current, pulse on and powder are significant factor. Current has most significant which has highest contribution in roughness. Remaining factors and all three interactions have insignificant. The interaction between workpiece and electrode is significant.

Table 7.4 ANOVA for S/N ratio of Roughness at position 1 (Center)

Sources	SS	v	V	F	F (Critical)	SS'	% contribution
Workpiece, A	11.03	2	5.52	5.40			
Dielectric, B	3.03	1	3.03	2.97			
Electrode, C	2.17	1	2.17	2.12			
Pulse off, D	0.79	2	0.39	0.39			
Pulse on, E	58.45	2	29.23	28.59	10.9	53.60	16.96
Current, F	128.45	2	64.23	62.84	10.9	123.61	39.11
Powder, G	40.48	2	20.24	19.80	10.9	35.63	11.28
A×C	45.00	2	22.50	22.01	10.9	40.15	12.71
A×G	16.71	4	4.18	4.09			
C×G	3.76	2	1.88	1.84			
Error	6.13	6	1.02				
TOTAL	316.01	26	12.15				
e-pooled	43.63	18	2.42			63.02	19.94

Table 7.5 Response table for S/N ratio of Roughness at position 1 (Center)

Level	workpiece	Dielectric	Electrode	Pulse off	Pulse on	Current	Powder
1	-15.77	-15.10	-15.53	-15.57	-13.57	-12.28	-16.40
2	-15.80	-15.10	-14.93	-15.20	-15.25	-16.50	-13.62
3	-14.43			-15.22	-17.17	-17.22	-15.98
Delta	1.37	0.71	0.60	0.37	3.60	4.94	2.78
Rank	4	5	6	7	2	1	3

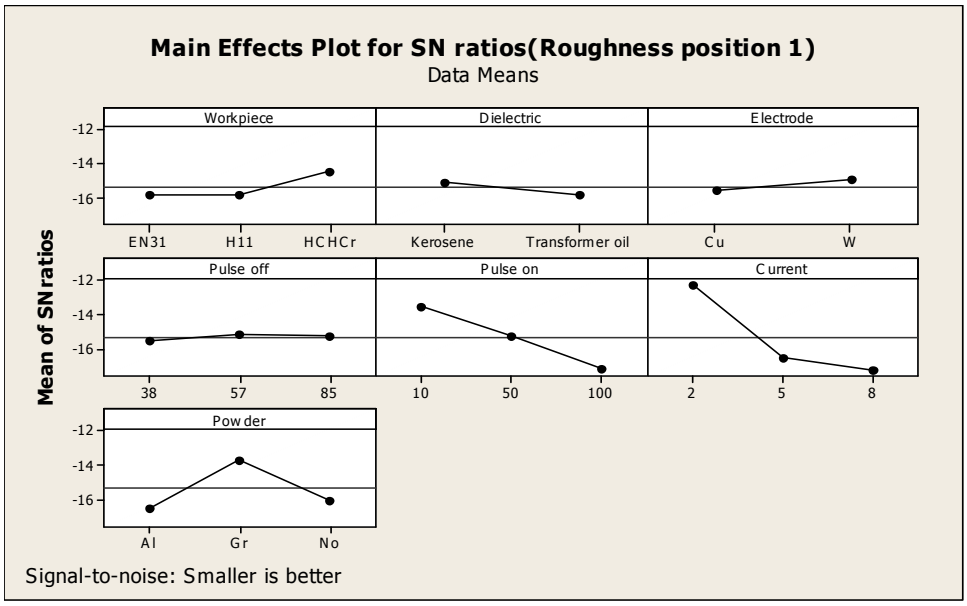

Figure 7.3 Main effects plot for S/N ratio of surface roughness at position 1

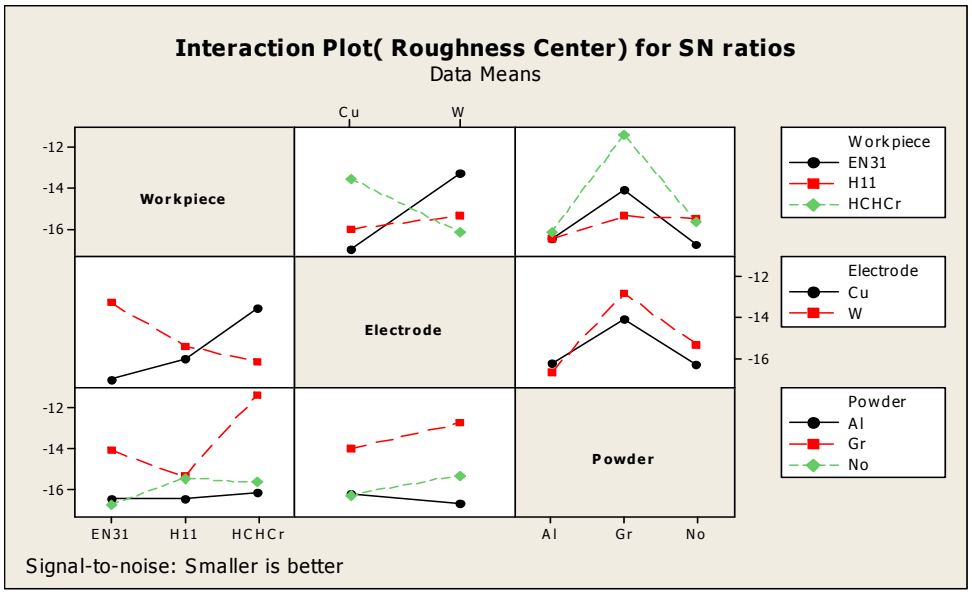

Figure 7.4 Interaction plot for of S/N ratio for roughness at position 1

7.4 OPTIMAL DESIGN FOR SURFACE ROUGHNESS (R_a) AT POSITION1

In this experimental analysis, the main effect plot and interaction plot in Figure 7.1 and Figure 7.2 used to estimate the mean surface roughness. From the, Table 7.6 it was concluded that lowest roughness value was to be observed when HCHCr was machined

with tungsten-copper electrode at pulse on time 10 µs, current 2Amp with graphite mixed powder in dielectric. In S/N ratio was to be observed at lowest roughness value when workpiece material was machined at pulse on time 10 µs, current 2Amp with graphite powder mixing. But the interactions had given contradiction between results. The best design was to be suggested if HCHCr workpiece was machined with copper electrode at pulse on time 10 µs, current 2Amp with graphite mixing in dielectric.

Table 7.6: Significant factors and interactions

Factor	Affecting mean		Affecting variation	
	Contribution	Best level	Contribution	Best level
Workpiece , *A*	significant	Level-3 (HCHcr)	insignificant	-
Dielectric, *B*	insignificant	-	insignificant	-
Electrode, C	significant	Level 2 (W-Cu)	insignificant	-
Pulse off , *D*	insignificant	-	insignificant	-
Pulse on, *E*	significant	Level-1(10µsec)	significant	Level-1(10µsec)
Current , *F*	significant	Level-1(2Amp)	significant	Level-1(2Amp)
Powder, G	significant	Level-2(Gr powder)	significant	Level-2(Gr powder)
A×C	significant	A_3C_3	significant	A_3C_3
A×G	significant	A_3G_2	insignificant	-
C×G	significant	C_2G_2	insignificant	-

Mean value for Micro hardness

$$\mu_{A_3E_1F_1G_2} = \overline{E_1} + \overline{F_1} + \overline{A_3C_3} + \overline{A_3G_2} - 3\overline{T}$$

$$= 4.42 + 5.50 + 4.91 + 4.16 - 3*6.22 = 0.33 \text{micron}$$

Confidence Interval around the Estimated Mean

Confidence Interval around the estimated Roughness value

$$CI_1 = \sqrt{\frac{F_{\alpha,\nu_1,\nu_2} V_e}{n_{eff}}} \quad \text{Where} \quad F_{\alpha\nu_1\nu_2} = F \ ratio$$

$\alpha = risk$ (0.01) $\qquad confidence = 1 - \alpha$

$\nu_1 = dof \ for \ mean which \ is \ always = 1$

$\nu_2 = dof \ for error = \nu_e$

$$n_{eff} = \frac{N}{1+dof} = \frac{27}{1+2+2+2+4} = 2.45$$

$$CI_1 = \sqrt{\frac{F_{\alpha,v_1,v_2} V_e}{n_{eff}}} = \sqrt{\frac{0.09 \times 0.04}{2.45}} = 0.038$$

So the confidence interval around the roughness is given by 0.33±0.038 micron.

7.5 ANALYSIS OF VARIANCE - SURFACE ROUGHNESS (R_A) AT POSITION 2

The results for surface roughness at position 2 (Left) for each of the 27 treatment conditions with repetition are given in Table 7.1. The experimental results for surface roughness were analyzed using ANOVA for identifying the significant factors affecting the performance measures. ANOVA for the mean surface roughness at 99% confidence interval is given in Table 7.7. The current and pulse on time are two input parameters which effects the surface roughness. The surface roughness increases with the current increase from 2 Amp to 8 Amp. The surface roughness increases pulse on time increases. All the interactions are insignificant. Table 7.8 shows the ranks to various factors according to significance in surface roughness. The current has higher rank which has the highest contribution in surface roughness.

Table 7.7: ANOVA for Roughness at position 2 (Left)

Sources	SS	v	V	F	F (Critical)	SS'	% contribution
Workpiece, A	4.51	2	2.25	7.15			
Dielectric, B	0.24	1	0.24	0.78			
Electrode, C	0.68	1	0.68	2.16			
Pulse off, D	0.88	2	0.44	1.40			
Pulse on, E	15.41	2	7.70	24.44	10.9	13.79	13.47
Current, F	69.13	2	34.57	109.67	10.9	67.51	65.97
Powder, G	2.35	2	1.18	3.73	10.9		
A×C	5.14	2	2.57	8.15			
A×G	1.43	4	0.36	1.13			
C×G	0.68	2	0.34	1.08	10.9		
Error	1.89	6	0.32				
TOTAL	102.35	26	3.94				
e-pooled	17.80	22	0.81			21.04	20.56

Table 7.8 Response table for means of Roughness at position 2 (Left)

Level	workpiece	Dielectric	Electrode	Pulse off	Pulse on	Current	Powder
1	6.616	6.297	6.476	6.156	5.424	4.256	6.755
2	6.688	6.498	6.139	6.341	6.394	6.705	6.043
3	5.788			6.596	7.273	8.131	6.293
Delta	0.900	0.202	0.337	0.441	1.850	3.875	0.712
Rank	3	7	6	5	2	1	4

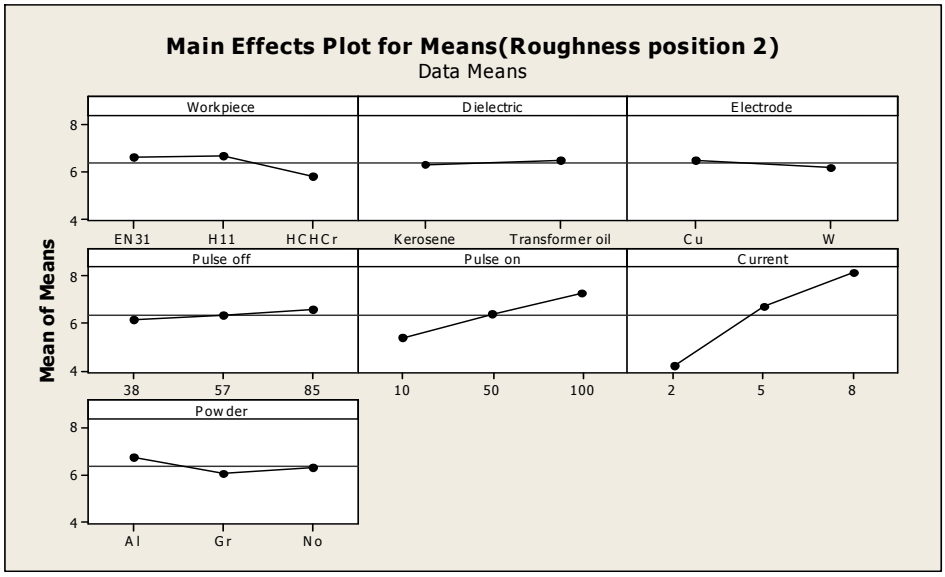

Figure 7.5 Main effects plot for surface roughness at position 2

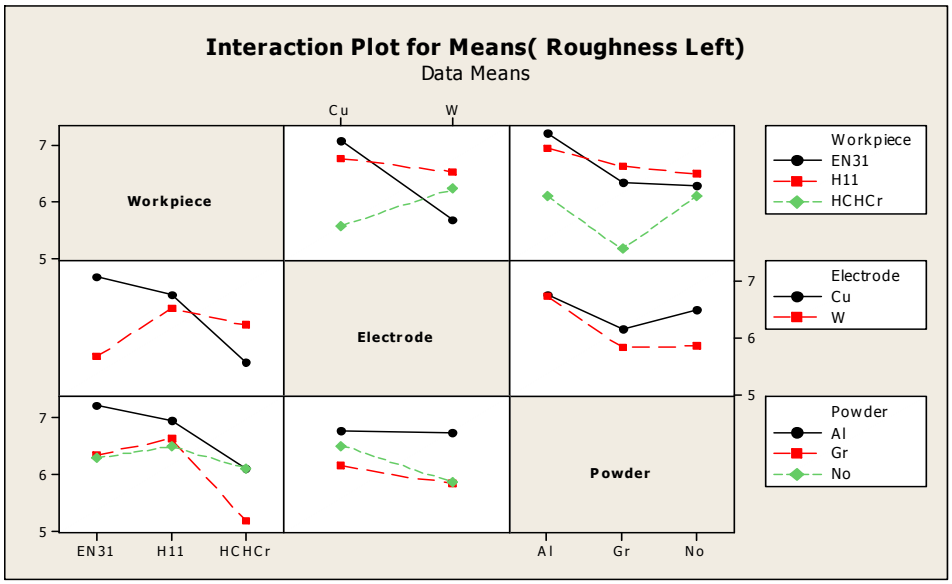

Figure 7.6 Interaction plot surface roughness at position 2

7.6 ANOVA FOR S/N RATIO FOR SURFACE ROUGHNESS(R_a) AT POSITION 2

Table 7.9 shows the ANOVA for S/N ratio for roughness at 99% confidence interval. Among all the factors current has most significant which has contribution in roughness. Remaining factors and all three interactions have insignificant.

Table 7.9 ANOVA for S / N of Roughness at position 2 (Left)

Sources	SS	v	V	F	F (Criti-cal)	SS'	% contribution
Workpiece, A	11.02	2	5.51	3.14	10.9		
Dielectric, B	2.70	1	2.70	1.54			
Electrode, C	1.32	1	1.32	0.75			
Pulse off, D	0.55	2	0.27	0.16			
Pulse on, E	34.13	2	17.07	9.72	10.9		
Current, F	168.93	2	84.47	48.10	10.9	160.32	58.88
Powder, G	11.68	2	5.84	3.33	10.9		
A×C	21.89	2	10.94	6.23			
A×G	6.02	4	1.50	0.86			
C×G	3.50	2	1.75	1.00	10.9		
Error	10.54	6	1.76				
TOTAL	272.28	26	10.47				
e-pooled	103.35	24	4.31			111.96	41.12

Table 7.10 Response table for S/N ratio of Roughness at position 2 (Left)

Level	workpiece	Dielectric	Electrode	Pulse off	Pulse on	Current	Powder
1	-15.68	-15.36	-15.74	-15.46	-14.27	-12.17	-16.32
2	-16.32	-16.03	-15.27	-15.50	-15.46	-16.49	-14.72
3	-14.76			-15.78	-17.02	-18.09	-15.71
Delta	1.56	0.67	0.47	0.32	2.75	5.92	1.60
Rank	4	5	6	7	2	1	3

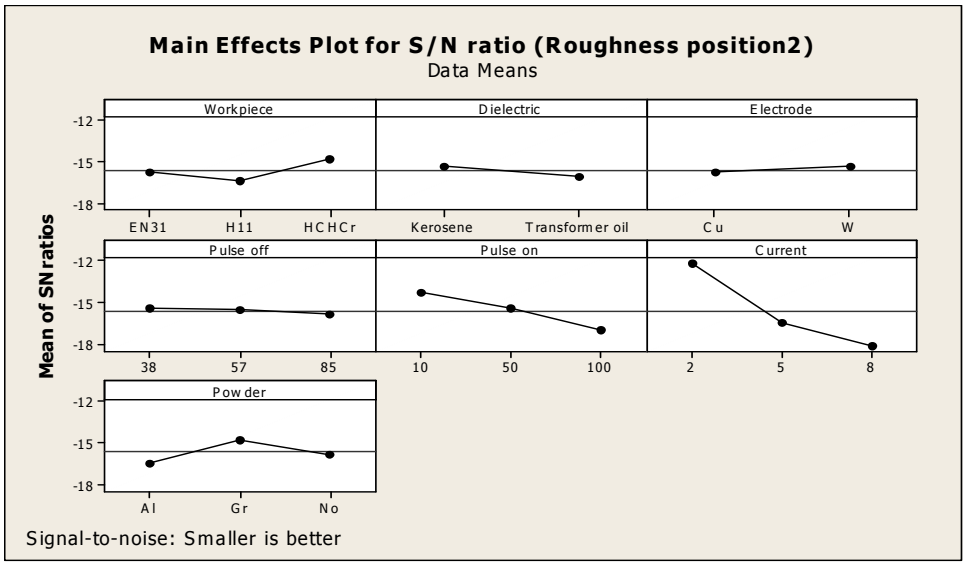

Figure 7.7 Main effects plot for S/N of surface roughness at position 2

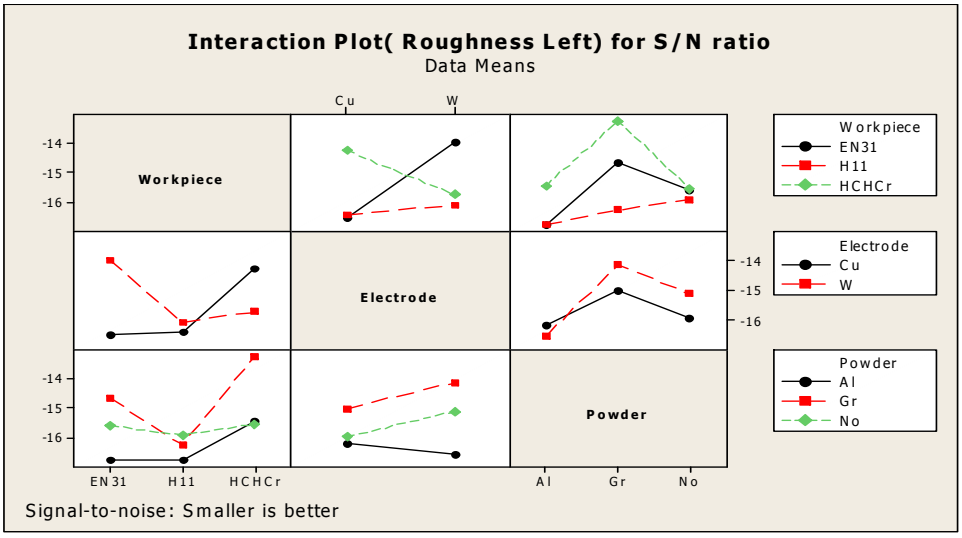

Figure 7.8 Interaction plot for S/N ratio of surface roughness at position 2

7.7 OPTIMAL DESIGN FOR ROUGHNESS (R_A) AT POSITION 2

In this experimental analysis, the main effect plot and interaction plot in Figure 7.5 and Figure 7.6 used to estimate the mean surface roughness. The best design was to be suggested if workpiece was machined at pulse on time 10 µs, current 2Amp.

Table 7.11: Significant factors and interactions

Factor	Affecting mean		Affecting variation	
	Contribution	Best level	Contribution	Best level
Workpiece , *A*	insignificant	-	insignificant	-
Dielectric, *B*	insignificant	-	insignificant	-
Electrode, C	insignificant	-	insignificant	-
Pulse off , *D*	insignificant	-	insignificant	-
Pulse on, *E*	significant	Level-1(10µsec)	significant	-
Current , *F*	significant	Level-1(2Amp)	significant	Level-1(2Amp)
Powder, G	insignificant	-	insignificant	-
A×C	insignificant	-	insignificant	-
A×G	insignificant	-	insignificant	-
C×G	insignificant	-	insignificant	-

Estimating the Mean value for roughness (left)

$$\mu_{E_1F_1} = \overline{E_1} + \overline{F_1} - \overline{T}$$

$$=5.42+4.25-6.36=3.31\text{micron}$$

Confidence Interval around the Estimated Mean

Confidence Interval around the estimated Roughness value

$$n_{eff} = \frac{N}{1+dof_{E,F}} = \frac{27}{1+2+2} = 5.4$$

$$CI_1 = \sqrt{\frac{F_{\alpha,v_1,v_2} V_e}{n_{eff}}} = \sqrt{\frac{0.22 \times 0.82}{5.4}} = 0.18$$

So the confidence interval around the roughness is given by 3.31±0.18 micron.

7.8 ANALYSIS OF VARIANCE - SURFACE ROUGHNESS (R_a) AT POSITION 3

The results for surface roughness at position 3 (right) for each of the 27 treatment conditions with repetition are given in Table 7.1. The results for surface roughness were analyzed using ANOVA for identifying the significant factors affecting the performance measures. ANOVA for the mean surface roughness at 99% confidence interval is given in

Table 7.12. The current, pulse on and powder are input parameters which effects the surface roughness at position 3.It is observed that as the current and pulse on time increase, surface roughness increases. The interaction between workpiece and electrode is significant in surface roughness. Table 7.13 shows the ranks to various factors according to significance in surface roughness, current is the highest affecting factor to surface roughness.

Table 7.12: ANOVA for Roughness at position 3 (Right)

Sources	SS	v	V	F	F (Criti-cal)	SS'	% contribution
Workpiece, A	7.00	2	3.50	20.07	10.9	6.04	5.78
Dielectric, B	0.44	1	0.44	2.54			
Electrode, C	0.37	1	0.37	2.14			
Pulse off, D	0.67	2	0.34	1.94			
Pulse on, E	17.23	2	8.62	49.44	10.9	16.28	15.58
Current, F	57.99	2	29.00	166.38	10.9	57.03	54.59
Powder, G	6.36	2	3.18	18.25	10.9	5.40	5.17
A×C	8.23	2	4.11	23.60		7.27	6.96
A×G	1.95	4	0.49	2.80			
C×G	3.18	2	1.59	9.11	10.9		
Error	1.05	6	0.17				
TOTAL	104.47	26	4.02				
e-pooled	7.66	16	0.48			12.45	11.92

Table 7.13: Response table for means of Roughness at position 3 (right)

Level	workpiece	Dielectric	Electrode	Pulse off	Pulse on	Current	Powder
1	6.664	6.197	6.370	6.233	5.231	4.329	6.863
2	6.630	6.468	6.121	6.502	6.469	6.678	5.676
3	5.567			6.126	7.162	7.854	6.323
Delta	1.097	0.272	0.249	0.376	1.932	3.525	1.187
Rank	4	6	6	7	2	1	3

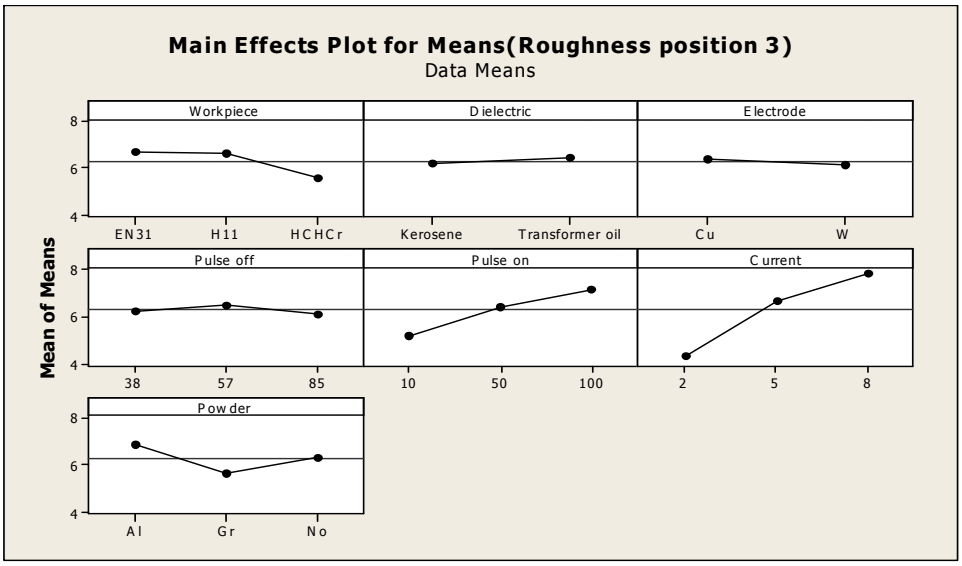

Figure 7.9: Main effects plot for surface roughness at position 3

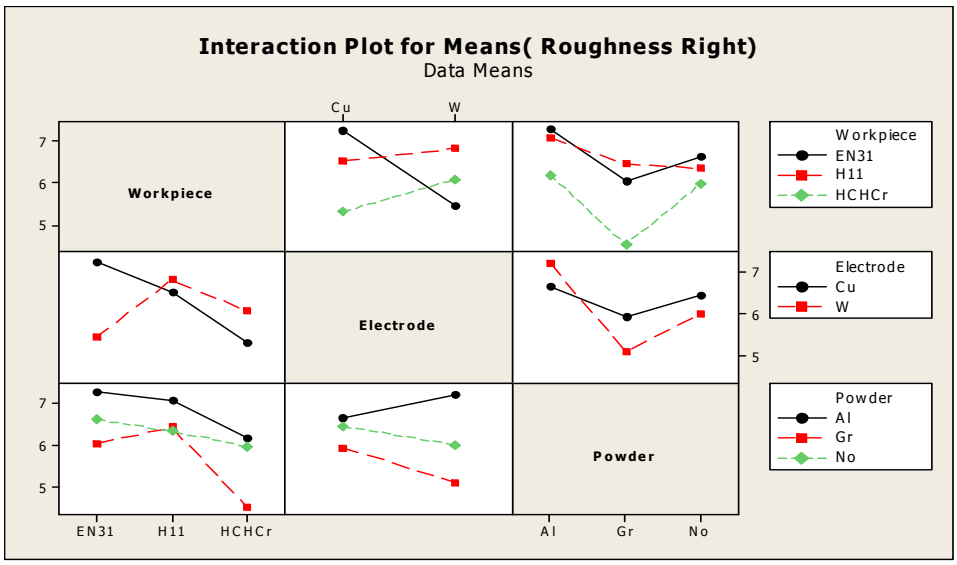

Figure 7.10: Interaction plot surface roughness at position 3

7.9 ANOVA FOR S/N RATIO FOR SURFACE ROUGHNESS (R_a) POSITION -3

Table 7.14 shows the ANOVA for S/N ratio for roughness at 99% confidence interval. Among all the factors current and pulse on time are significant factors. Remaining factors have insignificant. The interaction between workpiece and electrode has significant.

Table 7.14: ANOVA table for S/N ratio of Roughness at position 3

Sources	SS	v	V	F	F (Criti-cal)	SS'	% contribution
Workpiece, A	13.68	2	6.84	3.87			
Dielectric, B	5.36	1	5.36	3.03			
Electrode, C	6.27	1	6.27	3.54			
Pulse off, D	8.97	2	4.49	2.53			
Pulse on, E	55.45	2	27.73	15.66	10.9	44.41	11.70
Current, F	166.38	2	83.19	47.00	10.9	155.33	40.93
Powder, G	34.67	2	17.33	9.79	10.9		
A×C	44.55	2	22.27	12.58		33.50	8.83
A×G	12.95	4	3.24	1.83			
C×G	20.59	2	10.30	5.82	10.9		
Error	10.62	6	1.77				
TOTAL	379.49	26	14.60				
e-pooled	99.43	18	5.52			143.62	37.84

Table 7.15: Response table for S/N ratio of Roughness of position 3

Level	workpiece	Dielectric	Electrode	Pulse off	Pulse on	Current	Powder
1	-15.19	-15.05	-15.70	-15.66	-13.44	-11.93	-16.46
2	-16.31	-15.99	-14.68	-15.87	-15.77	-16.45	-13.80
3	-14.59			-14.56	-16.88	-17.71	-15.83
Delta	1.72	0.94	1.02	1.31	3.44	5.78	2.66
Rank	4	7	6	5	2	1	3

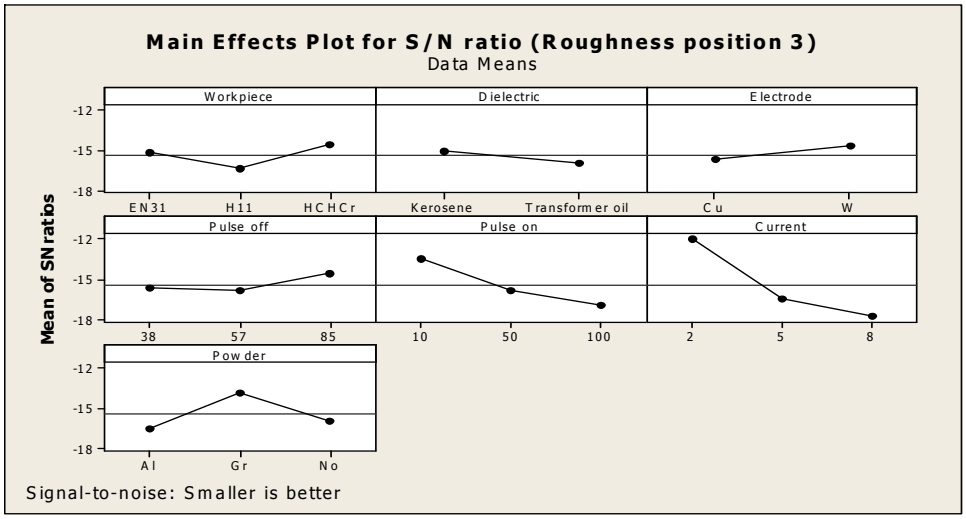

Figure 7.11 Main effects plot for S/N ratio of surface roughness at position 3

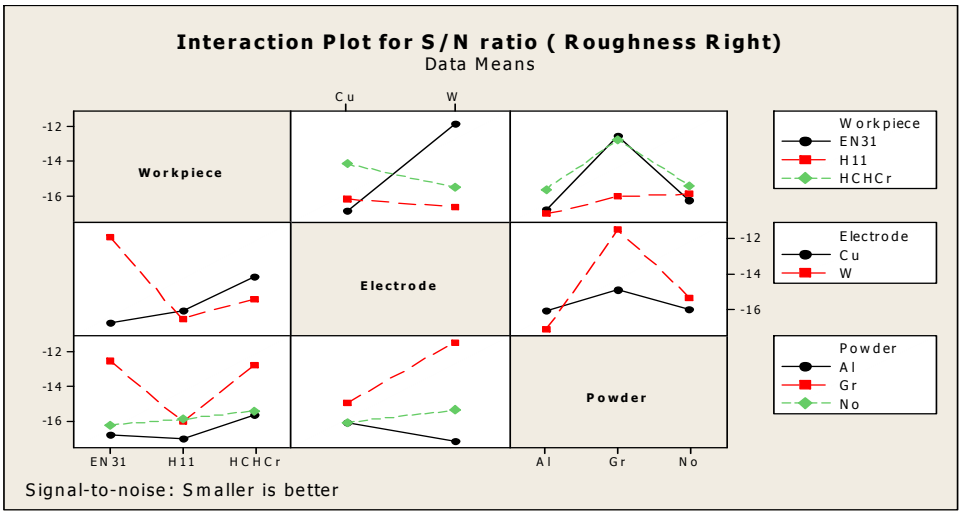

Figure 7.12 Interaction plot for S/N ratio of surface roughness at position 3

7.10 OPTIMAL DESIGN FOR ROUGHNESS AT POSITION 3

In this experimental analysis, the main effect plot and interaction plot in Figure 7.9 and Figure 7.10 used to estimate the mean surface roughness. From the, Table 7.14 it was concluded that lowest roughness value was to be observed when workpiece was machined at pulse on time 10 µs, current 2Amp with graphite mixed powder in dielectric. In S/N ratio was to be observed at lowest roughness value when workpiece material was machined at pulse on time 10 µs, current 2Amp without powder mixing. The best design was to be suggested if workpiece was machined with copper electrode at pulse on time 10 µs, current 2Amp with graphite mixing in dielectric.

Table 7.16: Significant factors and interactions

Factor	Affecting mean		Affecting variation	
	Contribution	Best level	Contribution	Best level
Workpiece , *A*	insignificant	-	insignificant	-
Dielectric, *B*	insignificant	-	insignificant	-
Electrode, C	insignificant	-	insignificant	-
Pulse off , *D*	insignificant	-	insignificant	-
Pulse on, *E*	significant	Level-1(10µsec)	significant	Level-1(10µsec)
Current , *F*	significant	Level-1(2Amp)	significant	Level-1(2Amp)
Powder, G	significant	Level-2(Gr powder)	insignificant	-
A×C	significant	A_3C_1	significant	A_3C_1
A×G	insignificant	-	insignificant	-
C×G	insignificant	-	insignificant	-

Estimating the Mean value for roughness (right)

$$\mu_{A_3E_3F_2G_2} = \overline{E_1} + \overline{F_1} + \overline{G_2} + \overline{A_3C_1} - 3\overline{T}$$

=5.23+3.84+5.67+5.27-3*6.28=1.17micron

Confidence Interval around the Estimated Mean

Confidence Interval around the estimated Roughness value

n_{eff} = Number of tests under that condition using the participating factors

$$n_{eff} = \frac{N}{1 + dof_{E,F,G,AC}} = \frac{27}{1+2+2+2+2} = 3$$

$$CI_1 = \sqrt{\frac{F_{\alpha,v_1,v_2} V_e}{n_{eff}}} = \sqrt{\frac{0.16 \times 0.48}{3}} = 0.16$$

So the confidence interval around the roughness is given by 1.17±0.16 micron.

CHAPTER 8

XRD RESULTS AND MICRO STRUCTURE ANALYSIS

8.1 INTRODUCTION

In the present work, the effect of various input parameters i.e. current, pulse on time, pulse off time, electrode material, dielectric, powder on the surface properties of the workpiece material has been evaluated. During machining, temperature between tool and workpiece is more than 5000^0C and this high temperature causes fusion or partial vaporization of the molten metal and the dielectric fluid at the point of discharge. Due to very high temperature workpiece material is subjected to, re-crystallization of the metal grains take place and subsequent cooling of the heated metal causes change in the micro structure. The heating and cooling rate decides the shape of grains and properties of surface of the machined area. Also, metal is transferred from the powder, which is suspended in the dielectric, as well as from the electrode to the machined surface. The chemical composition of the machined surface was determined with the help of X-ray diffraction (XRD) analysis. Micro structural analysis was carried out using a Scanning Electron Microscope (SEM) and Lieca Metallurgical Microscope. During this analysis chemical composition of machined surface and micro structure of machined surface was determined.

8.2 XRD ANALYSIS

During machining of the workpiece, material is transferred from suspended powder in the dielectric and from the electrode material, resulting in improvement of surface properties. The material is transferred to the workpiece, which forms various compounds. To analyze modification of surface of workpiece was tested by XRD on selected samples. The range of 2θ from the 5^0 to 100^0 was used at a scan speed of 5^0/minute for each test. After the XRD analysis, each sample was tested on Optical Emission Spectrometry to quantitatively confirm the results of XRD.

8.2.1 XRD Analysis of EN-31

The XRD pattern of EN-31 which has been machined with tungsten-copper electrode in aluminium mixed dielectric has shown in figure 8.1 The XRD shows that traces of

aluminium and copper was generated on the machined surface, which decreases surface roughness value. Also, aluminium and copper helps to improve the hardness and strength of steel. Peak list and pattern list are given shown in the Table 8.1 and Table 8.2 respectively. After the spectrometry analysis the copper percentage increases from 0.03% to 1.12%.

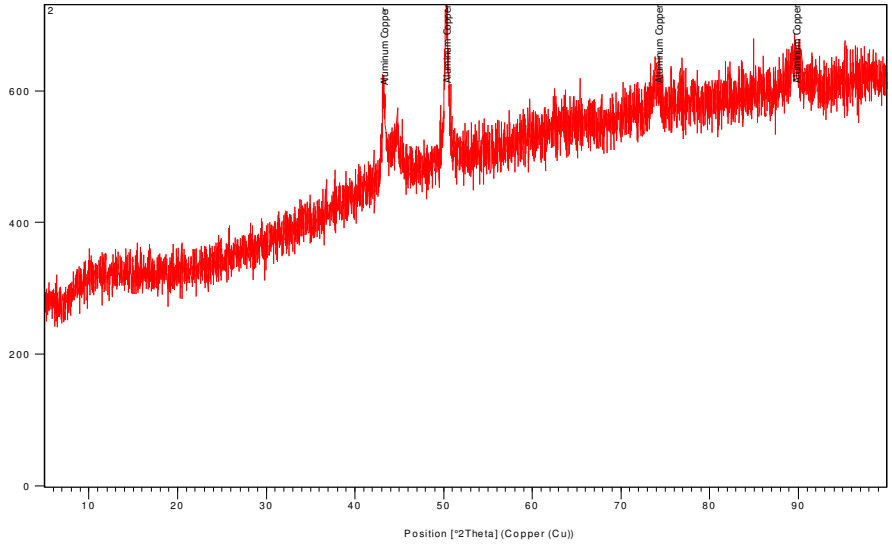

Fig 8.1 XRD pattern of EN31 workpiece machined with Tungsten-Copper electrode in Kerosene with aluminium powder mixing (current 6 Amp, pulse off 38, pulse On50)

Table 8.1 Pattern List

Visible	Ref. Code	Score	Compound Name	Scale Factor	Chemical Formula	Semi Quant [%]
1	01-074-5169	71	Aluminum Copper	0.737	Al0.0565 Cu0.9434	100

The XRD pattern of EN-31 machined with tungsten-copper electrode in without powder mixing dielectric has been shown in figure 8.2. XRD shows the traces carbon, iron, aluminium and copper. Carbon acts as a hardening agent, preventing dislocations in the iron atom crystal lattice from sliding past one another. Carbon imparts strength, hardness and wear resistance to workpiece but reduces ductility and toughness. As the carbon content increases workpiece become harder and stronger, also become more brittle. The maximum solubility of carbon in iron in austenite region; higher concentrations of carbon

or lower temperatures will produce cementite. The presence of copper is beneficial to corrosion resistance. Peak list and pattern list are given shown in the Table 8.3 and Table 8.4 respectively. After the spectrometry analysis the carbon percentage increases from 0.35% to 0.94% and copper increases0.03% to 0.08%.

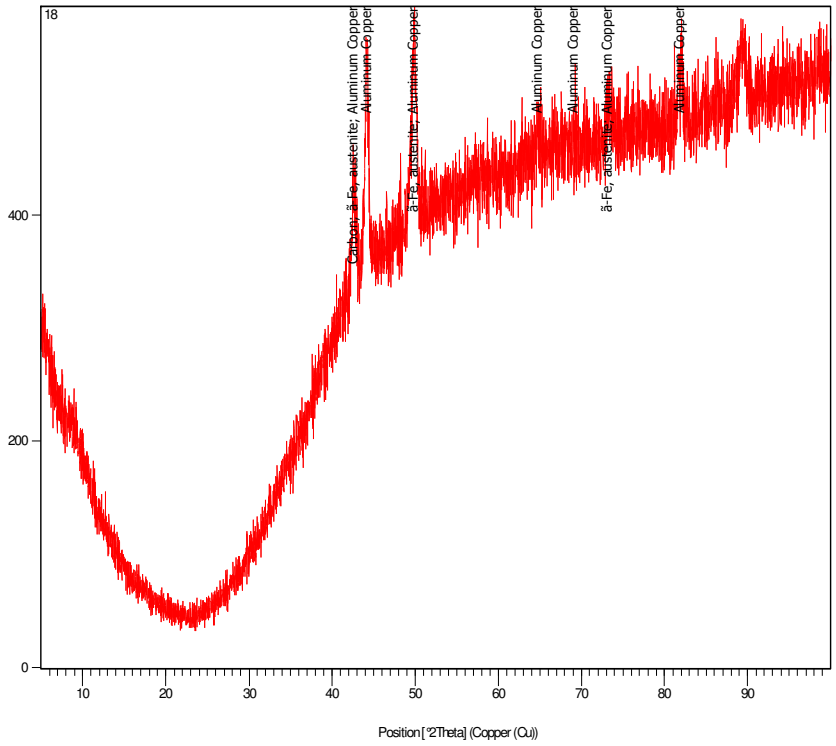

Fig 8.2 XRD pattern of EN31 workpiece machined with Copper electrode in Kerosene with aluminium powder mixing (current 8 Amp, pulse off 38, pulse On50)

Table 8.2 Pattern List

Visible	Ref. Code	Score	Compound Name	Scale Factor	Chemical Formula	Semi Quant [%]
1	00-054-0501	15	Carbon	0.509	C	-
2	00-052-0513	17	ã-Fe, austenite	0.720	Fe	-
3	01-072-3506	19	Aluminum Copper	0.726	Al35.472 Cu47.792	-

8.2.2 XRD ANALYSIS OF HOT DIE STEEL (H11)

The XRD pattern of H11 machined copper in kerosene oil with graphite powder mixing in dielectric medium is shown in the Figure 8.3. The pattern shows the presence of Cohenite synthetic (Fe_3C). The cohenite (Fe_3C) compound formed which increase the hardness of surface. Peak list and pattern list are given shown in the Table 8.7 and Table 8.8 respectively. After the spectrometer analysis, it was observed that carbon percentage increased from 1.60% to 1.65%.

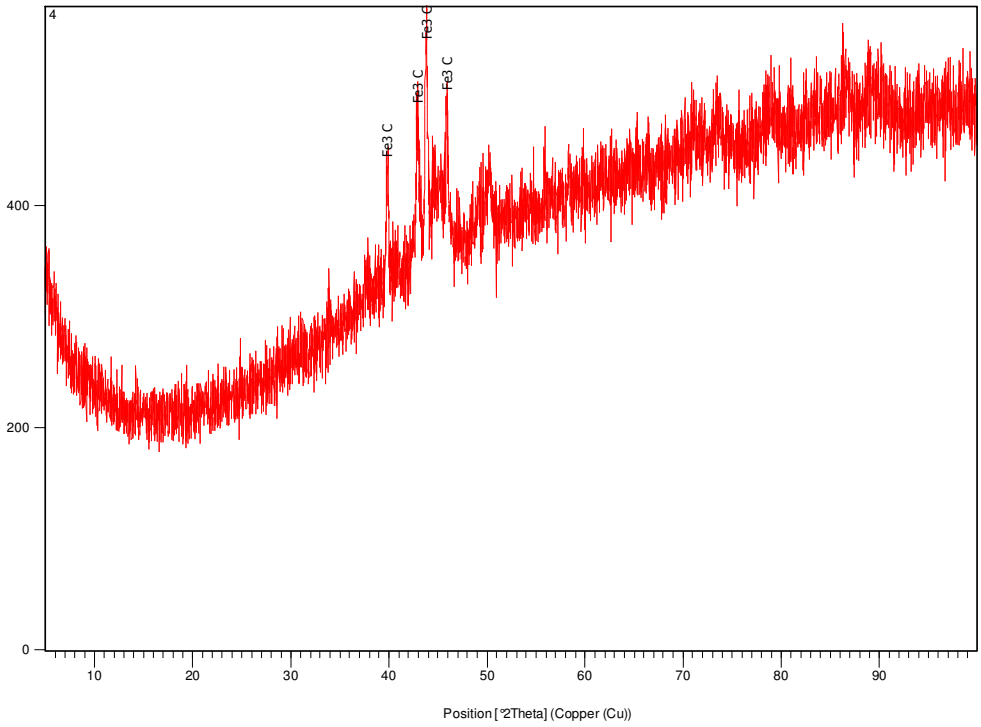

Figure 8.3: XRD pattern of H11 machined with Cu electrode in kerosene oil with graphite powder mixing. (I=2 Amp, Pulse on= 100µs, Pulse off=38µs)

Table 8.3: Pattern list

Visible	Score	Compound Name	Scale Factor	Chemical Formula	SemiQuant [%]
1	10	Cohenite – synthetic	1.274	Fe_3 C	100

The XRD pattern of H11 machined with copper electrode in kerosene oil with graphite powder mixing in dielectric medium is shown in the Figure 8.4. The pattern shows the presence of Cohenite synthetic (Fe_3C).The cohenite is rich iron meteorites, have carbon contents not more than 0.4-0.6% less than α-γ eutectoid composition. The presence of cohenite increases the hardness. Fe_3C compound formed which increase the hardness of surface. Peak list and pattern list are given shown in the Table 8.9 and Table 8.10 respectively. After the spectrometer analysis it was observed that copper increased at machined surface from 0.01% to 0.42% and carbon increased by 0.39% to 0.65%.

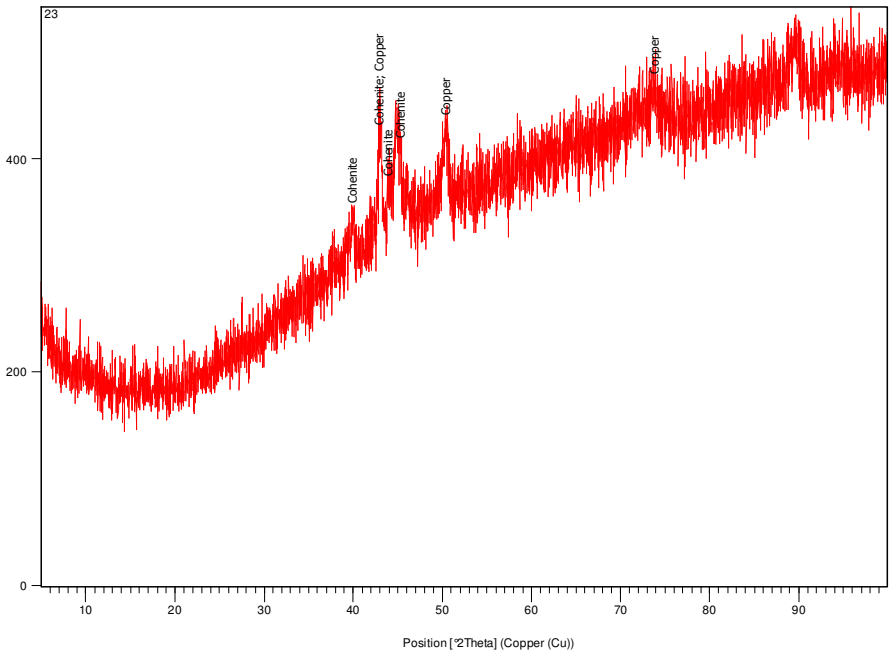

Figure 8.4: XRD pattern of H11 machined with W-Cu electrode in kerosene oil with graphite powder mixing. (I=8 Amp, Pulse on= 50µs, Pulse off=57µs)

Table 8.4 Pattern list

Visible	Ref. Code	Score	Compound Name	Scale Factor	Chemical Formula	SemiQuant [%]
1	00-006-0688	17	Cohenite	0.693	Fe_3C	-
2	01-070-3038	18	Copper	0.498	Cu	-

The XRD pattern of H11 machined with copper electrode with aluminium powder mixing in kerosene oil as dielectric has been shown in figure 8.5.The XRD pattern shows the traces of aluminium, chromium and cohenite. Aluminium decreases surface roughness value and helps to improve the hardness and strength of steel. The workpiece becomes highly resistant to corrosion with presence of chromium. The presence of cohenite increases the hardness. Peak list and pattern list are given shown in the Table 8.11 and Table 8.12 respectively. After the spectrometer analysis it was observed presence of aluminium on machined surface and copper was also increased from 0.01% to 0.35%.

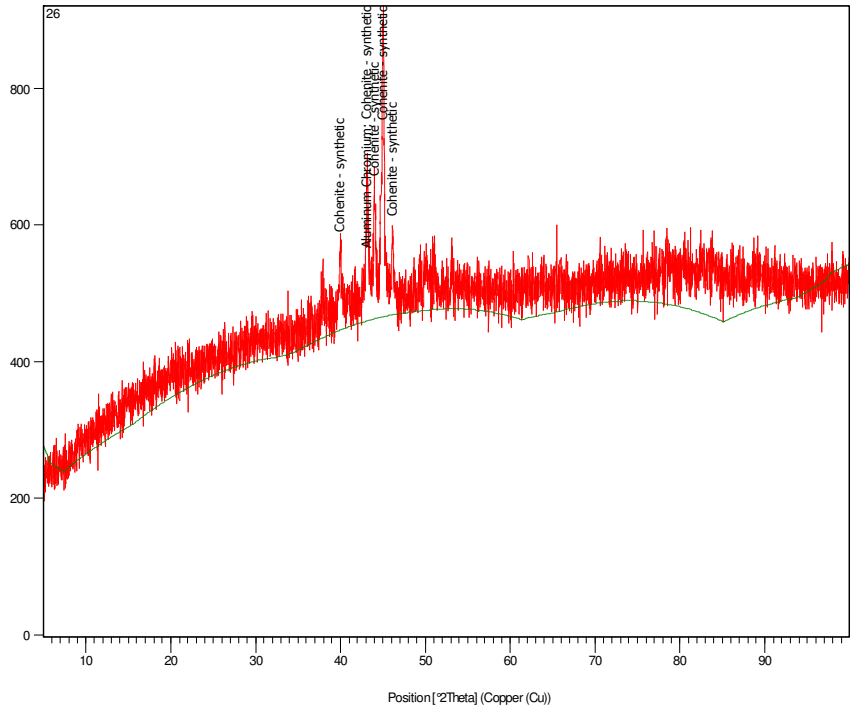

Figure 8.5: XRD pattern of H11 machined with Cu electrode in kerosene with aluminium powder mixing. (I=8 Amp, Pulse on= 50µs, Pulse off=38µs)

Table 8.12: Pattern List

Visible	Ref. Code	Score	Compound Name	Scale Factor	Chemical Formula	SemiQuant [%]
1	00-006-0688	17	Cohenite	0.693	Fe_3C	-
2	01-070-3038	18	Copper	0.498	Cu	-

8.2.1 XRD Analysis of HCHCr

The XRD pattern of HCHCr which has been machined with copper electrode in with aluminium powder mixing dielectric has shown in figure 8.6. The XRD pattern shows presence of aluminium, copper, tin and Heptachromium tricarbide (Cr_7C_3). Aluminum, copper and tin helps to improve the wear and friction resistance. Heptachromium tricarbide compound helps to increase hardness of the workpiece and decreases the wear of workpiece. Peak list and pattern list are given shown in the Table 8.13 and Table 8.14 respectively. . After the spectrometer analysis it was observed presence of aluminium on machined surface and copper was also increased from 0.01% to 0.23%.

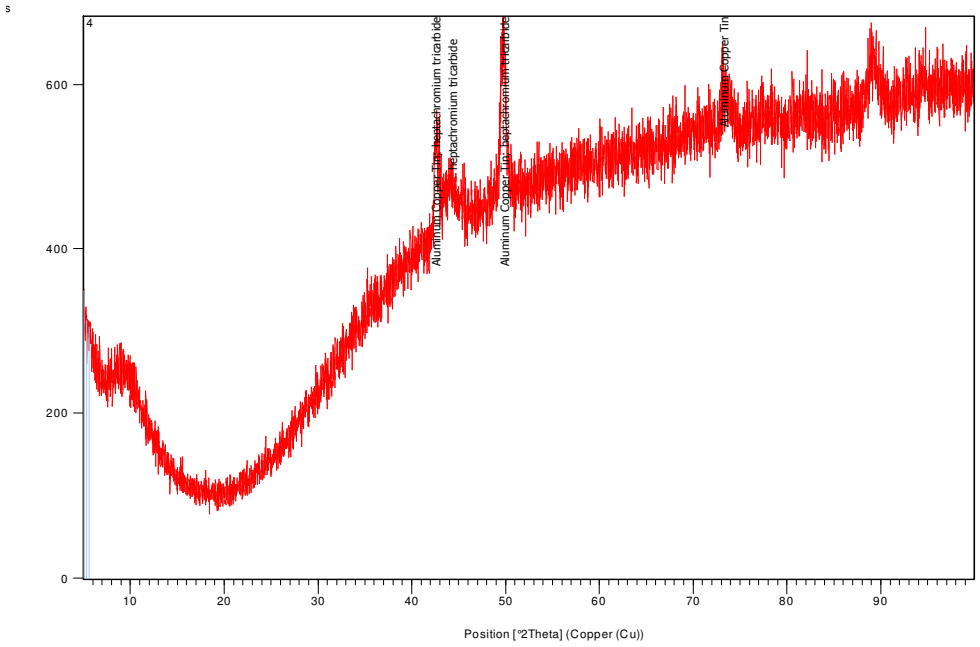

Fig 8.6: XRD pattern of HCHCr workpiece machined with Tungsten-Copper electrode in Kerosene with without powder mixing (current 8 Amp, pulse off 57, pulse On100)

Table 8.6: Pattern List

Visible	Ref. Code	Score	Compound Name	Scale Factor	Chemical Formula	Semi Quant [%]
1	01-074-5187	31	Aluminum Copper Tin	0.486	Al0.05 Cu0.9 Sn0.05	--
2	00-036-1482	10	Heptachromium tricarbide	0.191	$Cr_7 C_3$	--

The XRD pattern of HCHCr machined with tungsten-copper electrode with graphite powder mixing in transformer oil as dielectric medium is shown in the Figure 8.7. The pattern shows the some traces of chromium iron carbide and iron carbide. The chromium forms solid solution with iron and has high solubility in α-ferrite as well γ-iron. The iron atoms of cementite phase can be substitute in chromium atoms and forms carbides. The chromium carbides and chromium iron carbides formed by carburization of chromium at high temperature. The presence of chromium carbide improves the high temperature properties and corrosion resistance and also increases hardenability. The thermal expansion coefficient of chromium carbide helps to reduce the mechanical stress buildup at the layer boundary. . After the spectrometer analysis it was observed carbon was increased from 1.6% to 1.8%.

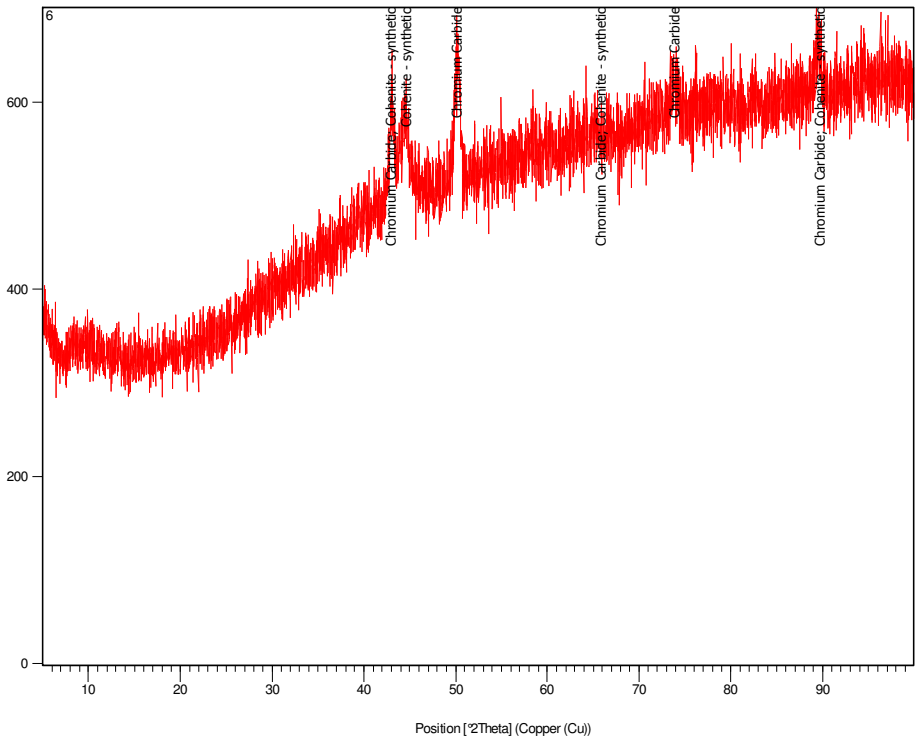

Figure 8.7: XRD pattern of HCHCr machined with W-Cu electrode in Transformer oil with graphite powder mixing. (I=5 Amp, Pulse on= 100µs, Pulse off=38µs)

Table 8.7: Pattern List

Visible	Ref. Code	Score	Compound Name	Scale Factor	Chemical Formula	SemiQuant [%]
1	01-075-2661	17	Chromium Carbide	0.802	$Cr_{23} C_6$	54
2	01-074-3857	6	Cohenite - synthetic	0.413	$Fe_3 C$	46

The XRD pattern of HCHCr machined with copper electrode in graphite powder mixed kerosene dielectric is shown in the Figure 8.8. The XRD pattern shows the traces of chromium carbide and carbon. Chromium Carbide helps to impart strength and hardness of workpiece. Chromium Carbide also improves the high temperature properties of the machined surface. The carbon imparts the strength, wear resistance and hardness but reduces the toughness and ductility. The carbon has contributed by electrode wear as well as the pyrolysis of the dielectric. . After the spectrometer analysis it was observed that carbon was increased from1.6% to 1.8%.

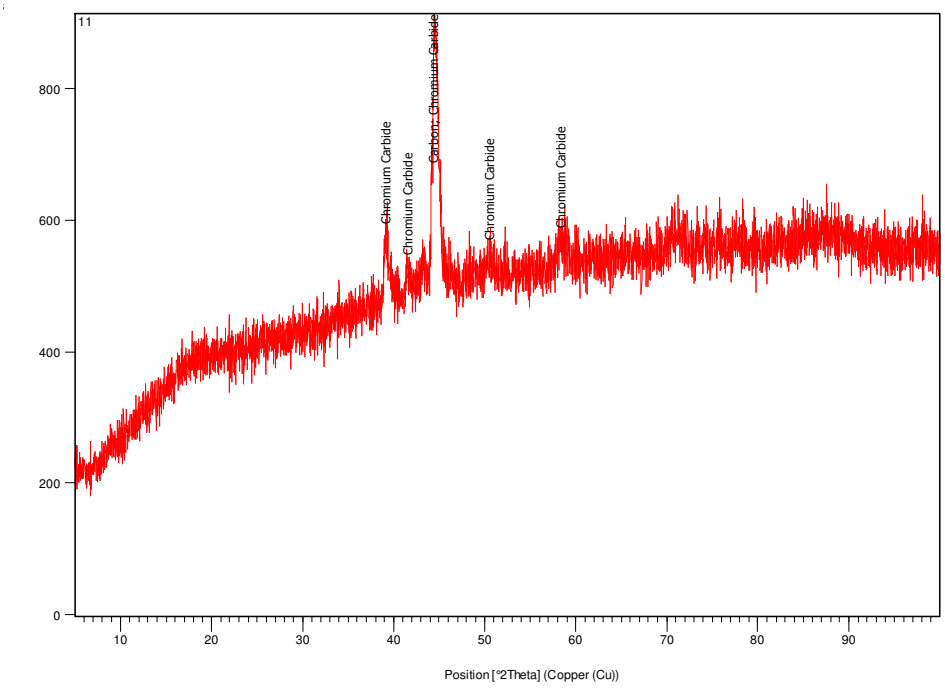

Figure 8.8: XRD pattern of HCHCr machined with Cu electrode in kerosene oil with graphite powder mixing. (I=2 Amp, Pulse on= 50µs, Pulse off=57µs)

Table 8.8: Pattern list

Visible	Ref. Code	Score	Compound Name	Scale Factor	Chemical Formula	SemiQuant [%]
1	01-080-0017	28	Carbon	0.488	C	43
2	01-089-5902	22	Chromium Carbide	0.596	$Cr_7 C_3$	57

Table 8.9: Results of XRD analysis

Work-piece	Electrode	Dielectric	Powder	XRD Analysis
EN31	W-Cu	Kerosene	Aluminium	• shows that traces of aluminium and copper • helps to decrease surface roughness value • improve the hardness and strength
EN31	W-Cu	Kerosene	No	• shows the traces carbon, iron, aluminium and copper • carbon imparts strength, hardness and wear resistance • copper improves corrosion resistance • aluminium and copper helps to improve the hardness and strength of steel.
H11	Cu	Kerosene	Graphite	• shows the presence of cohenite synthetic (Fe_3C). • The cohenite (Fe_3C) compound formed which increase the hardness of surface.
H11	Cu	Kerosene	Graphite	• shows the presence of cohenite synthetic • cohenite formation increases the hardness • copper improves thermal properties
H11	Cu	Kerosene	Aluminium	• shows the traces of aluminium, chromium and cohenite. • presence of chromium imparts resistant to corrosion.
HCHCr	Cu	Kerosene	Graphite	• shows presence of aluminium, copper, tin and Heptachromium tricarbide (Cr_7C_3).

				• Aluminum, copper and tin helps to improve the wear and friction resistance. • Cr_7C_3 helps to increase hardness of the workpiece.
HCHCr	W-Cu	Transformer oil	Graphite	• shows the traces of chromium iron carbide and iron carbide. • presence of chromium carbide improves the high temperature properties and corrosion resistance. • chromium carbide helps to reduce the mechanical stress buildup at the layer boundary.
HCHCr	Cu	Kerosene	Graphite	• XRD pattern shows the traces of chromium carbide and carbon. • carbon imparts the strength, wear resistance and hardness but reduces the toughness and ductility.

8.3 MICROSTRUCTURE ANALYSIS

Microstructure analysis was carried out on some selected samples using Scanning Electron Microscope to study the change in the microstructure after machining. The samples were prepared as per standard before SEM analysis on three different magnifications, namely, 200×, 500× and 1000×.

8.3.1 Method of Sample Preparation for SEM

The steps for the sample preparation for SEM are given below:

1) Cut out the samples in 14×16mm on wire cut EDM.
2) Clean the surface with wire brush.
3) Clean the samples with acetone.
4) Clean the samples with ultrasonic gel to remove any dust particles.

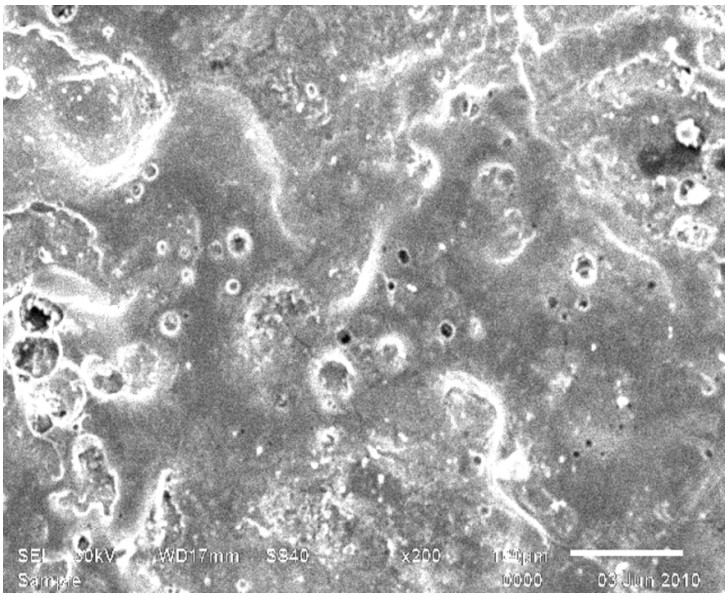

Figure 8.9: SEM micrograph at 200× of EN 31 machined with W-Cu electrode without mixing in transformer oil (I 8Amp, pulse on time 100µs, pulse off time 57µs)

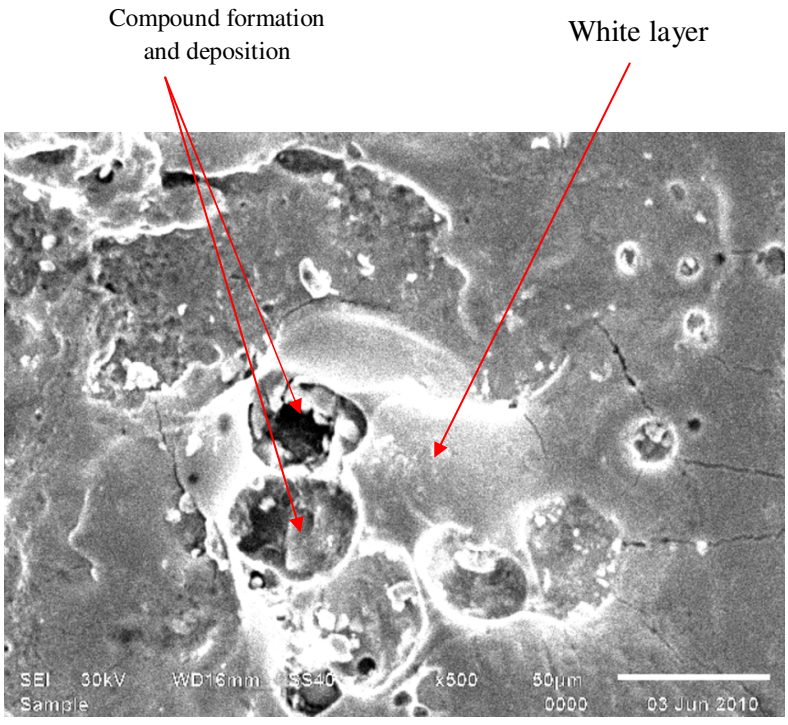

Figure 8.10: SEM micrograph at 500× of EN 31 machined with W-Cu electrode without mixing in transformer oil (I 8Amp, pulse on time 100µs, pulse off time 57µs)

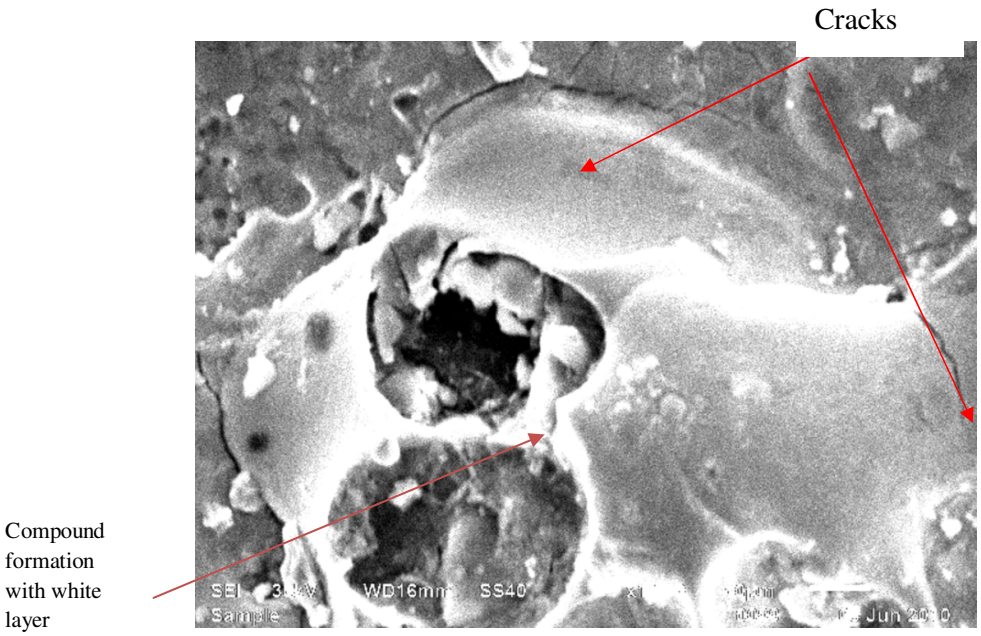

Figure 8.11: SEM micrograph at 1000× of EN 31 machined with W-Cu electrode without mixing in transformer oil (I 8Amp, pulse on time 100µs, pulse off time 57µs)

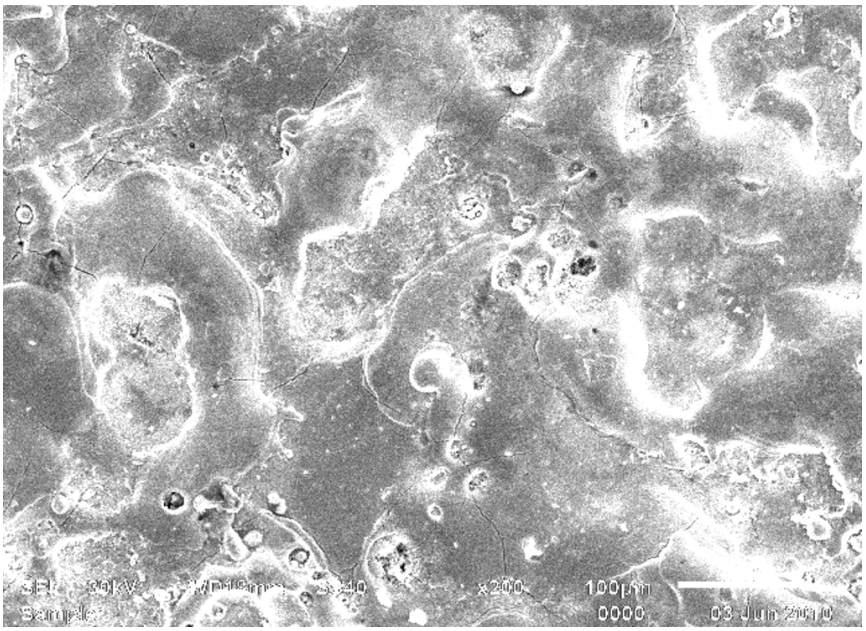

Figure 8.12: SEM micrograph at 200× of H11 machined with copper electrode in graphite mixed in kerosene (I 2Amp, pulse on time 100µs, pulse off time 38µs)

Figure 8.13: SEM micrograph at 500× of H11 machined with copper electrode in graphite mixed in kerosene (I 2Amp, pulse on time 100µs, pulse off time 38µs)

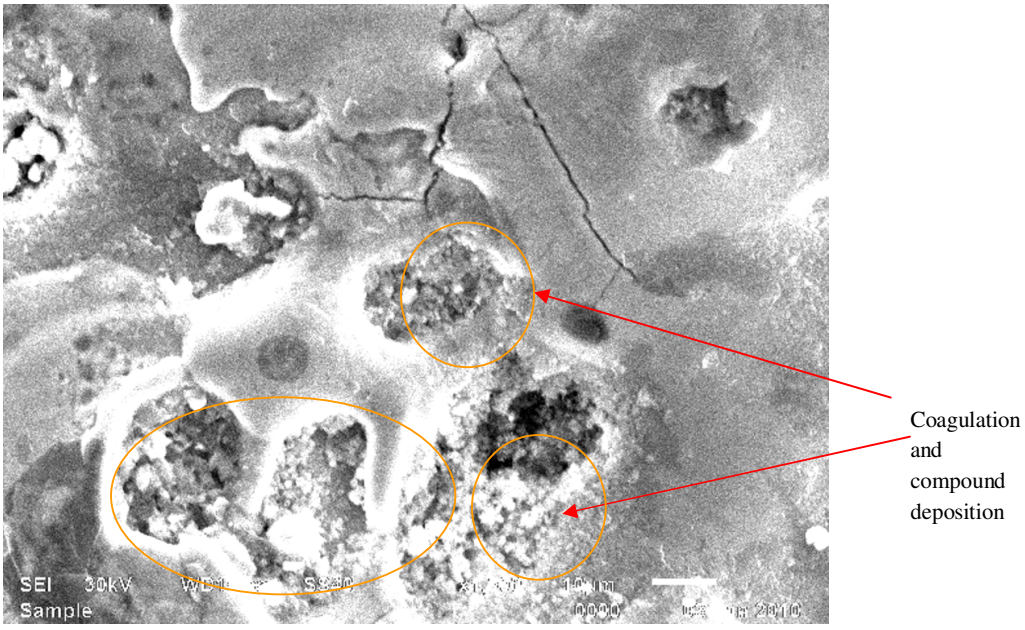

Figure 8.14: SEM micrograph at 1000× of H11 machined with copper electrode in graphite mixed in kerosene (I 2Amp, pulse on time 50µs, pulse off time 57µs)

SEM micrograph at 200×, 500× and 1000× of EN31 machined with tungsten-copper electrode in without powder mixed in transformer oil (I=8 Amp, pulse on 100µs, pulse off 57µs) are shown in the Figure 5.10-5.12 which shows formation of cracks on the white layer. The crater size is more when machined at 8Amp without powder in dielectric. Crater size increased with increase in current. There is recast layer is formed on the machined surface. The surface is rough because of debris which are not flashed away completely from the machining zone. Different layers which were formed in the machined are shown in the Figure 5.22. The discharge between the workpiece and tool melts the metal and metal vaporizes which creating thermally altered layers of the cavity. The white layer readily formed and remains stable on the surface. The white layer is typically fine grained and hard and alloyed with carbon from the material transferred from electrode. In the white layer material was taken to molten state but neither ejected nor removed by flushing action of dielectric. The depth of this top melted zone depends upon the pulse energy and duration. The carbon content in the layer can also be affected by carburization from the flushing fluid or electrode material, but decarburization also occurs. The action of EDM altered the metallurgical structure and characteristics in recast layer. The recast layer is formed by the un-expelled molten metal solidifying in the craters. The white layer is densely infiltrated with carbon to the point that its structure is different than that of the base material.

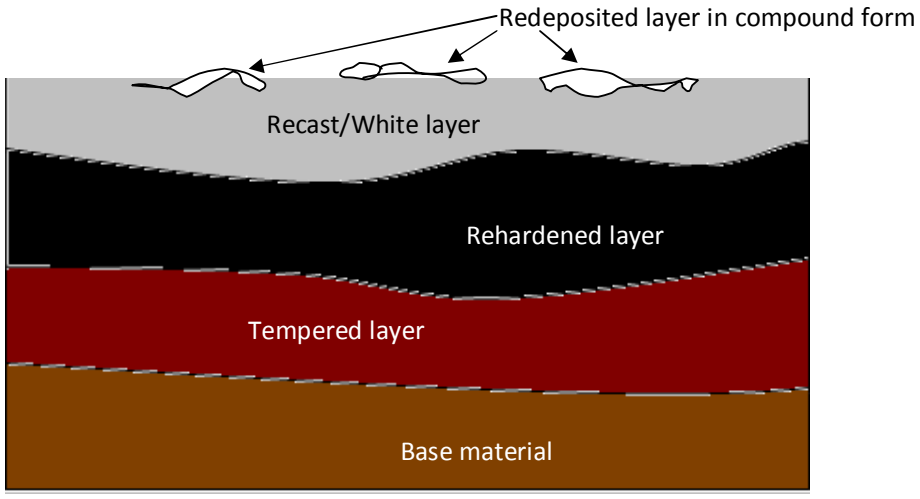

Figure 8.15: Different layers formed on the EDM machined surface

The white layer consists mainly of martensite, residual austenite, and some undissolved carbide. In addition, the high-temperature conditions induced during the EDM procedure prompt some carbon atoms from the kerosene dielectric fluid to migrate into the surface of the machined component. As the thickness of the white layer increases, it becomes more brittle and therefore fractures more readily. As a result, the fatigue life reduces as the thickness of the white layer increases. The next layer is rehardened layer, in this layer temperature has risen above the hardening temperature and martensite formed and which become more hard and brittle. The last layer which is formed that is tempered layer in which material has not heated up to reach hardening temperature and tempering back occurred. This layer retains the metallurgical structure same as the base material because temperature absorbed is not to the level to change the structure. Below the tempered layer is the base material and this is unaffected by EDM process. When workpiece material was machined without powder in the dielectric then crater size is more and more in the depth. Increasing the current or reducing the pulse-on duration suppresses the formation of surface cracks in the machined surface. The fundamental cause of cracking lies in the existence of the internal stresses which are created at the time of the machining operation. The surface density and the depth of these cracks are directly related to the machining conditions, more increase the current (2Amp-8Amp), more the appearance frequency of these cracks increases. The cracks are formed with the result of high thermal stresses prevailing at the workpiece surface as the latter was cooled at fast rate after the discharge.

CHAPTER 9

RESULTS, CONCLUSIONS AND RECOMMENDATIONS

9.1 RESULTS

The effect of parameters i.e. workpiece, dielectric, electrode, pulse on time, pulse off time, current, powder and some of their interactions were evaluated using ANOVA and factorial design analysis. The purpose of the ANOVA was to identify the important parameters in prediction of MRR, TWR, micro hardness, surface roughness. Some results consolidated from ANOVA and plots are given below:

9.1.1 MRR

Current was found to be the most significant factor highest (F value 186.82), and its contribution to MRR was 45.86% and followed by pulse on time (F value89.05),workpiece(F value 33.50) pulse off time (F value16.28) and powder (F value 11.30) were the factors that significantly affected the MRR which had contribution to MRR was 21.53%, 7.71%, 3.42%, 2.12% respectively. The interaction between electrode and powder (F value 47.16) was found to be significant which contributes 11.11%.

All others factors, namely, dielectric and electrode and other interactions were found to be insignificant to MRR.

For S/N ratio pulse on time and current were found to be significant to MRR for reducing the variation.

The best results for MRR would be achieved best result when EN-31workpicee is machined at pulse on time100 μs, pulse off time 38μs, current 5Amp with copper-tungsten electrode and aluminium powder mixing in dielectric. With 99% confidence interval mean value of MRR was found to be $28.32 \pm 0.37 mm^3/min$.

9.1.2 TWR

Current (F value 149.06), powder (F value 13.39), electrode (F value 12.54) were the significant factors which affects the TWR.

Factors, namely, workpiece material, dielectric, pulse on time, pulse off time and interactions were found to be insignificant for TWR.

In S/N ratio, the current is the most significant in affecting TWR followed by pulse on time, electrode in reducing the variation. The interaction between workpiece and electrode also affects TWR.

The best results for TWR would be suggested if EN31 workpiece machined at current 2 Amp and pulse on time10 μsec with tungsten-copper electrode without powder mixing in dielectric. The mean value with 99% confidence interval was found to be 1.237±0.07 mm^3/min.

9.1.3 MICRO HARDNESS

Powder (F value 30.34), pulse on time (F value 17.27), current (F value 14.47) and interaction between workpiece and powder were the factors that has significantly affected the micro hardness at non-deposited region.

The estimated mean value of micro hardness at non-deposited region when current 8Amp and pulse on time 50 μsec with graphite powder mixing in dielectric were considered with 99% confidence interval was found to be 772±8.18 *hvn*.

Current (F value 117.13), powder (F value 39.25) are significant factors were found to be significant for micro hardness at deposited black region. Also, the interaction between workpiece and electrode was found to be significant for the micro hardness at deposited region. All other factors studied in trials were found to be insignificant.

The best value of micro hardness was to be found when HCHCr workpiece was machined with tungsten-copper electrode at current of 8Amp in graphite powder mixed dielectric was considered with 99% confidence interval was found to be 1133±6.15 *hvn*.

Current (F value 108.8), powder (F value 54.9), workpiece (F value 38.6) and pulse on time (F value 16.6) were found to be significant for micro hardness at deposited red region. The interaction between electrode and powder is significant for the micro hardness at deposited red region.

The estimated mean value micro hardness was obtained when H11 workpiece machined at pulse off 100 µs and current at 8Amp with tungsten-copper electrode in graphite mixed dielectric. The estimated mean value of micro hardness of red region considered with 99% confidence interval found to be 1015±4.31 *hvn*.

9.1.4 SURFACE ROUGHNESS (R_a)

The current, pulse on time, powder, workpiece and electrode are input parameters which effects the surface roughness. Current (F value 764.81), pulse on time (F value 408.82), powder (F value 150.97), workpiece (F value 91.02), electrode (F value 30.26) were found to be significant in surface roughness at center. All interactions studied during trials were found to be significant for surface roughness. Current and pulse on time were observed to be significant for left position and right position. The interaction workpiece × electrode was found to be significant for roughness of right position.

The estimated mean values of roughness considered with 99% confidence interval found to be 0.33±0.038 micron (Center position), 3.31±0.16 micron (Left position) 1.17±0.16 micron(Right position)

9.1.5 SURFACE PROPERTIES

EN31

The presence of aluminium and copper was found on the machined surface, when workpiece was machined with aluminium powder in kerosene which decreases surface roughness value. Also, aluminium and copper helps to improve the hardness and strength of steel. Hardness, strength and wear resistance was improved when it was machined with tungsten-copper electrode in without powder mixing dielectric.

Hot Die Steel (H11)

Cohenite has been formed on the surface of H11 as machined with tungsten copper electrode in graphite mixed kerosene oil, which contributed to increase the hardness of material. Chromium and aluminium has been formed when machined with copper electrode in aluminium powder mixed kerosene.

HCHCr

Chromium carbide has been formed on the surface of HCHCr, which improves the high temperature properties, corrosion resistance and hardenability. Also, iron carbide has been formed, which improves hardness and strength.

9.1.6. MICROSTRUCTURE ANALYSIS

SEM micrograph carried out on selected samples at three different magnifications, namely at 200×, 500× and 1000×. It was observed that crater size was more when machined at 8Amp without powder in dielectric as compared to when machined with powder mixed in dielectric. The white layer formed readily and remained stable on the surface. The white layer is typically fine grained and hard and is alloyed with carbon from the material transferred from electrode. With increase in current micro cracks on the white layer also increased. The fundamental cause of cracking lies in the existence of the internal stresses which were created at the time of the machining operation. The uniform dispersion of the particles and less micro cracks on the surface of machined was observed when machined with aluminium powder mixed dielectric.

9.2 CONCLUSIONS

The present study was carried out to study the effect of input parameters on the MRR, TWR, surface roughness, micro hardness and on the surface properties. The following conclusions have been drawn from the study:

- The MRR and TWR are mainly affected by the current and powder.
- With mixing of graphite powder MRR can be decreased.
- Higher micro hardness can be achieved with the mixing of graphite powder in dielectric.
- All three workpiece materials showed improvement in micro hardness when machining has been carried out with graphite powder and the highest value of micro hardness 1133 *hvn* has been achieved in HCHCr.
- Micro hardness also affected with current.
- Surface roughness was mainly affected by the current and pulse on time. At higher value of current causes the more surface roughness. Higher surface finish can be achieved value can be achieved at lower current.
- Surface roughness can be decreased with aluminium powder.
- The dielectric medium is the least effective in roughness and micro hardness.
- Aluminium, copper and cohenite were found on the surface of workpiece material when machining was carried out with tungsten-copper electrode and with graphite or aluminium suspended in the dielectric medium.
- With addition of powder in dielectric medium, crater size reduced and with aluminium crater size was less as compared with graphite powder.
- Thickness of cracks increased with increase in current.
- Urea has no effect on surface properties due lack of solubility in transformer oil.

9.3 RECOMMENDATIONS FOR FUTURE WORK

Only three workpiece materials, namely, HCHCr, H11 and EN31 had been used. Other materials such as titanium, OHNS die steel and tungsten hot work die steel can be machined. Machining was carried out only with two powders, graphite and aluminium. Other powders, namely, silicon, nickel, vanadium can be used. Particle size and powder concentration can also be varied.

APPENDIX-A

TECHNICAL SPECIFICATION OF EDM MACHINE

The experiment has been conducted on Electrical Discharge Machine model T-3822M, Victory Electromech, Kolhapur, India. Technical data of machine is as under:

1. Electrical Data

Supply voltage	415V, 3Ø, 50 Hz
Connected load	3 KVA
Open gap voltage output	135±5% V
Max. Machine current	12Amp
Current range	3 ranges of 4Amp each
Current adjustment	0-4Amp in each current range

2. *Machine Tool*

Height	1300mm
Width	730mm
Depth	840mm
Net weight	325 kg
Quill travel	150mm

3. Work Tank

Length	600mm
Width	350mm
Height	240mm

APPENDIX-B

SPECIFICATIONS OF MEASURING INSTRUMENTS

1. OPTICAL EMISSION SPECTROMETER

Make and model	Baird, DV-6, USA
Base	Iron, Aluminum, Copper
Medium	Argon gas
Accuracy	0.0001%

2. PERTHOMETER

Make and model	Mahr. M4Pi, Germany
Measurement method	Stylus
Profile resolution	100nm
Cut-off wavelength	0.8mm
Tracing length	4.8mm

3. MICRO HARDNESS TESTER

Make and model	Metatech, MVH-2, Pune, India,
Software used	Quantimet
Load	1 kg
Dwell time	20 sec

4. SCANNING ELETRON MICROSCOPE

Make and model	JSM-840A Joel, Japan
Magnification range	10× to 3,00,000×

5. X-RAY DIFFRACTION TESTER

Make and model	ME 210 LA 2, Rigaku corporation
Scan speed	5^0/minute
Range of 2θ	5^0 to 100^0

APPENDIX -C

TECHNICAL SPECIFICATIONS OF DIELECTRIC MEDIUM

1. TRANSFORMER OIL

Appearance	Clear, transparent, light
Density ($g/cm^{3)}$	0.89
Kinematic Viscosity (cSt)	27
Interfacial Tension, N/m	0.04
Flash Point (^oC)	140
Pour Point (^oC)	-6
Corrosive Sulphur	Non Corrosive
Electrical Strength, KV	50
Water content (max)	15 ppm
Specific Resistance (Ohm-cm)At 27^oC	3200×10^{12}

2. KEROSENE OIL

Appearance	Clear, transparent, light
Density (kg/m^3)	817.15
Flash Point (^0C)	40
Boiling Point (^0C)	600
G.C.V. (Kcal/kg)	11200
Viscosity (centistokes)	2.71

REFERENCES

[1] Marafona J.D., Jo A.A. (2009), "Influence of workpiece hardness on EDM performance", *International Journal of Machine Tools & Manufacture,* Vol. 49, pp. 744–748.

[2] Ho K.H., Newman S.T. (2003), "State of the art electrical discharge machining (EDM)", *International Journal of Machine Tools & Manufacture*, Vol.43, pp. 1287–1300.

[3] McGeough J.A. (1988), "Advanced Methods of Machining", Chapman and Hall, USA, ISBN 0-412-31970-5.

[4] Panday P.C., Shan H.S. (2007), "Modern Machining Processes", Tata McGraw-Hill, New Delhi, India, ISBN -07-096553-6.

[5] Kunieda M., Lauwers B., Rajurkar K. P., Schumacher B. M. (2005), "Advancing EDM through Fundamental Insight into the Process", *Journal of Materials Processing Technology, Annals of CIRP,* Vol. 54(2), pp. 599-622.

[6] Lin J.L., Lin C.L. (2002), "The use of the orthogonal array with grey relational analysis to optimize the electrical discharge machining process with multiple performance characteristics", *International Journal of Machine Tools & Manufacture*, Vol. 42, pp. 237–244.

[7] Jain V. K. (2004) "Advanced Machining Processes", Allied Publishers, New Delhi, India, ISBN 81-7764-294-4.

[8] Kumar S., Singh R., Singh T.P., Sethi B.L. (2009), "Surface modification by electrical discharge machining: A review",*Journal of Materials Processing Technology,* Vol. 209, pp. 3675–3687.

[9] Leao F. N., Pashby I. R. (2004), "A review on the use of environmentally-friendly dielectric fluids in electrical discharge machining", *Journal of Materials Processing Technology*, Vol. 149, pp. 341–346.

[10] Abbas N. M., Solomon D. G., Bahari M. F. (2007),**"**A review on current research trends in electrical discharge machining", *International Journal of Machine Tools & Manufacture,* Vol. 47, pp.1214–1228.

[11] Wu K. L., Yan B. H., Huang F. Y, Chen S.C. (2005) ,"Improvement of surface finish on SKD steel using electro-discharge machining with aluminum and surfactant added dielectric", *International Journal of Machine Tools & Manufacture,* Vol.45, pp. 1195–1201.

[12] Uno Y., Okada A., Cetin S. (2001), "Surface Modification of EDMed Surface with Powder Mixed Fluid", *2nd International Conference on Design and Production of dies and molds*.

[13] Pecas P., Henriques E. (2008), "Effect of the powder concentration and dielectric flow in the surface morphology in electrical discharge machining with powder-mixed dielectric (PMD-EDM)" , *Int J Adv Manuf Technol* ,Vol. 37, pp. 1120–1132.

[14] Kansal H.K., Singh S., Kumar P. (2005) , "Parametric optimization of powder mixed electrical discharge machining by response surface methodology", *Journal of Materials Processing Technology,* Vol. 169, pp. 427–436.

[15] Chiang K.T. (2008) , "Modeling and analysis of the effects of machining parameters on the performance characteristics in the EDM process of Al_2O_3+TiC mixed ceramic", *Int J Adv Manuf Technol* Vol. 37, pp. 523–533.

[16] Yan B.H., Tsai H. C., Huang F.Y. (2005), "The effect in EDM of a dielectric of a urea solution in water on modifying the surface of titanium", *International Journal of Machine Tools & Manufacture,* Vol. 45, pp. 194–200.

[17] Prihandana G. S., Mahardika M., Hamdi M., Wong Y.S., Mitsui K. (2009), "Effect of micro-powder suspension and ultrasonic vibration of dielectric fluid in micro-EDM processes—Taguchi approach", *International Journal of Machine Tools & Manufacture*, Vol. 49, pp. 1035–1041.

[18] Chowa H.M., Yangb L.D., Lina C.T., Chena Y.F. "The use of SiC powder in water as dielectric for micro-slit EDM machining", *Journal of materials processing technology,* Vol. 195, pp. 160–170.

[19] Pecas P., Henriques E. (2008), "Electrical discharge machining using simple and powder-mixed dielectric: The effect of the electrode area in the surface roughness and topography", *Journal of materials processing technology*, Vol. 200, pp. 250–258.

[20] K.Y.Kung, J.T. Horng, K.T.Chiang (2009) "Material removal rate and electrode wear ratio study on the powder mixed electrical discharge machining of cobalt-bonded tungsten carbide" *Int J Adv Manuf Technol* ,Vol. 40, pp. 95–104.

[21] Pecas P., Henriques E. (2003),"Influence of silicon powder-mixed dielectric on conventional electrical discharge machining", *International Journal of Machine Tools & Manufacture* Vol. 43, pp. 1465–1471.

[22] Furutani K., Sato H., Suzuki M. (2009) "Influence of electrical conditions on performance of electrical discharge machining with powder suspended in working oil for titanium carbide deposition process" *Int J Adv Manuf Technol* , Vol. 40, pp. 1093–1101.

[23] Wong Y. S, Lim L.C, Rahuman I., Tee W. M, (1998), "Near-mirror-finish phenomena in EDM using powder-mixed dielectric", *Journal of Material Processing Technology,* Vol. 79, pp. 30-40.

[24] Che Haron C.H., Ghani J.A., Burhanuddin Y. , Seong Y.K., Swee C.Y. (2008) "Copper and graphite electrodes performance in electrical-discharge machining of XW42 tool steel", *Journal of materials processing technology*, Vol. 201, pp. 570–573.

[25] Tsai H.C., Yan B.H., Huang F.Y. (2003), "EDM performance of Cr/Cu-based composite electrodes", *International Journal of Machine Tools & Manufacture*, Vol. 43, pp. 245–252.

[26] Simao J., Lee H.G., Aspinwall D.K., Dewes R.C., Aspinwall E.M. (2003), "Workpiece surface modification using electrical discharge Machining", *International Journal of Machine Tools & Manufacture,* Vol. 43, pp.121–128.

[27] Mohri N., Satio N., Tsunekawa Y., Kinoshtia N. (1993), " Metal surface modification by electrical discharge machining with composite electrode", *CIRP Annals Manufacturing Technology,* Vol 42, pp. 219-222.

[28] Koshy P., Jain V.K., Lal G.K. (1993), "Experimental investigation into electrical discharge machining with a rotating disk electrode", *Precision Engineering,* Vol. 15, pp. 6-15.

[29] Kanlayasiri K., Boonmungb S. (2007), "Effects of wire-EDM machining variables on surface roughness of newly developed DC 53 die steel: Design of experiments and regression model", *Journal of Materials Processing Technology*, Vol. 192–193, pp. 459–464.

[30] Wanga C. C., Chowb H. M., Yangb L. D., Luc C. T. (2009), "Recast layer removal after electrical discharge machining via Taguchi analysis: A feasibility study**"**, *Journal of Materials Processing Technology ,* Vol. 209, pp. 4134–4140.

[31] Keskin Y., Halkaci H. S., Kizil M. (2006), "An experimental study for determination of the effects of machining parameters on surface roughness in electrical discharge machining", *Int J Adv Manuf Technol*, Vol. 28, pp. 1118–1121.

[32] Singh S., Maheshwari S., Pandey P.C. (2004) ,**"**Some investigations into the electric discharge machining of hardened tool steel using different electrode materials", *Journal of Materials Processing Technology*, Vol.149, pp. 272–277.

[33] Ross Phillip J., (1990), “Taguchi Techniques for Quality Engineering”, McGraw-Hill, ISBN 0-07-053866-2

[34] Krawczyk J., Pacyna J., (2006), “Effect of the tool microstructure on the white layer formation”, *Journal of Achievements in Materials and Manufacturing Engineering,* Vol. 17, pp. 93-96.